

World Journal of *Stem Cells*

World J Stem Cells 2018 December 26; 10(12): 183-227



**MINIREVIEWS**

- 183 Cancer stem cell impact on clinical oncology

Toledo-Guzmán ME, Bigoni-Ordóñez GD, Ibáñez Hernández M, Ortiz-Sánchez E

ORIGINAL ARTICLE**Basic Study**

- 196 Functional and molecular mechanism of intracellular pH regulation in human inducible pluripotent stem cells

Chao SC, Wu GJ, Huang SF, Dai NT, Huang HK, Chou MF, Tsai YT, Lee SP, Loh SH

- 196 Platelet-rich plasma enhances adipose-derived stem cell-mediated angiogenesis in a mouse ischemic hindlimb model

Chen CF, Liao HT

Contents

World Journal of Stem Cells
Volume 10 Number 12 December 26, 2018

ABOUT COVER

Editorial Board Member of *World Journal of Stem Cells*, Nils O Schmidt, MD, Associate Professor, Department of Neurosurgery, University Medical Center Hamburg-Eppendorf, Hamburg 20246, Germany

AIM AND SCOPE

World Journal of Stem Cells (*World J Stem Cells*, *WJSC*, online ISSN 1948-0210, DOI: 10.4252), is a peer-reviewed open access academic journal that aims to guide clinical practice and improve diagnostic and therapeutic skills of clinicians.

WJSC covers topics concerning all aspects of stem cells: embryonic, neural, hematopoietic, mesenchymal, tissue-specific, and cancer stem cells; the stem cell niche, stem cell genomics and proteomics, and stem cell techniques and their application in clinical trials.

We encourage authors to submit their manuscripts to *WJSC*. We will give priority to manuscripts that are supported by major national and international foundations and those that are of great basic and clinical significance.

INDEXING/ABSTRACTING

World Journal of Stem Cells (*WJSC*) is now indexed in PubMed, PubMed Central, Science Citation Index Expanded (also known as SciSearch®), Journal Citation Reports/Science Edition, Biological Abstracts, and BIOSIS Previews. The 2018 Edition of Journal Citation Reports cites the 2017 impact factor for *WJSC* as 4.376 (5-year impact factor: N/A), ranking *WJSC* as 7 among 24 journals in Cell and Tissue Engineering (quartile in category Q2), and 65 among 190 journals in Cell Biology (quartile in category Q2).

EDITORS FOR THIS ISSUE

Responsible Assistant Editor: *Xiang Li*
Responsible Electronic Editor: *Han Song*
Proofing Editor-in-Chief: *Lian-Sheng Ma*

Responsible Science Editor: *Fang-Fang Ji*
Proofing Editorial Office Director: *Jin-Lei Wang*

NAME OF JOURNAL
World Journal of Stem Cells

ISSN
ISSN 1948-0210 (online)

LAUNCH DATE
December 31, 2009

FREQUENCY
Monthly

EDITORS-IN-CHIEF
Tong Cao, BM BCh, DDS, PhD, Associate Professor, Doctor, Department of Oral Sciences, National University of Singapore, Singapore 119083, Singapore

EDITORIAL BOARD MEMBERS
All editorial board members resources online at <https://www.wjgnet.com/1948-0210/editorialboard.htm>

EDITORIAL OFFICE
Jin-Lei Wang, Director
World Journal of Stem Cells

Baishideng Publishing Group Inc
7901 Stoneridge Drive, Suite 501, Pleasanton, CA 94588, USA
Telephone: +1-925-2238242
Fax: +1-925-2238243
E-mail: editorialoffice@wjgnet.com
Help Desk: <https://www.f6publishing.com/helpdesk>
<https://www.wjgnet.com>

PUBLISHER
Baishideng Publishing Group Inc
7901 Stoneridge Drive, Suite 501, Pleasanton, CA 94588, USA
Telephone: +1-925-2238242
Fax: +1-925-2238243
E-mail: bpgoffice@wjgnet.com
Help Desk: <https://www.f6publishing.com/helpdesk>
<https://www.wjgnet.com>

PUBLICATION DATE
December 26, 2018

COPYRIGHT

© 2018 Baishideng Publishing Group Inc. Articles published by this Open-Access journal are distributed under the terms of the Creative Commons Attribution Non-commercial License, which permits use, distribution, and reproduction in any medium, provided the original work is properly cited, the use is non-commercial and is otherwise in compliance with the license.

SPECIAL STATEMENT

All articles published in journals owned by the Baishideng Publishing Group (BPG) represent the views and opinions of their authors, and not the views, opinions or policies of the BPG, except where otherwise explicitly indicated.

INSTRUCTIONS TO AUTHORS

<https://www.wjgnet.com/bpg/gerinfo/204>

ONLINE SUBMISSION

<https://www.f6publishing.com>

Cancer stem cell impact on clinical oncology

Mariel E Toledo-Guzmán, Gabriele D Bigoni-Ordóñez, Miguel Ibáñez Hernández, Elizabeth Ortiz-Sánchez

Mariel E Toledo-Guzmán, Gabriele D Bigoni-Ordóñez, Elizabeth Ortiz-Sánchez, Subdirección de Investigación Básica, Instituto Nacional de Cancerología, Mexico City 14080, Mexico

Mariel E Toledo-Guzmán, Miguel Ibáñez Hernández, Departamento de Bioquímica, Laboratorio de Terapia Génica, Escuela Nacional de Ciencias Biológicas, Posgrado de Biomedicina y Biotecnología Molecular, Instituto Politécnico Nacional, Mexico City 11340, Mexico

ORCID number: Mariel E Toledo-Guzmán (0000-0003-4992-8486); Gabriele D Bigoni-Ordóñez (0000-0003-2091-6107); Miguel Ibáñez Hernández (0000-0003-4013-6888); Elizabeth Ortiz-Sánchez (0000-0001-9855-9491).

Author contributions: Toledo-Guzmán ME participated in the conception and writing of the manuscript; Bigoni-Ordóñez GD generated the figures; Ibáñez Hernández M reviewed and suggested modifications to the content; Ortiz-Sánchez E designed the aim of the editorial, participated in the conception and contributed to the writing of the manuscript.

Supported by Institutional funding at Instituto Nacional de Cancerología.

Conflict-of-interest statement: The authors declare no conflict of interest.

Open-Access: This article is an open-access article which was selected by an in-house editor and fully peer-reviewed by external reviewers. It is distributed in accordance with the Creative Commons Attribution Non Commercial (CC BY-NC 4.0) license, which permits others to distribute, remix, adapt, build upon this work non-commercially, and license their derivative works on different terms, provided the original work is properly cited and the use is non-commercial. See: <http://creativecommons.org/licenses/by-nc/4.0/>

Manuscript source: Invited manuscript

Corresponding author to: Elizabeth Ortiz-Sánchez, MD, PhD, Academic Research, Professor, Research Scientist, Senior Researcher, Subdirección de Investigación Básica, Instituto Nacional de Cancerología, Av San Fernando 22, Colonia Sección XVI, Mexico City 14080, Mexico. elinfbk@yahoo.com.mx

Telephone: +52-55-54280400

Received: September 13, 2018

Peer-review started: September 13, 2018

First decision: October 5, 2018

Revised: October 15, 2018

Accepted: November 15, 2018

Article in press: November 16, 2018

Published online: December 26, 2018

Abstract

Cancer is a widespread worldwide chronic disease. In most cases, the high mortality rate from cancer correlates with a lack of clear symptoms, which results in late diagnosis for patients, and consequently, advanced tumor disease with poor probabilities for cure, since many patients will show chemo- and radio-resistance. Several mechanisms have been studied to explain chemo- and radio-resistance to anti-tumor therapies, including cell signaling pathways, anti-apoptotic mechanisms, stemness, metabolism, and cellular phenotypes. Interestingly, the presence of cancer stem cells (CSCs), which are a subset of cells within the tumors, has been related to therapy resistance. In this review, we focus on evaluating the presence of CSCs in different tumors such as breast cancer, gastric cancer, lung cancer, and hematological neoplasias, highlighting studies where CSCs were identified in patient samples. It is evident that there has been a great drive to identify the cell surface phenotypes of CSCs so that they can be used as a tool for anti-tumor therapy treatment design. We also review the potential effect of nanoparticles, drugs, natural compounds, aldehyde dehydrogenase inhibitors, cell signaling inhibitors, and antibodies to treat CSCs from specific tumors. Taken together, we present an overview of the role of CSCs in tumorigenesis and how research is advancing to target these highly tumorigenic cells to improve oncology patient outcomes.

Key words: Cancer; Targeted therapy; Clinical outcome; Drug resistance; Cancer stem cells

© The Author(s) 2018. Published by Baishideng Publishing Group Inc. All rights reserved.

Core tip: Tumor heterogeneity can explain the presence of cells that display high tumorigenic capacity along with chemo- and radio-resistance properties. These cells, identified as cancer stem cells (CSCs), are partially responsible for recurrence and tumor progression. Most tumors follow the CSC model, which indicates the existence of a subset of highly tumorigenic cells. This has been shown to be the case for several patients with several types of tumors. In this review, we focus on the phenotypes used for the study and identification of CSCs from human samples, as well as promising strategies to target CSCs.

Toledo-Guzmán ME, Bigoni-Ordóñez GD, Ibáñez Hernández M, Ortiz-Sánchez E. Cancer stem cell impact on clinical oncology. *World J Stem Cells* 2018; 10(12): 183-195

URL: <https://www.wjgnet.com/1948-0210/full/v10/i12/183.htm>
DOI: <https://dx.doi.org/10.4252/wjsc.v10.i12.183>

INTRODUCTION

Cancer stem cells (CSCs) comprise a cell population within a tumor that, among other factors, is responsible for cancer initiation, propagation, metastasis and recurrence. It is known that solid tumors are composed of heterogeneous cell populations^[1-3] with different phenotypic characteristics at different stages of development, with variable abilities to proliferate. However, only the CSC population is clonogenic *in vitro* and *in vivo*, suggesting that these cells are the only ones with the highest tumorigenic potential^[4,5].

The existence of a subset of cancer cells that possesses an extensive proliferative capacity was reported in leukemia and multiple myeloma in the 1970s^[6,7]. In both cancer types, only a cell population derived from a tumor was able to grow in clonogenic assays, where they formed spherical colonies, and induce tumors in mice that recapitulated the original tumor. At that time, the most reliable criterion for CSC identification was the capacity of these cells to produce colonies^[6].

The first CSCs were isolated from acute myeloid leukemia (AML) by transplantation into severe combined immune-deficient (SCID) mice. They were identified as CD34⁺CD38⁻ cells and named AML-initiating cells because of their ability to establish human leukemia in SCID mice. Since the identified CD34⁺CD38⁻ cells were less differentiated than colony-forming cells, a hierarchy or heterogeneity in AML was proposed^[1]. Later, in 1997, the model was reproduced in non-obese diabetic mice with severe combined immunodeficiency disease (NOD/SCID) mice, where CD34⁺CD38⁻ CSCs were capable of differentiating into leukemic blasts *in vivo*, supporting the existence of a hierarchy in leukemia^[8].

Some years later, enriched CSC populations were obtained from human brain tumors^[9], using cells with a

CD133⁺ phenotype that showed a higher capacity for proliferation, self-renewal, and differentiation. CD133⁺ cells were xenotransplanted into NOD/SCID mice and formed tumors that, when serially transplanted, recapitulated the original human tumor^[10,11]. Since then, CSCs from various solid tumors have been reported^[5].

In recent years, several research groups have focused on the identification and isolation of these cells. Besides leukemia and multiple myeloma, CSCs from solid tumors have been identified and isolated through the use of surface and functional markers^[12-15], their growing capacity as spheroids *in vitro*^[16,17], the evaluation of CSC clonogenic capacity^[18,19] and their *in vivo* tumorigenic capacity in xenotransplant experiments^[16,17,20,21].

Due to the reported participation of CSCs in chemo- and radio-resistance^[22-24], an increasing interest in implementing strategies against CSCs in patients to improve their clinical outcome has grown in recent years because conventional therapies are effective in controlling tumor growth at the beginning, but over time, relapse is a main problem due to remaining CSCs^[22,25,26].

CSC GENERALITIES

A CSC is defined as a cell within a tumor that is able to produce an identical cell with the same properties to give rise heterogeneous differentiated progeny, and has the ability to modulate differentiation and self-renewal (homeostatic control). These CSCs possess the ability to propagate themselves, as well as recapitulate a tumor^[2,3,27].

A major characteristic of CSCs relies on their ability to regulate stemness pathways such as Wnt/ β -catenin, Sonic hedgehog (Shh), transforming growth factor beta (TGF- β), *etc*^[28]. These pathways are dysregulated in CSCs, and targeting them has been proposed as a strategy to increase the effectiveness of cancer therapies.

The CSC model postulates that solid tumors and leukemia are hierarchically organized, with CSCs at the apex of this hierarchy, driving tumor growth, relapse, metastasis and drug resistance^[5,29]. Cell heterogeneity is responsible for varying cell morphology, different proliferative index, genetic changes and therapeutic response^[30]. For a successful therapy, all CSCs should be specifically eliminated to avoid relapse.

Typically, CSCs are defined as a small or a rare cell population^[2,31] that forms tumors after being xenotransplanted into immunodeficient mice. However, recent reports have suggested that the percentage of CSCs within a tumor can vary from 0.02% to 25% depending on the tumor type, where higher CSC proportions are found in undifferentiated tumors^[31-34]. Typically, higher CSC frequencies have been found in mouse models, leukemias and lymphomas, while lower frequencies are frequently found in solid tumors^[35]. Based on this information, it has been suggested that not all cancers follow the CSC model^[27]. Instead, a dynamic or plastic CSC model has been proposed, where CSCs and non-CSCs could alternate between two phenotypic states^[36].

In this dynamic model, both cell types show varying levels of tumor-forming capacity, drug response and the ability to give rise to differentiated cells^[29,35]. CSCs and non-CSCs can still be easily distinguished through surface and functional markers, but mainly by their self-renewal capacity.

It is very important to note that the CSC model is widely reported in several cancer types (Figure 1), although there are a few publications about cancers that do not follow a CSC model or a dynamic CSC model, specifically in lymphoma mice models^[37] and melanoma^[32], where the tumors are homogeneous. In 2007, Strasser and his group inoculated 10 to 10⁵ pre-B/B lymphoma cells into recipient mice. All of the animals developed lymphoma within 35 d, regardless of the number of inoculated cells, differing only in tumor growth rate^[37].

Although CSCs are able to self-renew and differentiate, they do not necessarily originate from the malignant transformation of stem cells^[33]. The cell of origin refers only to the cell type that received the first genetic or epigenetic hit, which confers the ability for self-renewal or tumor growth^[35]. Examples of these cells are: normal stem cells, restricted progenitor cells and more differentiated cells. All of them could have acquired or maintained self-renewal capacity, and some of them can even undergo epithelial to mesenchymal transition (EMT), giving rise to metastatic CSCs^[36].

In conclusion, the variable phenotype of the CSC population in patients and tumor types proposed in the CSC dynamic model constitutes the main challenge for the possible use of anti-CSC therapy.

CSC CHARACTERISTICS WITH CLINICAL RELEVANCE

The CSC population possesses several characteristics that can be useful for cancer therapy development, primarily focusing on the elimination of these cells.

Usually, a distinctive profile of surface and functional markers characterizes the CSC population, and their identification and purification usually begins with the description of such markers^[3,29]. Moreover, there is an increasing interest in identifying the role of each marker in CSCs, as well as targeting CSC-specific pathways, which could increase the radio- and chemo-sensitivity of CSCs.

To date, several CSC markers from distinct tumor types have been proposed and validated through different experimental models (Table 1 and Figure 1). Some of these markers are discussed below.

Surface markers

Nowadays, there are CSC markers that are widely used to identify several tumor types. Such markers have been reported in CSC-enrichment culture models from cell lines or primary cultures derived from patient samples and serial xenotransplantation of putative CSCs

in mouse models, which must be able to recapitulate the original heterogeneous populations and be directly validated in human tumor samples. It is important to note that the use of a single marker to define a CSC population is not recommended. For this purpose, a phenotypic profile that combines various markers should be established, as well as carrying out self-renewal assays (Figure 1)^[2,25].

CD133, also known as prominin-1, is a transmembrane cell surface glycoprotein traditionally used as a hematopoietic stem cell marker that is effective for detection of non-stem cells from various tumor and tissue samples. The Dirks laboratory used the CSC marker CD133 for brain CSC identification. The purified CD133⁺ population from primary human brain tumors samples showed higher proliferation and self-renewal capacity in neurosphere formation assays than CD133⁻ cells^[10]. Moreover, the inoculation of only a few CD133⁺ cells was sufficient to produce a tumor, which was then successfully transplanted^[11]. In 2013, the Pelicci laboratory reported that CD133 was found in an interconvertible state in glioblastoma patient-derived neurospheres and that the use of short hairpin RNA (shRNA) against CD133 diminished their self-renewal and tumorigenicity potential^[18]. Interestingly, some studies have proposed that CD133 could maintain CSC properties through the Wnt/ β -catenin signaling pathway^[38].

CD133 has also been tested in colorectal cancer cell lines and tumor tissue samples^[39,40] through the use of various techniques, including flow cytometry and serial xenotransplantation in mice^[41]. Additionally, CD133⁺ CSCs have been reported in many other solid cancer models, including endometrial cancer^[42], lung cancer^[43], small cell lung cancer^[44], laryngeal cancer^[45,46], liver cancer^[47], colorectal cancer^[48], and gastric cancer^[49].

CD133 has been found in samples that represent higher stage tumors and are predictors of poor prognosis. For this reason, CD133 is considered a promising therapeutic target. This year, a phase I trial for testing the efficacy of CD133-directed CAR-T cells showed that CD133⁺ cells were successfully eliminated after CART-133 infusion^[50].

CD44 is a multifunctional glycoprotein involved in cell adhesion, signaling, proliferation, migration, hematopoiesis, and lymphocyte activation^[51]. It functions as a receptor for hyaluronan and other extracellular matrix components^[52]. CD44 is widely used as a CSC marker, especially for tumors of epithelial origin, and it is used alone or in combination with CD24 for the identification of breast CSCs^[5]. CD24 is a small surface protein that is found in many tumor types. However, reports from cancer cell lines show that there is a substantial variation in CD24 expression even among the same tumor types^[53].

Though CD24⁻ cells are commonly associated with CSC phenotypes, there are some cases in which CD24⁺ has been found to be a marker for cell populations with CSC features. For example, in nasopharyngeal carcinoma (NPC) cell lines^[54] and in HPV-16 SiHa cervical cancer

Table 1 Cancer stem cells markers in solid tumors

| Cancer type | Phenotype | Model | References |
|------------------------------|---|---|------------|
| Prostate cancer | CD44 ⁺ | PCa cell line and tumor xenograft in mice | [58] |
| Breast cancer | CD44 ⁺ CD24 ^{-/low} | Patient-derived tumor xenograft in mice | [5] |
| Cervical cancer | CD44 ⁺ CD24 ⁺ | SiHa cell line | [55] |
| Gastric cancer | CD44 ⁺ CD24 ⁺ | AGS cell line and patient tissue samples | [56] |
| Nasopharyngeal carcinoma | CD24 ⁻ | NPC cell lines, mice | [54] |
| Gastric adenocarcinoma | CD44 ⁺ CD133 ⁺ | Patient tissue samples | [51] |
| Oral squamous cell carcinoma | CD44 ⁺ ALDH1 | Metastatic lymph nodes | [153] |
| Breast cancer | CD44v | Clinical samples | [154] |
| Prostate cancer | CD133 | Primary prostate cancer cell lines | [155] |
| Endometrial cancer | CD133 | Human endometrial cell lines | [42] |
| Liver cancer | CD133 | Huh-7 cells and tumor xenograft in mice | [47] |
| Prostate cancer | CD133 | Primary human prostate cancer cell lines | [155] |
| Cervical cancer | CD49f | SiHa and HeLa cell lines | [156] |
| Non-small cell lung cancer | CD49f | Patient-derived sphere-forming assays | [157] |
| Gastric cancer | CD49f | Gastric tumor tissues and tumor xenograft in mice | [75] |
| Colon cancer | CD49f | HT29 and Caco2 cell lines, clinical samples | [77] |
| Cervical cancer | ALDH | SiHa and HeLa cell lines, mice model | [85] |
| Colon cancer | ALDH1A3 | HT29 cell line | [158] |
| Colon cancer | ALDH1A1 | HT29 cell line and tumor xenograft in mice | [159] |
| Breast cancer | ALDH | Breast cancer tumor tissues | [160] |

CSCs: Cancer stem cells; ALDH: Aldehyde dehydrogenase; NPC: Nasopharyngeal carcinoma.

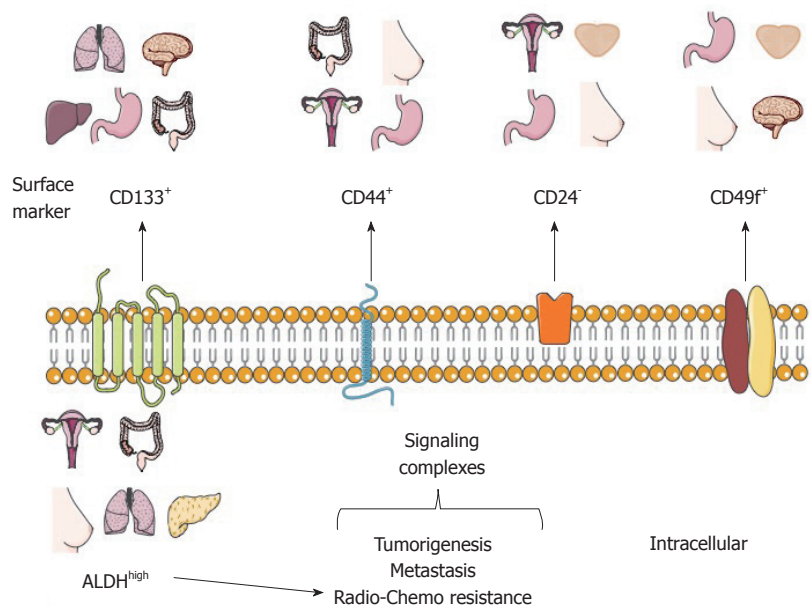


Figure 1 Schematic representation of common cancer stem cell markers. CD133, CD44, CD24 and CD49f are common phenotype markers used for the identification of cancer stem cells (CSCs) and their isolation from tissue samples from cancer patients, such as the stomach, lung, liver, ovary, breast, prostate and colon carcinoma. In addition, the metabolic and functional marker aldehyde dehydrogenase (ALDH) is represented in CSCs derived from ovarian carcinoma, colon carcinoma, breast, lung and liver cancer. The CSC markers shown have a specific and relevant function in the high tumorigenic capacity of CSCs, metastasis, and resistance to radio- and chemotherapy.

cells, isolated CD44⁺CD24⁺ cells were radioresistant and more tumorigenic than those negative for the same markers^[55]. The same CD44⁺CD24⁺ phenotype was used to identify gastric CSCs^[56].

A known classic publication demonstrated that only a small population isolated from breast tumors, defined as CD44⁺CD24^{-/low}, has the capacity to sustain tumor growth in NOD/SCID mice and generate heterogeneous cell populations as the original breast tumor^[5]. Later, in

human prostate cancer samples, CSCs characterized through immunofluorescence with the CD44⁺/β₂β₁^{hi}/CD133⁺ phenotype were identified and characterized^[57]. The next year, CD44⁺ prostate cancer cell populations were obtained^[58]. Also, CD44 and CD133 expression was evaluated in gastric adenocarcinoma tumors by immunohistochemistry, and it was found that both markers could be correlated with clinical and pathological parameters^[51].

Although CD44 is widely reported as a CSC marker, it is very important to note that it is a ubiquitously expressed molecule derived from a gene with 18 exons. When all variable exons are spliced out, the standard form (CD44s) is expressed, and when alternative splicing occurs, variant forms (CD44v) are expressed^[59]. In spite of this, there are only a few reports in which CD44 isoforms are considered when evaluating CSCs. In 2005, Mackenzie and his group demonstrated the existence of two CSC populations, both expressing CD44^{high} (and CD44⁺), derived from head and neck cutaneous squamous cell carcinoma. One was associated with EMT properties and the other one possessed an epithelial phenotype^[60]. They demonstrated that the CD44^{high} cells that undergo EMT preferably expressed the CD44s isoform; while the epithelial CD44^{high} cells expressed the CD44v isoform. Using RNAseq, another group later confirmed these results. The CD44v6 isoform was identified as the predominant isoform in a prostate cancer epithelial cell line^[61].

A very important contribution from the Mackenzie laboratory is that they demonstrated that the use of enzymes (for example, trypsin or collagenase) for cell extraction from tissues caused destruction of cell surface CD44v isoforms, leaving only the CD44s isoform^[62]. Moreover, CD44-specific antibodies are not able to distinguish between all isoforms. Specifically, in breast cancer, CD44v was found to be associated with better prognosis while CD44s was related to poor prognosis^[63]. As a consequence, CD44 is the most frequently found CSC marker^[64,65]. Other examples are found in colorectal cancer, in which CD44 was found together with CD133^[66,67], head and neck squamous cell carcinoma^[68,69], ovarian CSCs^[70], and gastric cancer using the specific isoform CD44v8-10^[71].

CD49f or integrin $\alpha 6$, is a transmembrane glycoprotein that functions as the receptor for the extracellular matrix protein laminin^[72,73]. CD49f is widely distributed in stem cells and in the brain^[73]; because of its role in tumor cell proliferation, survival, self-renewal and tumor growth, it has been proposed that it could be used as a CSC marker^[73].

In sphere colony forming cell culture using prostate cancer cells, CD49f was shown to be a better marker than CD133 and CD44^[74]. In gastric cancer, CD49^{high} cells displayed CSC characteristics, including resistance to doxorubicin, 5-fluorouracil and doxifluridine^[75]. This has also been reported in breast^[76] and colon cancer^[77]. Besides the examples mentioned above, there are other surface markers that have been proposed as CSC markers, such as CXCR4 and LGR5, among others.

Functional markers

Another strategy for CSC identification and purification is the use of functional or intracellular markers (Figure 1), which are considered to be more stable than surface markers. The principal functional CSC marker is aldehyde dehydrogenase or ALDH, part of an enzy-

me superfamily encoded by 19 genes that metabolize endogenous and exogenous aldehydes. It is present in practically all organisms, and its levels and isozymes vary depending on tissue and organ^[78].

For ALDH identification, specific ALDH antibodies are available; nonetheless, we suggest that the most appropriate way for ALDH identification is the measurement of its activity using the commercial ALDH fluorescent substrate ALDEFLUOR® kit assay by Stem Cells Technologies, Inc. (Vancouver, BC, Canada). Cells that display high ALDH activity, (named ALDH^{high} or ALDH⁺ or ALDH^{br}), can be identified and isolated using flow cytometry^[79]. Several works have shown that high ALDH activity is often associated with CSCs derived from solid tumor types^[80]. These cells are generally characterized by a higher proliferation potential, colony-forming capacity, self-renewal, *in vivo* tumorigenic capacity, metastasis, and drug resistance. For instance, ALDH^{high} CSCs have been identified in colon cancer^[81,82], lung cancer^[83], cervical cancer^[14,84,85], breast cancer^[86], pancreatic cancer^[87,88], and melanoma^[89,90], to mention some examples.

As for surface markers, ALDH is often reported in combination with other cell markers to increase the accuracy of CSC validation. In some cases, high ALDH activity is found together with high expression of markers like CD133. Some cases have been identified in ovarian cancer^[91,92], invasive ductal breast carcinoma tumors^[93], and lung cancer^[94]. The combination ALDH⁺/CD44⁺ has been evaluated in various tumors such as breast cancer^[95] and lung cancer^[96].

CSCs AND THERAPY RESISTANCE

Several cancers acquire drug resistance during or after treatment, which is the case for cancers that possess cells that are more resistant than the rest of the tumor. Generally, resistant cells have proteins that remove drugs from cells^[97]. One of the most studied mechanisms of drug resistance in CSCs is their ability to actively expel therapeutic drugs *via* transport proteins. Such proteins are a family known as ATP-binding cassette transporters. These proteins use ATP-dependent drug efflux pumps for drug elimination, mostly into the extracellular space, and they have been found to be overexpressed in CSCs using side population assays^[41,98-100].

Additionally, high ALDH activity is directly related to a higher resistance to several drugs, for example, cyclophosphamide, temozolomide, irinotecan, paclitaxel, and doxorubicin^[101-103]. Resistance conferred by ALDH has been observed in numerous cell lines and patient samples^[97,104]. A well known case is the resistance to cyclophosphamide, where ALDH irreversibly oxidizes aldophosphamide, an active metabolite of cyclophosphamide, into an inert compound^[105]. In breast cancer, the inhibition of ALDH activity in ALDH^{high} CD44⁺ cells leads to a reduction in chemoresistance to doxorubicin and paclitaxel^[106]. This information suggests that the

inhibition of ALDH activity leads to cell sensitization to chemotherapeutics^[99].

Besides higher resistance to conventional cancer treatments, evidence shows that highly metastatic tumors correlate with a higher percentage of CSCs^[28].

CSCs IN PATIENTS: PHENOTYPE AND TYPE OF STUDIES

Most publications about the identification of CSCs have been performed in cell lines. However, in this section, we will discuss the cases in which CSCs were identified in patient samples.

CD133 was analyzed in a meta-analysis of 32 studies of non-small cell lung cancer, and a higher CD133 expression was associated with poor tumor differentiation and lymph node metastasis^[107].

Gastric CSCs have been identified in tumor tissues and peripheral blood using the CD44⁺CD54⁺ phenotype^[108]. Nevertheless, in another study, CD133⁺/CD44⁺ cells sorted from 44 patients who underwent gastrectomy failed to produce tumors in mice and did not show any CSC properties^[109].

The presence of ALDH has been analyzed in normal mammary and breast cancer tissues^[110]. The activity of ALDH1A3 is associated with metastasis in patient breast cancer samples by microarray analysis^[86]. In another analysis of formalin-fixed paraffin-embedded tissue samples from primary stage IV breast cancer, ALDH and CD44/CD24 expression was correlated with response to endocrine therapy and clinical outcome but was not statistically significant^[111].

CSC approaching therapy

Despite the broad variety of CSC publications in the last years, the discovery of effective therapies has remained elusive. However, some advances have been made in the field that could be getting us closer to direct CSC elimination. A brief outline of some of these strategies is showed in Figure 2.

Targeting deregulated pathways in CSCs aims at developing effective strategies against CSCs. In adult pancreas, the Hedgehog (Hh) signaling pathway is dormant, but it is upregulated in pancreatic ductal adenocarcinoma, specifically in CD44⁺/CD24⁺/ESA⁺CSCs. In a phase I study, 68 patients were treated with GDC-0449 or Vismodegib, a Hh pathway antagonist^[112], alone or in combination with gemcitabine. GDC-0449 inhibited Hh signaling, but there was no correlation with survival or other parameters^[113]. Other drugs that show promising results in inhibiting this pathway are PF-04449913^[114] and thioistrepon, which attenuates CD44⁺/CD24⁺ triple-negative breast CSCs^[115].

In addition, γ -secretase inhibitors target the Notch pathway and possess a stronger anti-neoplastic activity when combined with chemotherapeutic agents^[116]. Nevertheless, adverse effects have been reported, as patients developed cutaneous rash in phase I clinical

trials^[117,118].

Several drugs that aim to inhibit the Wnt/ β -catenin signaling pathway are being developed. One such drug is Celecoxib, a non-steroidal anti-inflammatory drug that inhibits β -catenin signaling by cyclo-oxygenase (commonly known as COX)-dependent and COX-independent mechanisms^[116]. This drug downregulates CD133 expression in colon cancer cells by inhibiting Wnt signaling^[119] and intestinal cancer growth^[120]. The Wnt inhibitor LGK-974 inhibits porcupine, an O-acyl-transferase required for Wnt secretion. In liver cancer cells, LGK-974 blocks secretion of the Wnt3A protein, and as a consequence, cells become more sensitive to radiation^[121]. A recent study showed that LGK-974 downregulates ALDH1A3 and reduces chemoresistance in glioblastoma cells^[122].

Curcumin is an antioxidant derived from turmeric whose anti-cancer effect is well documented. Referring specifically to CSCs, curcumin has shown the potential to regulate the CSC self-renewal pathways, as well as specific microRNAs^[123]. In CD133⁺ lung CSCs, curcumin suppresses the activation of Wnt/ β -catenin and Shh pathways, as well as other CSC traits^[124]. It has been demonstrated that in bladder cancer, curcumin suppress the Shh pathway^[125] and in laryngeal carcinoma treatment, curcumin enhances the effectiveness of cisplatin, reducing CD133⁺ cells *in vitro*^[46]. Additionally, a combination of curcumin and FOLFOX chemotherapy inhibits colorectal CSCs in *ex vivo* models^[126].

An interesting strategy is to target CSCs using nanoparticles to reduce side effects on surrounding normal cells. In 2015, construction of glucose-coated gold nanoparticles (Glu-GNPs) that used glucose to facilitate GNP entry into leukemic stem cells overexpressing CD44 (TH1-P) was reported. Leukemic cells were cultured for one hour in the absence of glucose for better Glu-GNP uptake, and then X-ray irradiation tests were performed. Results showed that Glu-GNPs enhanced cell death compared to either irradiation or GNPs alone^[127]. Formulated mangostin-encapsulated poly(lactic-co-glycolic acid) nanoparticles (Mang-NPs) successfully downregulated the known stemness genes c-Myc, Nanog and Oct4, two CSC markers, CD24 and CD133, and the Shh pathway^[128]. Salinomycin and paclitaxel nanoparticles are also being used to eliminate breast cancer cells including CD44 breast CSCs^[129].

Interestingly, CSCs have a strict dependence on mitochondrial biogenesis. Five classes of FDA-approved antibiotics that inhibit mitochondrial biogenesis were used on eight different cancer cell lines, and the results suggested that the observed therapeutic effects were infection-independent^[130]. Clinical trials using doxycycline showed positive results in cancer patients^[131]. Another drug that has been shown to specifically eliminate CSCs is metformin, and its effects are enhanced when it is used in combination with doxorubicin^[132]. Moreover, it has been observed that metformin reduces metastasis by targeting both EMT

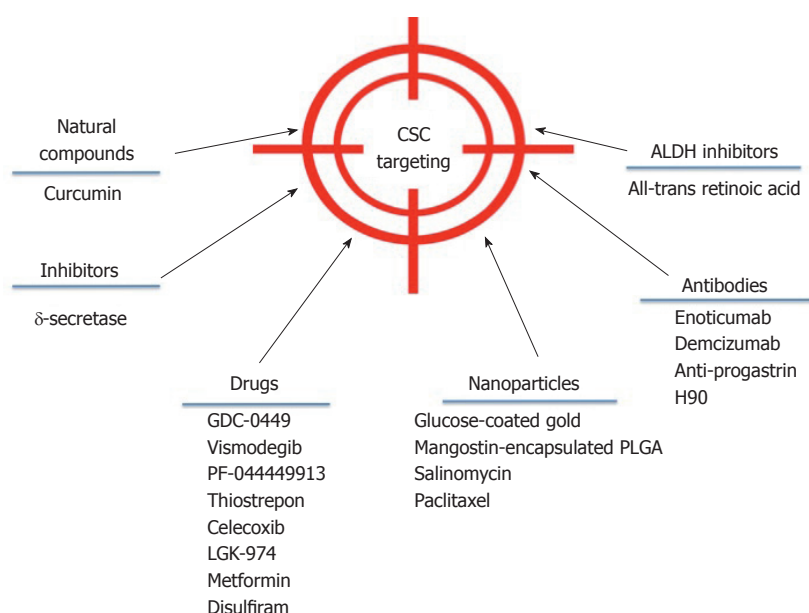


Figure 2 Drugs that may target cancer stem cells. Promising therapeutics to treat cancer patients. The flowchart highlights the new and more promising cancer therapies that can be directed toward cancer stem cells to eliminate them. CSC: Cancer stem cell.

and CSCs^[133]. In the ovarian cancer cell line SKOV3, low doses of metformin diminished CD44⁺CD117⁺ CSCs in xenograft tissue and enhanced the effect of cisplatin^[134]. In esophageal cancer, metformin reduced the number of ALDH⁺ cells, tumor growth *in vivo*^[135], and in pancreatic cancer, it increased radiation sensitivity^[136].

Using antibodies is another strategy to block CSC signaling pathways and reduce tumor activity in different models. For instance, the anti-DLL4 (Enoticumab) antibody that targets the dominant Notch ligand DLL4 has shown anti-tumor activity, especially in VEGF-resistant tumors in human phase I studies^[137]. Furthermore, another anti-DLL4 antibody (Demcizumab) is effective in decreasing tumor size but produces hypertension^[138]. In colon cancer patients, increased progastrin levels in the blood have been observed, which is a tumor-promoting peptide that participates in colon CSC self-renewal and is also a direct target gene of β -catenin/Tcf4. Based on this information, specific anti-progastrin antibodies have been developed and tested in colon cancer cell lines and in mice. The antibodies, alone or in combination with chemotherapy, decreased self-renewal, migration and invasion. Moreover, they mitigated Wnt-driven intestinal neoplasia and induced tumor cell differentiation *in vivo*^[139]. H90 is a mouse IgG1 mAb against human CD44 that directly targets CSCs to induce differentiation and proliferation in AML xenograft mouse models^[140]. Additionally, anti-CD44s-specific antibodies are effective in eliminating pancreatic stem cells^[141]. For more extensive information about antibodies against CSCs, we recommend reference^[142].

ALDH is an important CSC marker that is overexpressed in several cancers. Specific ALDH inhibitors are effective in modulating cell growth, apoptosis and differentiation. Additionally, increased chemo- and radio-sensitivity is usually observed. All-trans retinoic

acid (commonly known as ATRA) is a first generation systemic retinoid that promotes cell differentiation^[143,144] and has been used in clinical trials^[145]. ATRA has also been tested in breast cancer cells^[106,146,147] and in gastric cancer, where it inhibited tumor growth^[148], and in head and neck cancer, where it suppressed Wnt/ β -catenin signaling^[149]. In a phase I / II trial, advanced breast cancer patients did not show a significant improvement when treated with ATRA and tamoxifen compared with tamoxifen alone^[150].

Disulfiram is a drug used for treating alcoholism, and it shows anti-cancer activity *in vitro* and *in vivo*, further potentiating the chemotherapeutic response. Its effectiveness has been demonstrated on paclitaxel-resistant triple-negative breast cancer cells^[151], in non-small cell lung cancer cells^[152], and glioblastoma.

CONCLUSION

CSCs are potential cancer therapy targets due to their tumorigenic capabilities, such as chemo- and radio-resistance, phenomena involved in tumor relapse in patients. Several efforts have been made to continue to identify the CSCs in several tumors to better understand the mechanisms related to tumor resistance in oncologic patients. It is known that de-regulated cell signaling pathways are partially responsible for maintaining CSC stemness. Consequently, Wnt, Notch and Hh signaling pathways have been studied to develop an efficient anti-CSC therapy. However, innovative anti-cancer treatments need to be developed to improve the lifespan and quality of life of cancer patients. Finally, we suggest that there cannot be a generalized CSC phenotype to design and promote new drugs, antibodies, nanoparticles, and cellular treatments to treat oncological patients. Taken together, we suggest

the full characterization of phenotypes and capabilities of CSCs in patients, a cellular component responsible for tumor progression, tumor relapse and metastasis.

ACKNOWLEDGEMENTS

The authors thank Marco Antonio Meraz Rodríguez for his constructive suggestions and Dra. Elizabeth Langley McCarron for her editing and we thank Instituto Nacional de Cancerología, Instituto Politécnico Nacional and Posgrado de Biomedicina y Biotecnología Molecular.

REFERENCES

- Lapidot T**, Sirard C, Vormoor J, Murdoch B, Hoang T, Caceres-Cortes J, Minden M, Paterson B, Caligiuri MA, Dick JE. A cell initiating human acute myeloid leukaemia after transplantation into SCID mice. *Nature* 1994; **367**: 645-648 [PMID: 7509044 DOI: 10.1038/367645a0]
- Clarke MF**, Dick JE, Dirks PB, Eaves CJ, Jamieson CH, Jones DL, Visvader J, Weissman IL, Wahl GM. Cancer stem cells—perspectives on current status and future directions: AACR Workshop on cancer stem cells. *Cancer Res* 2006; **66**: 9339-9344 [PMID: 16990346 DOI: 10.1158/0008-5472.CAN-06-3126]
- Dalerba P**, Cho RW, Clarke MF. Cancer stem cells: models and concepts. *Annu Rev Med* 2007; **58**: 267-284 [PMID: 17002552 DOI: 10.1146/annurev.med.58.062105.204854]
- Reya T**, Morrison SJ, Clarke MF, Weissman IL. Stem cells, cancer, and cancer stem cells. *Nature* 2001; **414**: 105-111 [PMID: 11689955 DOI: 10.1038/35102167]
- Al-Hajj M**, Wicha MS, Benito-Hernandez A, Morrison SJ, Clarke MF. Prospective identification of tumorigenic breast cancer cells. *Proc Natl Acad Sci USA* 2003; **100**: 3983-3988 [PMID: 12629218 DOI: 10.1073/pnas.0530291100]
- Park CH**, Bergsagel DE, McCulloch EA. Mouse myeloma tumor stem cells: a primary cell culture assay. *J Natl Cancer Inst* 1971; **46**: 411-422 [PMID: 5115909]
- Hamburger AW**, Salmon SE. Primary bioassay of human tumor stem cells. *Science* 1977; **197**: 461-463 [PMID: 560061 DOI: 10.1126/science.560061]
- Bonnet D**, Dick JE. Human acute myeloid leukemia is organized as a hierarchy that originates from a primitive hematopoietic cell. *Nat Med* 1997; **3**: 730-737 [PMID: 9212098 DOI: 10.1038/nm0797-730]
- Hemmati HD**, Nakano I, Lazareff JA, Masterman-Smith M, Geschwind DH, Bronner-Fraser M, Kornblum HI. Cancerous stem cells can arise from pediatric brain tumors. *Proc Natl Acad Sci USA* 2003; **100**: 15178-15183 [PMID: 14645703 DOI: 10.1073/pnas.2036535100]
- Singh SK**, Clarke ID, Terasaki M, Bonn VE, Hawkins C, Squire J, Dirks PB. Identification of a cancer stem cell in human brain tumors. *Cancer Res* 2003; **63**: 5821-5828 [PMID: 14522905]
- Singh SK**, Hawkins C, Clarke ID, Squire JA, Bayani J, Hide T, Henkelman RM, Cusimano MD, Dirks PB. Identification of human brain tumour initiating cells. *Nature* 2004; **432**: 396-401 [PMID: 15549107 DOI: 10.1038/nature03128]
- Ginestier C**, Hur MH, Charafe-Jauffret E, Monville F, Dutcher J, Brown M, Jacquemier J, Viens P, Kleer CG, Liu S, Schott A, Hayes D, Birnbaum D, Wicha MS, Dontu G. ALDH1 is a marker of normal and malignant human mammary stem cells and a predictor of poor clinical outcome. *Cell Stem Cell* 2007; **1**: 555-567 [PMID: 18371393 DOI: 10.1016/j.stem.2007.08.014]
- Greve B**, Kelsch R, Spaniol K, Eich HT, Götte M. Flow cytometry in cancer stem cell analysis and separation. *Cytometry A* 2012; **81**: 284-293 [PMID: 22311742 DOI: 10.1002/cyto.a.22022]
- Rao QX**, Yao TT, Zhang BZ, Lin RC, Chen ZL, Zhou H, Wang LJ, Lu HW, Chen Q, Di N, Lin ZQ. Expression and functional role of ALDH1 in cervical carcinoma cells. *Asian Pac J Cancer Prev* 2012; **13**: 1325-1331 [PMID: 22799327 DOI: 10.7314/APJCP.2012.13.4.1325]
- Shackleton M**. Normal stem cells and cancer stem cells: similar and different. *Semin Cancer Biol* 2010; **20**: 85-92 [PMID: 20435143 DOI: 10.1016/j.semcancer.2010.04.002]
- Yu SC**, Ping YF, Yi L, Zhou ZH, Chen JH, Yao XH, Gao L, Wang JM, Bian XW. Isolation and characterization of cancer stem cells from a human glioblastoma cell line U87. *Cancer Lett* 2008; **265**: 124-134 [PMID: 18343028 DOI: 10.1016/j.canlet.2008.02.010]
- Qiang L**, Yang Y, Ma YJ, Chen FH, Zhang LB, Liu W, Qi Q, Lu N, Tao L, Wang XT, You QD, Guo QL. Isolation and characterization of cancer stem like cells in human glioblastoma cell lines. *Cancer Lett* 2009; **279**: 13-21 [PMID: 19232461 DOI: 10.1016/j.canlet.2009.01.016]
- Brescia P**, Ortensi B, Fornasari L, Levi D, Broggi G, Pelicci G. CD133 is essential for glioblastoma stem cell maintenance. *Stem Cells* 2013; **31**: 857-869 [PMID: 23307586 DOI: 10.1002/stem.1317]
- Wang L**, Guo H, Lin C, Yang L, Wang X. Enrichment and characterization of cancer stem-like cells from a cervical cancer cell line. *Mol Med Rep* 2014; **9**: 2117-2123 [PMID: 24676900 DOI: 10.3892/mmr.2014.2063]
- Fillmore CM**, Kuperwasser C. Human breast cancer cell lines contain stem-like cells that self-renew, give rise to phenotypically diverse progeny and survive chemotherapy. *Breast Cancer Res* 2008; **10**: R25 [PMID: 18366788 DOI: 10.1186/bcr1982]
- Bertolini G**, Roz L, Perego P, Tortoreto M, Fontanella E, Gatti L, Pratesi G, Fabbri A, Andriani F, Tinelli S, Roz E, Caserini R, Lo Vullo S, Camerini T, Mariani L, Delia D, Calabrò E, Pastorino U, Sozzi G. Highly tumorigenic lung cancer CD133+ cells display stem-like features and are spared by cisplatin treatment. *Proc Natl Acad Sci USA* 2009; **106**: 16281-16286 [PMID: 19805294 DOI: 10.1073/pnas.0905653106]
- Li X**, Lewis MT, Huang J, Gutierrez C, Osborne CK, Wu MF, Hilsenbeck SG, Pavlick A, Zhang X, Chamness GC, Wong H, Rosen J, Chang JC. Intrinsic resistance of tumorigenic breast cancer cells to chemotherapy. *J Natl Cancer Inst* 2008; **100**: 672-679 [PMID: 18445819 DOI: 10.1093/jnci/djn123]
- Liao J**, Qian F, Tchabo N, Mhawech-Fauceglia P, Beck A, Qian Z, Wang X, Huss WJ, Lele SB, Morrison CD, Odunsi K. Ovarian cancer spheroid cells with stem cell-like properties contribute to tumor generation, metastasis and chemotherapy resistance through hypoxia-resistant metabolism. *PLoS One* 2014; **9**: e84941 [PMID: 24409314 DOI: 10.1371/journal.pone.0084941]
- Bao S**, Wu Q, McLendon RE, Hao Y, Shi Q, Hjelmeland AB, Dewhirst MW, Bigner DD, Rich JN. Glioma stem cells promote radioresistance by preferential activation of the DNA damage response. *Nature* 2006; **444**: 756-760 [PMID: 17051156 DOI: 10.1038/nature05236]
- Clarke MF**. A self-renewal assay for cancer stem cells. *Cancer Chemother Pharmacol* 2005; **56** Suppl 1: 64-68 [PMID: 16273355 DOI: 10.1007/s00280-005-0097-1]
- Eyler CE**, Rich JN. Survival of the fittest: cancer stem cells in therapeutic resistance and angiogenesis. *J Clin Oncol* 2008; **26**: 2839-2845 [PMID: 18539962 DOI: 10.1200/JCO.2007.15.1829]
- Gupta PB**, Chaffer CL, Weinberg RA. Cancer stem cells: mirage or reality? *Nat Med* 2009; **15**: 1010-1012 [PMID: 19734877 DOI: 10.1038/nm0909-1010]
- Ajani JA**, Song S, Hochster HS, Steinberg IB. Cancer stem cells: the promise and the potential. *Semin Oncol* 2015; **42** Suppl 1: S3-S17 [PMID: 25839664 DOI: 10.1053/j.seminoncol.2015.01.001]
- Vlashi E**, Pajonk F. Cancer stem cells, cancer cell plasticity and radiation therapy. *Semin Cancer Biol* 2015; **31**: 28-35 [PMID: 25025713 DOI: 10.1016/j.semcancer.2014.07.001]
- Visvader JE**. Cells of origin in cancer. *Nature* 2011; **469**: 314-322 [PMID: 21248838 DOI: 10.1038/nature09781]
- Ishizawa K**, Rasheed ZA, Karisch R, Wang Q, Kowalski J, Susky E, Pereira K, Karamboulas C, Moghal N, Rajeshkumar NV, Hidalgo M, Tsao M, Ailles L, Waddell TK, Maitra A, Neel BG, Matsui W. Tumor-initiating cells are rare in many human tumors.

- Cell Stem Cell* 2010; **7**: 279-282 [PMID: 20804964 DOI: 10.1016/j.stem.2010.08.009]
- 32 **Quintana E**, Shackleton M, Foster HR, Fullen DR, Sabel MS, Johnson TM, Morrison SJ. Phenotypic heterogeneity among tumorigenic melanoma cells from patients that is reversible and not hierarchically organized. *Cancer Cell* 2010; **18**: 510-523 [PMID: 21075313 DOI: 10.1016/j.ccr.2010.10.012]
 - 33 **Visvader JE**, Lindeman GJ. Cancer stem cells: current status and evolving complexities. *Cell Stem Cell* 2012; **10**: 717-728 [PMID: 22704512 DOI: 10.1016/j.stem.2012.05.007]
 - 34 **Eppert K**, Takenaka K, Lechman ER, Waldron L, Nilsson B, van Galen P, Metzeler KH, Poepl A, Ling V, Beyene J, Canty AJ, Danska JS, Bohlander SK, Buske C, Minden MD, Golub TR, Jurisica I, Ebert BL, Dick JE. Stem cell gene expression programs influence clinical outcome in human leukemia. *Nat Med* 2011; **17**: 1086-1093 [PMID: 21873988 DOI: 10.1038/nm.2415]
 - 35 **Visvader JE**, Lindeman GJ. Cancer stem cells in solid tumours: accumulating evidence and unresolved questions. *Nat Rev Cancer* 2008; **8**: 755-768 [PMID: 18784658 DOI: 10.1038/nrc2499]
 - 36 **Khan IN**, Al-Karim S, Bora RS, Chaudhary AG, Saini KS. Cancer stem cells: a challenging paradigm for designing targeted drug therapies. *Drug Discov Today* 2015; **20**: 1205-1216 [PMID: 26143148 DOI: 10.1016/j.drudis.2015.06.013]
 - 37 **Kelly PN**, Dakic A, Adams JM, Nutt SL, Strasser A. Tumor growth need not be driven by rare cancer stem cells. *Science* 2007; **317**: 337 [PMID: 17641192 DOI: 10.1126/science.1142596]
 - 38 **Alvarado-Ortiz E**, Sarabia-Sanchez MA, Garcia-Carranca A. Molecular mechanisms underlying the functions of cellular markers associated with the phenotype of Cancer Stem Cells. *Curr Stem Cell Res Ther* 2018 [PMID: 30147013]
 - 39 **Ren F**, Sheng WQ, Du X. CD133: a cancer stem cells marker, is used in colorectal cancers. *World J Gastroenterol* 2013; **19**: 2603-2611 [PMID: 23674867 DOI: 10.3748/wjg.v19.i17.2603]
 - 40 **Lin L**, Fuchs J, Li C, Olson V, Bekaii-Saab T, Lin J. STAT3 signaling pathway is necessary for cell survival and tumorsphere forming capacity in ALDH⁺/CD133⁺ stem cell-like human colon cancer cells. *Biochem Biophys Res Commun* 2011; **416**: 246-251 [PMID: 22074823 DOI: 10.1016/j.bbrc.2011.10.112]
 - 41 **Catalano V**, Di Franco S, Iovino F, Dieli F, Stassi G, Todaro M. CD133 as a target for colon cancer. *Expert Opin Ther Targets* 2012; **16**: 259-267 [PMID: 22385077 DOI: 10.1517/14728222.2012.667404]
 - 42 **Nakamura M**, Zhang X, Mizumoto Y, Maida Y, Bono Y, Takakura M, Kyo S. Molecular characterization of CD133⁺ cancer stem-like cells in endometrial cancer. *Int J Oncol* 2014; **44**: 669-677 [PMID: 24366104 DOI: 10.3892/ijo.2013.2230]
 - 43 **Wang S**, Xu ZY, Wang LF, Su W. CD133⁺ cancer stem cells in lung cancer. *Front Biosci (Landmark Ed)* 2013; **18**: 447-453 [PMID: 23276935 DOI: 10.2741/4113]
 - 44 **Sarvi S**, Mackinnon AC, Avlonitis N, Bradley M, Rintoul RC, Rassl DM, Wang W, Forbes SJ, Gregory CD, Sethi T. CD133⁺ cancer stem-like cells in small cell lung cancer are highly tumorigenic and chemoresistant but sensitive to a novel neuropeptide antagonist. *Cancer Res* 2014; **74**: 1554-1565 [PMID: 24436149 DOI: 10.1158/0008-5472.CAN-13-1541]
 - 45 **Wu CP**, Du HD, Gong HL, Li DW, Tao L, Tian J, Zhou L. Hypoxia promotes stem-like properties of laryngeal cancer cell lines by increasing the CD133⁺ stem cell fraction. *Int J Oncol* 2014; **44**: 1652-1660 [PMID: 24573690 DOI: 10.3892/ijo.2014.2307]
 - 46 **Zhang H**, Yu T, Wen L, Wang H, Fei D, Jin C. Curcumin enhances the effectiveness of cisplatin by suppressing CD133⁺ cancer stem cells in laryngeal carcinoma treatment. *Exp Ther Med* 2013; **6**: 1317-1321 [PMID: 24223665 DOI: 10.3892/etm.2013.1297]
 - 47 **Piao LS**, Hur W, Kim TK, Hong SW, Kim SW, Choi JE, Sung PS, Song MJ, Lee BC, Hwang D, Yoon SK. CD133⁺ liver cancer stem cells modulate radioresistance in human hepatocellular carcinoma. *Cancer Lett* 2012; **315**: 129-137 [PMID: 22079466 DOI: 10.1016/j.canlet.2011.10.012]
 - 48 **Abbasi M**, Mousavi E, Arab-Bafarani Z, Sahebkar A. The most reliable surface marker for the identification of colorectal cancer stem-like cells: A systematic review and meta-analysis. *J Cell Physiol* 2018; [PMID: 30317669 DOI: 10.1002/jcp.27619]
 - 49 **Lee HH**, Seo KJ, An CH, Kim JS, Jeon HM. CD133 expression is correlated with chemoresistance and early recurrence of gastric cancer. *J Surg Oncol* 2012; **106**: 999-1004 [PMID: 22674531 DOI: 10.1002/jso.23178]
 - 50 **Wang Y**, Chen M, Wu Z, Tong C, Dai H, Guo Y, Liu Y, Huang J, Lv H, Luo C, Feng KC, Yang QM, Li XL, Han W. CD133-directed CAR T cells for advanced metastasis malignancies: A phase I trial. *Oncoimmunology* 2018; **7**: e1440169 [PMID: 29900044 DOI: 10.1080/2162402X.2018.1440169]
 - 51 **Nosrati A**, Naghshvar F, Khanari S. Cancer Stem Cell Markers CD44, CD133 in Primary Gastric Adenocarcinoma. *Int J Mol Cell Med* 2014; **3**: 279-286 [PMID: 25635255]
 - 52 **Yan Y**, Zuo X, Wei D. Concise Review: Emerging Role of CD44 in Cancer Stem Cells: A Promising Biomarker and Therapeutic Target. *Stem Cells Transl Med* 2015; **4**: 1033-1043 [PMID: 26136504 DOI: 10.5966/sctm.2015-0048]
 - 53 **Jaggupilli A**, Elkord E. Significance of CD44 and CD24 as cancer stem cell markers: an enduring ambiguity. *Clin Dev Immunol* 2012; **2012**: 708036 [PMID: 22693526 DOI: 10.1155/2012/708036]
 - 54 **Yang CH**, Wang HL, Lin YS, Kumar KP, Lin HC, Chang CJ, Lu CC, Huang TT, Martel J, Ojcius DM, Chang YS, Young JD, Lai HC. Identification of CD24 as a cancer stem cell marker in human nasopharyngeal carcinoma. *PLoS One* 2014; **9**: e99412 [PMID: 24955581 DOI: 10.1371/journal.pone.0099412]
 - 55 **Liu H**, Wang YJ, Bian L, Fang ZH, Zhang QY, Cheng JX. CD44⁺/CD24⁺ cervical cancer cells resist radiotherapy and exhibit properties of cancer stem cells. *Eur Rev Med Pharmacol Sci* 2016; **20**: 1745-1754 [PMID: 27212166]
 - 56 **Zhang C**, Li C, He F, Cai Y, Yang H. Identification of CD44⁺CD24⁺ gastric cancer stem cells. *J Cancer Res Clin Oncol* 2011; **137**: 1679-1686 [PMID: 21882047 DOI: 10.1007/s00432-011-1038-5]
 - 57 **Collins AT**, Berry PA, Hyde C, Stower MJ, Maitland NJ. Prospective identification of tumorigenic prostate cancer stem cells. *Cancer Res* 2005; **65**: 10946-10951 [PMID: 16322242 DOI: 10.1158/0008-5472.CAN-05-2018]
 - 58 **Patrawala L**, Calhoun T, Schneider-Broussard R, Li H, Bhatia B, Tang S, Reilly JG, Chandra D, Zhou J, Claypool K, Coghlan L, Tang DG. Highly purified CD44⁺ prostate cancer cells from xenograft human tumors are enriched in tumorigenic and metastatic progenitor cells. *Oncogene* 2006; **25**: 1696-1708 [PMID: 16449977 DOI: 10.1038/sj.onc.1209327]
 - 59 **Prochazka L**, Tesarik R, Turanek J. Regulation of alternative splicing of CD44 in cancer. *Cell Signal* 2014; **26**: 2234-2239 [PMID: 25025570 DOI: 10.1016/j.cellsig.2014.07.011]
 - 60 **Biddle A**, Liang X, Gammon L, Fazil B, Harper LJ, Emich H, Costea DE, Mackenzie IC. Cancer stem cells in squamous cell carcinoma switch between two distinct phenotypes that are preferentially migratory or proliferative. *Cancer Res* 2011; **71**: 5317-5326 [PMID: 21685475 DOI: 10.1158/0008-5472.CAN-11-1059]
 - 61 **Hernandez JR**, Kim JJ, Verdone JE, Liu X, Torga G, Pienta KJ, Mooney SM. Alternative CD44 splicing identifies epithelial prostate cancer cells from the mesenchymal counterparts. *Med Oncol* 2015; **32**: 159 [PMID: 25850653 DOI: 10.1007/s12032-015-0593-z]
 - 62 **Biddle A**, Gammon L, Fazil B, Mackenzie IC. CD44 staining of cancer stem-like cells is influenced by down-regulation of CD44 variant isoforms and up-regulation of the standard CD44 isoform in the population of cells that have undergone epithelial-to-mesenchymal transition. *PLoS One* 2013; **8**: e57314 [PMID: 23437366 DOI: 10.1371/journal.pone.0057314]
 - 63 **Inoue K**, Fry EA. Aberrant Splicing of Estrogen Receptor, HER2, and CD44 Genes in Breast Cancer. *Genet Epigenet* 2015; **7**: 19-32 [PMID: 26692764 DOI: 10.4137/GEG.S35500]
 - 64 **Zöller M**. CD44: can a cancer-initiating cell profit from an abundantly expressed molecule? *Nat Rev Cancer* 2011; **11**: 254-267 [PMID: 21390059 DOI: 10.1038/nrc3023]
 - 65 **Lobo NA**, Shimono Y, Qian D, Clarke MF. The biology of cancer stem cells. *Annu Rev Cell Dev Biol* 2007; **23**: 675-699 [PMID: 17551111 DOI: 10.1146/annurev.celldev.23.010107.11551111]

- 17645413 DOI: 10.1146/annurev.cellbio.22.010305.104154]
- 66 **Zhang L**, Zheng W, Wang Y, Wang Y, Huang H. Human bone marrow mesenchymal stem cells support the derivation and propagation of human induced pluripotent stem cells in culture. *Cell Reprogram* 2013; **15**: 216-223 [PMID: 23713432 DOI: 10.1089/cell.2012.0064]
- 67 **Jing F**, Kim HJ, Kim CH, Kim YJ, Lee JH, Kim HR. Colon cancer stem cell markers CD44 and CD133 in patients with colorectal cancer and synchronous hepatic metastases. *Int J Oncol* 2015; **46**: 1582-1588 [PMID: 25625240 DOI: 10.3892/ijo.2015.2844]
- 68 **Joshua B**, Kaplan MJ, Doweck I, Pai R, Weissman IL, Prince ME, Ailles LE. Frequency of cells expressing CD44, a head and neck cancer stem cell marker: correlation with tumor aggressiveness. *Head Neck* 2012; **34**: 42-49 [PMID: 21322081 DOI: 10.1002/hed.21699]
- 69 **Faber A**, Barth C, Hörmann K, Kassner S, Schultz JD, Sommer U, Stern-Straeter J, Thorn C, Goessler UR. CD44 as a stem cell marker in head and neck squamous cell carcinoma. *Oncol Rep* 2011; **26**: 321-326 [PMID: 21617876 DOI: 10.3892/or.2011.1322]
- 70 **Meng E**, Long B, Sullivan P, McClellan S, Finan MA, Reed E, Shevde L, Rocconi RP. CD44+/CD24- ovarian cancer cells demonstrate cancer stem cell properties and correlate to survival. *Clin Exp Metastasis* 2012; **29**: 939-948 [PMID: 22610780 DOI: 10.1007/s10585-012-9482-4]
- 71 **Lau WM**, Teng E, Chong HS, Lopez KA, Tay AY, Salto-Tellez M, Shabbir A, So JB, Chan SL. CD44v8-10 is a cancer-specific marker for gastric cancer stem cells. *Cancer Res* 2014; **74**: 2630-2641 [PMID: 24618343 DOI: 10.1158/0008-5472.CAN-13-2309]
- 72 **Watt FM**. Role of integrins in regulating epidermal adhesion, growth and differentiation. *EMBO J* 2002; **21**: 3919-3926 [PMID: 12145193 DOI: 10.1093/emboj/cdf399]
- 73 **Lathia JD**, Gallagher J, Heddleston JM, Wang J, Eyler CE, Macswords J, Wu Q, Vasanji A, McLendon RE, Hjelmeland AB, Rich JN. Integrin alpha 6 regulates glioblastoma stem cells. *Cell Stem Cell* 2010; **6**: 421-432 [PMID: 20452317 DOI: 10.1016/j.stem.2010.02.018]
- 74 **Yamamoto H**, Masters JR, Dasgupta P, Chandra A, Popert R, Freeman A, Ahmed A. CD49f is an efficient marker of monolayer- and spheroid colony-forming cells of the benign and malignant human prostate. *PLoS One* 2012; **7**: e46979 [PMID: 23071686 DOI: 10.1371/journal.pone.0046979]
- 75 **Fukamachi H**, Seol HS, Shimada S, Funasaka C, Baba K, Kim JH, Park YS, Kim MJ, Kato K, Inokuchi M, Kawachi H, Yook JH, Eishi Y, Kojima K, Kim WH, Jang SJ, Yuasa Y. CD49f(high) cells retain sphere-forming and tumor-initiating activities in human gastric tumors. *PLoS One* 2013; **8**: e72438 [PMID: 24015244 DOI: 10.1371/journal.pone.0072438]
- 76 **Ye F**, Zhong X, Qiu Y, Yang L, Wei B, Zhang Z, Bu H. CD49f Can Act as a Biomarker for Local or Distant Recurrence in Breast Cancer. *J Breast Cancer* 2017; **20**: 142-149 [PMID: 28690650 DOI: 10.4048/jbc.2017.20.2.142]
- 77 **Haraguchi N**, Ishii H, Mimori K, Ohta K, Uemura M, Nishimura J, Hata T, Takemasa I, Mizushima T, Yamamoto H, Doki Y, Mori M. CD49f-positive cell population efficiently enriches colon cancer-initiating cells. *Int J Oncol* 2013; **43**: 425-430 [PMID: 23708747 DOI: 10.3892/ijo.2013.1955]
- 78 **Sládek NE**. Human aldehyde dehydrogenases: potential pathological, pharmacological, and toxicological impact. *J Biochem Mol Toxicol* 2003; **17**: 7-23 [PMID: 12616643 DOI: 10.1002/jbt.10057]
- 79 **Storms RW**, Trujillo AP, Springer JB, Shah L, Colvin OM, Ludeman SM, Smith C. Isolation of primitive human hematopoietic progenitors on the basis of aldehyde dehydrogenase activity. *Proc Natl Acad Sci USA* 1999; **96**: 9118-9123 [PMID: 10430905 DOI: 10.1073/pnas.96.16.9118]
- 80 **Toledo-Guzmán ME**, Ibañez Hernández M, Gomez-Gallegos AA, Ortiz-Sánchez E. ALDH as a Stem Cell marker in solid tumors. *Curr Stem Cell Res Ther* 2018 [PMID: 30095061 DOI: 10.2174/1574888X13666180810120012]
- 81 **Huang EH**, Hynes MJ, Zhang T, Ginestier C, Dontu G, Appelman H, Fields JZ, Wicha MS, Boman BM. Aldehyde dehydrogenase 1 is a marker for normal and malignant human colonic stem cells (SC) and tracks SC overpopulation during colon tumorigenesis. *Cancer Res* 2009; **69**: 3382-3389 [PMID: 19336570 DOI: 10.1158/0008-5472.CAN-08-4418]
- 82 **Shenoy A**, Butterworth E, Huang EH. ALDH as a marker for enriching tumorigenic human colonic stem cells. *Methods Mol Biol* 2012; **916**: 373-385 [PMID: 22914954 DOI: 10.1007/978-1-61779-980-8_27]
- 83 **Jiang F**, Qiu Q, Khanna A, Todd NW, Deepak J, Xing L, Wang H, Liu Z, Su Y, Stass SA, Katz RL. Aldehyde dehydrogenase 1 is a tumor stem cell-associated marker in lung cancer. *Mol Cancer Res* 2009; **7**: 330-338 [PMID: 19276181 DOI: 10.1158/1541-7786.MCR-08-0393]
- 84 **Liu SY**, Zheng PS. High aldehyde dehydrogenase activity identifies cancer stem cells in human cervical cancer. *Oncotarget* 2013; **4**: 2462-2475 [PMID: 24318570 DOI: 10.18632/oncotarget.1578]
- 85 **Ortiz-Sánchez E**, Santiago-López L, Cruz-Domínguez VB, Toledo-Guzmán ME, Hernández-Cueto D, Muñoz-Hernández S, Garrido E, Cantú De León D, García-Carrancá A. Characterization of cervical cancer stem cell-like cells: phenotyping, stemness, and human papilloma virus co-receptor expression. *Oncotarget* 2016; **7**: 31943-31954 [PMID: 27008711 DOI: 10.18632/oncotarget.8218]
- 86 **Marcato P**, Dean CA, Pan D, Araslanova R, Gillis M, Joshi M, Helyer L, Pan L, Leidal A, Gujar S, Giacomantonio CA, Lee PW. Aldehyde dehydrogenase activity of breast cancer stem cells is primarily due to isoform ALDH1A3 and its expression is predictive of metastasis. *Stem Cells* 2011; **29**: 32-45 [PMID: 21280157 DOI: 10.1002/stem.563]
- 87 **Kim SK**, Kim H, Lee DH, Kim TS, Kim T, Chung C, Koh GY, Kim H, Lim DS. Reversing the intractable nature of pancreatic cancer by selectively targeting ALDH-high, therapy-resistant cancer cells. *PLoS One* 2013; **8**: e78130 [PMID: 24194908 DOI: 10.1371/journal.pone.0078130]
- 88 **Hoshino Y**, Nishida J, Katsuno Y, Koinuma D, Aoki T, Kokudo N, Miyazono K, Ehata S. Smad4 Decreases the Population of Pancreatic Cancer-Initiating Cells through Transcriptional Repression of ALDH1A1. *Am J Pathol* 2015; **185**: 1457-1470 [PMID: 25769430 DOI: 10.1016/j.ajpath.2015.01.011]
- 89 **Luo Y**, Nguyen N, Fujita M. Isolation of human melanoma stem cells using ALDH as a marker. *Curr Protoc Stem Cell Biol* 2013; **26**: Unit 3.8. [PMID: 24510792 DOI: 10.1002/9780470151808.sc0308s26]
- 90 **Luo Y**, Dallaglio K, Chen Y, Robinson WA, Robinson SE, McCarter MD, Wang J, Gonzalez R, Thompson DC, Norris DA, Roop DR, Vasiliou V, Fujita M. ALDH1A isozymes are markers of human melanoma stem cells and potential therapeutic targets. *Stem Cells* 2012; **30**: 2100-2113 [PMID: 22887839 DOI: 10.1002/stem.1193]
- 91 **Kryczek I**, Liu S, Roh M, Vatan L, Szeliga W, Wei S, Banerjee M, Mao Y, Kotarski J, Wicha MS, Liu R, Zou W. Expression of aldehyde dehydrogenase and CD133 defines ovarian cancer stem cells. *Int J Cancer* 2012; **130**: 29-39 [PMID: 21480217 DOI: 10.1002/ijc.25967]
- 92 **Silva IA**, Bai S, McLean K, Yang K, Griffith K, Thomas D, Ginestier C, Johnston C, Kueck A, Reynolds RK, Wicha MS, Buckanovich RJ. Aldehyde dehydrogenase in combination with CD133 defines angiogenic ovarian cancer stem cells that portend poor patient survival. *Cancer Res* 2011; **71**: 3991-4001 [PMID: 21498635 DOI: 10.1158/0008-5472.CAN-10-3175]
- 93 **Mansour SF**, Atwa MM. Clinicopathological Significance of CD133 and ALDH1 Cancer Stem Cell Marker Expression in Invasive Ductal Breast Carcinoma. *Asian Pac J Cancer Prev* 2015; **16**: 7491-7496 [PMID: 26625750 DOI: 10.7314/APJCP.2015.16.17.7491]
- 94 **Roudi R**, Korourian A, Sharifabrizi A, Madjd Z. Differential Expression of Cancer Stem Cell Markers ALDH1 and CD133 in Various Lung Cancer Subtypes. *Cancer Invest* 2015; **33**: 294-302 [PMID: 26046383 DOI: 10.3109/07357907.2015.1034869]
- 95 **Qiu Y**, Pu T, Guo P, Wei B, Zhang Z, Zhang H, Zhong X, Zheng H, Chen L, Bu H, Ye F. ALDH(+)/CD44(+) cells in breast cancer are associated with worse prognosis and poor clinical outcome. *Exp*

- Mol Pathol* 2016; **100**: 145-150 [PMID: 26687806 DOI: 10.1016/j.yexmp.2015.11.032]
- 96 **Liu J**, Xiao Z, Wong SK, Tin VP, Ho KY, Wang J, Sham MH, Wong MP. Lung cancer tumorigenicity and drug resistance are maintained through ALDH(hi)CD44(hi) tumor initiating cells. *Oncotarget* 2013; **4**: 1698-1711 [PMID: 24091605 DOI: 10.18632/oncotarget.1246]
 - 97 **Januchowski R**, Wojtowicz K, Zabel M. The role of aldehyde dehydrogenase (ALDH) in cancer drug resistance. *Biomed Pharmacother* 2013; **67**: 669-680 [PMID: 23721823 DOI: 10.1016/j.biopha.2013.04.005]
 - 98 **Leonard GD**, Fojo T, Bates SE. The role of ABC transporters in clinical practice. *Oncologist* 2003; **8**: 411-424 [PMID: 14530494 DOI: 10.1634/theoncologist.8-5-411]
 - 99 **Abdullah LN**, Chow EK. Mechanisms of chemoresistance in cancer stem cells. *Clin Transl Med* 2013; **2**: 3 [PMID: 23369605 DOI: 10.1186/2001-1326-2-3]
 - 100 **Eyre R**, Harvey I, Stemke-Hale K, Lennard TW, Tyson-Capper A, Meeson AP. Reversing paclitaxel resistance in ovarian cancer cells via inhibition of the ABCB1 expressing side population. *Tumour Biol* 2014; **35**: 9879-9892 [PMID: 24993095 DOI: 10.1007/s13277-014-2277-2]
 - 101 **Zhao J**. Cancer stem cells and chemoresistance: The smartest survives the raid. *Pharmacol Ther* 2016; **160**: 145-158 [PMID: 26899500 DOI: 10.1016/j.pharmthera.2016.02.008]
 - 102 **Pearce DJ**, Taussig D, Simpson C, Allen K, Rohatiner AZ, Lister TA, Bonnet D. Characterization of cells with a high aldehyde dehydrogenase activity from cord blood and acute myeloid leukemia samples. *Stem Cells* 2005; **23**: 752-760 [PMID: 15917471 DOI: 10.1634/stemcells.2004-0292]
 - 103 **Tanei T**, Morimoto K, Shimazu K, Kim SJ, Tanji Y, Taguchi T, Tamaki Y, Noguchi S. Association of breast cancer stem cells identified by aldehyde dehydrogenase 1 expression with resistance to sequential Paclitaxel and epirubicin-based chemotherapy for breast cancers. *Clin Cancer Res* 2009; **15**: 4234-4241 [PMID: 19509181 DOI: 10.1158/1078-0432.CCR-08-1479]
 - 104 **Sreerama L**, Sladek NE. Cellular levels of class I and class 3 aldehyde dehydrogenases and certain other drug-metabolizing enzymes in human breast malignancies. *Clin Cancer Res* 1997; **3**: 1901-1914 [PMID: 9815579]
 - 105 **Vasiliou V**, Pappa A, Estey T. Role of human aldehyde dehydrogenases in endobiotic and xenobiotic metabolism. *Drug Metab Rev* 2004; **36**: 279-299 [PMID: 15237855 DOI: 10.1081/DMR-120034001]
 - 106 **Crocker AK**, Allan AL. Inhibition of aldehyde dehydrogenase (ALDH) activity reduces chemotherapy and radiation resistance of stem-like ALDH^{hi}CD44⁺ human breast cancer cells. *Breast Cancer Res Treat* 2012; **133**: 75-87 [PMID: 21818590 DOI: 10.1007/s10549-011-1692-y]
 - 107 **Chen E**, Zeng Z, Bai B, Zhu J, Song Z. The prognostic value of CSCs biomarker CD133 in NSCLC: a meta-analysis. *Oncotarget* 2016; **7**: 56526-56539 [PMID: 27489355 DOI: 10.18632/oncotarget.10964]
 - 108 **Chen T**, Yang K, Yu J, Meng W, Yuan D, Bi F, Liu F, Liu J, Dai B, Chen X, Wang F, Zeng F, Xu H, Hu J, Mo X. Identification and expansion of cancer stem cells in tumor tissues and peripheral blood derived from gastric adenocarcinoma patients. *Cell Res* 2012; **22**: 248-258 [PMID: 21727908 DOI: 10.1038/cr.2011.109]
 - 109 **Rocco A**, Liguori E, Pirozzi G, Tirino V, Compare D, Franco R, Tatangelo F, Palaia R, D'Armiento FP, Pollastrone G, Affuso A, Bottazzi EC, Masone S, Persico G, Nardone G. CD133 and CD44 cell surface markers do not identify cancer stem cells in primary human gastric tumors. *J Cell Physiol* 2012; **227**: 2686-2693 [PMID: 21898409 DOI: 10.1002/jcp.23013]
 - 110 **Singer CF**, Zabkova P, Rappaport C, Muhr D, Pfeiler G, Gschwantler-Kaulich D, Fink-Retter A, Staudigl C, Walter I, Hudelist G, Spiess AC, Kubista E. Presence of intratumoral stem cells in breast cancer patients with or without BRCA germline mutations. *Curr Cancer Drug Targets* 2012; **12**: 44-50 [PMID: 22111833 DOI: 10.2174/156800912798888938]
 - 111 **Hashimoto K**, Shimizu C, Tsuda H, Saji S, Osaki A, Shigekawa T, Aogi K. Immunohistochemical detection of breast cancer stem cells in hormone receptor-positive breast cancer and their role in response to endocrine therapy and clinical outcome. *Oncology* 2012; **82**: 168-174 [PMID: 22433454 DOI: 10.1159/000336078]
 - 112 **Singh BN**, Fu J, Srivastava RK, Shankar S. Hedgehog signaling antagonist GDC-0449 (Vismodegib) inhibits pancreatic cancer stem cell characteristics: molecular mechanisms. *PLoS One* 2011; **6**: e27306 [PMID: 22087285 DOI: 10.1371/journal.pone.0027306]
 - 113 **Kim EJ**, Sahai V, Abel EV, Griffith KA, Greenson JK, Takebe N, Khan GN, Blau JL, Craig R, Balis UG, Zalupski MM, Simeone DM. Pilot clinical trial of hedgehog pathway inhibitor GDC-0449 (vismodegib) in combination with gemcitabine in patients with metastatic pancreatic adenocarcinoma. *Clin Cancer Res* 2014; **20**: 5937-5945 [PMID: 25278454 DOI: 10.1158/1078-0432.CCR-14-1269]
 - 114 **Sadarangani A**, Pineda G, Lennon KM, Chun HJ, Shih A, Schairer AE, Court AC, Goff DJ, Prashad SL, Geron I, Wall R, McPherson JD, Moore RA, Pu M, Bao L, Jackson-Fisher A, Munchhof M, VanArsdale T, Reya T, Morris SR, Minden MD, Messer K, Mikkola HK, Marra MA, Hudson TJ, Jamieson CH. GLI2 inhibition abrogates human leukemia stem cell dormancy. *J Transl Med* 2015; **13**: 98 [PMID: 25889765 DOI: 10.1186/s12967-015-0453-9]
 - 115 **Yang N**, Zhou TC, Lei XX, Wang C, Yan M, Wang ZF, Liu W, Wang J, Ming KH, Wang BC, Xu BL, Liu Q. Inhibition of Sonic Hedgehog Signaling Pathway by Thiazole Antibiotic Thiostrepton Attenuates the CD44⁺/CD24⁻Stem-Like Population and Sphere-Forming Capacity in Triple-Negative Breast Cancer. *Cell Physiol Biochem* 2016; **38**: 1157-1170 [PMID: 26963129 DOI: 10.1159/000443066]
 - 116 **Takebe N**, Miele L, Harris PJ, Jeong W, Bando H, Kahn M, Yang SX, Ivy SP. Targeting Notch, Hedgehog, and Wnt pathways in cancer stem cells: clinical update. *Nat Rev Clin Oncol* 2015; **12**: 445-464 [PMID: 25850553 DOI: 10.1038/nrclinonc.2015.61]
 - 117 **Krop I**, Demuth T, Guthrie T, Wen PY, Mason WP, Chinnaiyan P, Butowski N, Groves MD, Kesari S, Freedman SJ, Blackman S, Watters J, Loboda A, Podtelezhnikov A, Lunceford J, Chen C, Giannotti M, Hing J, Beckman R, Lorusso P. Phase I pharmacologic and pharmacodynamic study of the gamma secretase (Notch) inhibitor MK-0752 in adult patients with advanced solid tumors. *J Clin Oncol* 2012; **30**: 2307-2313 [PMID: 22547604 DOI: 10.1200/JCO.2011.39.1540]
 - 118 **Messersmith WA**, Shapiro GI, Cleary JM, Jimeno A, Dasari A, Huang B, Shaik MN, Cesari R, Zheng X, Reynolds JM, English PA, McLachlan KR, Kern KA, LoRusso PM. A Phase I, dose-finding study in patients with advanced solid malignancies of the oral γ -secretase inhibitor PF-03084014. *Clin Cancer Res* 2015; **21**: 60-67 [PMID: 25231399 DOI: 10.1158/1078-0432.CCR-14-0607]
 - 119 **Deng Y**, Su Q, Mo J, Fu X, Zhang Y, Lin EH. Celecoxib downregulates CD133 expression through inhibition of the Wnt signaling pathway in colon cancer cells. *Cancer Invest* 2013; **31**: 97-102 [PMID: 23245395 DOI: 10.3109/07357907.2012.754458]
 - 120 **Egashira I**, Takahashi-Yanaga F, Nishida R, Arioka M, Igawa K, Tomooka K, Nakatsu Y, Tsuzuki T, Nakabeppu Y, Kitazono T, Sasaguri T. Celecoxib and 2,5-dimethylcelecoxib inhibit intestinal cancer growth by suppressing the Wnt/ β -catenin signaling pathway. *Cancer Sci* 2017; **108**: 108-115 [PMID: 27761963 DOI: 10.1111/cas.13106]
 - 121 **Tian D**, Shi Y, Chen D, Liu Q, Fan F. The Wnt inhibitor LGK-974 enhances radiosensitivity of HepG2 cells by modulating Nrf2 signaling. *Int J Oncol* 2017; **51**: 545-554 [PMID: 28627706 DOI: 10.3892/ijo.2017.4042]
 - 122 **Suwala AK**, Koch K, Rios DH, Aretz P, Uhlmann C, Ogorek I, Felsberg J, Reifemberger G, Köhrer K, Deenen R, Steiger HJ, Kahlert UD, Maciacyk J. Inhibition of Wnt/ β -catenin signaling downregulates expression of aldehyde dehydrogenase isoform 3A1 (ALDH3A1) to reduce resistance against temozolomide in glioblastoma in vitro. *Oncotarget* 2018; **9**: 22703-22716 [PMID: 29854309 DOI: 10.18632/oncotarget.25210]

- 123 **Li Y**, Zhang T. Targeting cancer stem cells by curcumin and clinical applications. *Cancer Lett* 2014; **346**: 197-205 [PMID: 24463298 DOI: 10.1016/j.canlet.2014.01.012]
- 124 **Zhu JY**, Yang X, Chen Y, Jiang Y, Wang SJ, Li Y, Wang XQ, Meng Y, Zhu MM, Ma X, Huang C, Wu R, Xie CF, Li XT, Geng SS, Wu JS, Zhong CY, Han HY. Curcumin Suppresses Lung Cancer Stem Cells via Inhibiting Wnt/ β -catenin and Sonic Hedgehog Pathways. *Phytother Res* 2017; **31**: 680-688 [PMID: 28198062 DOI: 10.1002/ptr.5791]
- 125 **Wang D**, Kong X, Li Y, Qian W, Ma J, Wang D, Yu D, Zhong C. Curcumin inhibits bladder cancer stem cells by suppressing Sonic Hedgehog pathway. *Biochem Biophys Res Commun* 2017; **493**: 521-527 [PMID: 28870814 DOI: 10.1016/j.bbrc.2017.08.158]
- 126 **James MI**, Iwuji C, Irving G, Karmokar A, Higgins JA, Griffin-Teal N, Thomas A, Greaves P, Cai H, Patel SR, Morgan B, Dennison A, Metcalfe M, Garcea G, Lloyd DM, Berry DP, Steward WP, Howells LM, Brown K. Curcumin inhibits cancer stem cell phenotypes in ex vivo models of colorectal liver metastases, and is clinically safe and tolerable in combination with FOLFOX chemotherapy. *Cancer Lett* 2015; **364**: 135-141 [PMID: 25979230 DOI: 10.1016/j.canlet.2015.05.005]
- 127 **Hu C**, Niestroj M, Yuan D, Chang S, Chen J. Treating cancer stem cells and cancer metastasis using glucose-coated gold nanoparticles. *Int J Nanomedicine* 2015; **10**: 2065-2077 [PMID: 25844037 DOI: 10.2147/IJN.S72144]
- 128 **Verma RK**, Yu W, Shrivastava A, Shankar S, Srivastava RK. α -Mangostin-encapsulated PLGA nanoparticles inhibit pancreatic carcinogenesis by targeting cancer stem cells in human, and transgenic (Kras(G12D), and Kras(G12D)/tp53R270H) mice. *Sci Rep* 2016; **6**: 32743 [PMID: 27624879 DOI: 10.1038/srep32743]
- 129 **Muntmadugu E**, Kumar R, Saladi S, Rafeeqi TA, Khan W. CD44 targeted chemotherapy for co-eradication of breast cancer stem cells and cancer cells using polymeric nanoparticles of salinomycin and paclitaxel. *Colloids Surf B Biointerfaces* 2016; **143**: 532-546 [PMID: 27045981 DOI: 10.1016/j.colsurfb.2016.03.075]
- 130 **Lamb R**, Ozsvári B, Lisanti CL, Tanowitz HB, Howell A, Martinez-Outschoorn UE, Sotgia F, Lisanti MP. Antibiotics that target mitochondria effectively eradicate cancer stem cells, across multiple tumor types: treating cancer like an infectious disease. *Oncotarget* 2015; **6**: 4569-4584 [PMID: 25625193 DOI: 10.18632/oncotarget.3174]
- 131 **Lamb R**, Fiorillo M, Chadwick A, Ozsvári B, Reeves KJ, Smith DL, Clarke RB, Howell SJ, Cappello AR, Martinez-Outschoorn UE, Peiris-Pagès M, Sotgia F, Lisanti MP. Doxycycline down-regulates DNA-PK and radiosensitizes tumor initiating cells: Implications for more effective radiation therapy. *Oncotarget* 2015; **6**: 14005-14025 [PMID: 26087309 DOI: 10.18632/oncotarget.4159]
- 132 **Hirsch HA**, Iliopoulos D, Tsiachlis PN, Struhl K. Metformin selectively targets cancer stem cells, and acts together with chemotherapy to block tumor growth and prolong remission. *Cancer Res* 2009; **69**: 7507-7511 [PMID: 19752085 DOI: 10.1158/0008-5472.CAN-09-2994]
- 133 **Rattan R**, Ali Fehmi R, Munkarah A. Metformin: an emerging new therapeutic option for targeting cancer stem cells and metastasis. *J Oncol* 2012; **2012**: 928127 [PMID: 22701483 DOI: 10.1155/2012/928127]
- 134 **Zhang R**, Zhang P, Wang H, Hou D, Li W, Xiao G, Li C. Inhibitory effects of metformin at low concentration on epithelial-mesenchymal transition of CD44(+)CD117(+) ovarian cancer stem cells. *Stem Cell Res Ther* 2015; **6**: 262 [PMID: 26718286 DOI: 10.1186/s13287-015-0249-0]
- 135 **Honjo S**, Ajani JA, Scott AW, Chen Q, Skinner HD, Stroehlein J, Johnson RL, Song S. Metformin sensitizes chemotherapy by targeting cancer stem cells and the mTOR pathway in esophageal cancer. *Int J Oncol* 2014; **45**: 567-574 [PMID: 24859412 DOI: 10.3892/ijo.2014.2450]
- 136 **Fasih A**, Elbaz HA, Hüttemann M, Konski AA, Zielske SP. Radio-sensitization of pancreatic cancer cells by metformin through the AMPK pathway. *Radiat Res* 2014; **182**: 50-59 [PMID: 24909911 DOI: 10.1667/RR13568.1]
- 137 **Chiorean EG**, LoRusso P, Strother RM, Diamond JR, Younger A, Messersmith WA, Adriaens L, Liu L, Kao RJ, DiCioccio AT, Kostic A, Leek R, Harris A, Jimeno A. A Phase I First-in-Human Study of Enoticumab (REGN421), a Fully Human Delta-like Ligand 4 (Dl4) Monoclonal Antibody in Patients with Advanced Solid Tumors. *Clin Cancer Res* 2015; **21**: 2695-2703 [PMID: 25724527 DOI: 10.1158/1078-0432.CCR-14-2797]
- 138 **Smith DC**, Eisenberg PD, Manikhas G, Chugh R, Gubens MA, Stagg RJ, Kapoun AM, Xu L, Dupont J, Sikic B. A phase I dose escalation and expansion study of the anticancer stem cell agent demcizumab (anti-DLL4) in patients with previously treated solid tumors. *Clin Cancer Res* 2014; **20**: 6295-6303 [PMID: 25324140 DOI: 10.1158/1078-0432.CCR-14-1373]
- 139 **Prieur A**, Cappellini M, Habif G, Lefranc MP, Mazard T, Morency E, Pascussi JM, Flacelière M, Cahuzac N, Vire B, Dubuc B, Durochat A, Liaud P, Ollier J, Pfeiffer C, Poupeau S, Saywell V, Planque C, Assenat E, Bibeau F, Bourgaux JF, Pujol P, Sézeur A, Ychou M, Joubert D. Targeting the Wnt Pathway and Cancer Stem Cells with Anti-progastrin Humanized Antibodies as a Potential Treatment for K-RAS-Mutated Colorectal Cancer. *Clin Cancer Res* 2017; **23**: 5267-5280 [PMID: 28600477 DOI: 10.1158/1078-0432.CCR-17-0533]
- 140 **Jin L**, Hope KJ, Zhai Q, Smadja-Joffe F, Dick JE. Targeting of CD44 eradicates human acute myeloid leukemic stem cells. *Nat Med* 2006; **12**: 1167-1174 [PMID: 16998484 DOI: 10.1038/nm1483]
- 141 **Li L**, Hao X, Qin J, Tang W, He F, Smith A, Zhang M, Simeone DM, Qiao XT, Chen ZN, Lawrence TS, Xu L. Antibody against CD44s inhibits pancreatic tumor initiation and postradiation recurrence in mice. *Gastroenterology* 2014; **146**: 1108-1118 [PMID: 24397969 DOI: 10.1053/j.gastro.2013.12.035]
- 142 **Naujokat C**. Monoclonal antibodies against human cancer stem cells. *Immunotherapy* 2014; **6**: 290-308 [PMID: 24762074 DOI: 10.2217/imt.14.4]
- 143 **Pérez-Alea M**, McGrail K, Sánchez-Redondo S, Ferrer B, Fournet G, Cortés J, Muñoz E, Hernandez-Losa J, Tenbaum S, Martin G, Costello R, Ceylan I, Garcia-Patos V, Recio JA. ALDH1A3 is epigenetically regulated during melanocyte transformation and is a target for melanoma treatment. *Oncogene* 2017; **36**: 5695-5708 [PMID: 28581514 DOI: 10.1038/onc.2017.160]
- 144 **Gudas LJ**, Wagner JA. Retinoids regulate stem cell differentiation. *J Cell Physiol* 2011; **226**: 322-330 [PMID: 20836077 DOI: 10.1002/jcp.22417]
- 145 **Petrie K**, Zelent A, Waxman S. Differentiation therapy of acute myeloid leukemia: past, present and future. *Curr Opin Hematol* 2009; **16**: 84-91 [PMID: 19468269 DOI: 10.1097/MOH.0b013e3283257aee]
- 146 **Ginestier C**, Wicinski J, Cervera N, Monville F, Finetti P, Bertucci F, Wicha MS, Birnbaum D, Charafe-Jauffret E. Retinoid signaling regulates breast cancer stem cell differentiation. *Cell Cycle* 2009; **8**: 3297-3302 [PMID: 19806016 DOI: 10.4161/cc.8.20.9761]
- 147 **Yan Y**, Li Z, Xu X, Chen C, Wei W, Fan M, Chen X, Li JJ, Wang Y, Huang J. All-trans retinoic acids induce differentiation and sensitize a radioresistant breast cancer cells to chemotherapy. *BMC Complement Altern Med* 2016; **16**: 113 [PMID: 27036550 DOI: 10.1186/s12906-016-1088-y]
- 148 **Nguyen PH**, Giraud J, Staedel C, Chambonnier L, Dubus P, Chevret E, Bœuf H, Gauthereau X, Rousseau B, Fevre M, Soubeyran I, Belleannée G, Evrard S, Collet D, Mégraud F, Varon C. All-trans retinoic acid targets gastric cancer stem cells and inhibits patient-derived gastric carcinoma tumor growth. *Oncogene* 2016; **35**: 5619-5628 [PMID: 27157616 DOI: 10.1038/onc.2016.87]
- 149 **Lim YC**, Kang HJ, Kim YS, Choi EC. All-trans-retinoic acid inhibits growth of head and neck cancer stem cells by suppression of Wnt/ β -catenin pathway. *Eur J Cancer* 2012; **48**: 3310-3318 [PMID: 22640830 DOI: 10.1016/j.ejca.2012.04.013]
- 150 **Budd GT**, Adamson PC, Gupta M, Homayoun P, Sandstrom SK, Murphy RF, McLain D, Tuason L, Peereboom D, Bukowski RM, Ganapathi R. Phase I/II trial of all-trans retinoic acid and tamoxifen

- in patients with advanced breast cancer. *Clin Cancer Res* 1998; **4**: 635-642 [PMID: 9533531]
- 151 **Liu P**, Kumar IS, Brown S, Kannappan V, Tawari PE, Tang JZ, Jiang W, Armesilla AL, Darling JL, Wang W. Disulfiram targets cancer stem-like cells and reverses resistance and cross-resistance in acquired paclitaxel-resistant triple-negative breast cancer cells. *Br J Cancer* 2013; **109**: 1876-1885 [PMID: 24008666 DOI: 10.1038/bjc.2013.534]
 - 152 **Duan L**, Shen H, Zhao G, Yang R, Cai X, Zhang L, Jin C, Huang Y. Inhibitory effect of Disulfiram/copper complex on non-small cell lung cancer cells. *Biochem Biophys Res Commun* 2014; **446**: 1010-1016 [PMID: 24657266 DOI: 10.1016/j.bbrc.2014.03.047]
 - 153 **Ortiz RC**, Lopes NM, Amôr NG, Ponce JB, Schmerling CK, Lara VS, Moyses RA, Rodini CO. CD44 and ALDH1 immunore-expression as prognostic indicators of invasion and metastasis in oral squamous cell carcinoma. *J Oral Pathol Med* 2018; **47**: 740-747 [PMID: 29791975 DOI: 10.1111/jop.12734]
 - 154 **Hu J**, Li G, Zhang P, Zhuang X, Hu G. A CD44v+ subpopulation of breast cancer stem-like cells with enhanced lung metastasis capacity. *Cell Death Dis* 2017; **8**: e2679 [PMID: 28300837 DOI: 10.1038/cddis.2017.72]
 - 155 **Kanwal R**, Shukla S, Walker E, Gupta S. Acquisition of tumorigenic potential and therapeutic resistance in CD133+ subpopulation of prostate cancer cells exhibiting stem-cell like characteristics. *Cancer Lett* 2018; **430**: 25-33 [PMID: 29775627 DOI: 10.1016/j.canlet.2018.05.014]
 - 156 **Bigoni-Ordóñez GD**, Ortiz-Sánchez E, Rosendo-Chalma P, Valencia-González HA, Aceves C, García-Carrancá A. Molecular iodine inhibits the expression of stemness markers on cancer stem-like cells of established cell lines derived from cervical cancer. *BMC Cancer* 2018; **18**: 928 [PMID: 30257666 DOI: 10.1186/s12885-018-4824-5]
 - 157 **Zhang Y**, Xu W, Guo H, Zhang Y, He Y, Lee SH, Song X, Li X, Guo Y, Zhao Y, Ding C, Ning F, Ma Y, Lei QY, Hu X, Li S, Guo W. NOTCH1 Signaling Regulates Self-Renewal and Platinum Chemoresistance of Cancer Stem-like Cells in Human Non-Small Cell Lung Cancer. *Cancer Res* 2017; **77**: 3082-3091 [PMID: 28416482 DOI: 10.1158/0008-5472.CAN-16-1633]
 - 158 **Durinkova E**, Kozovska Z, Poturnajova M, Plava J, Cierna Z, Babelova A, Bohovic R, Schmidtova S, Tomas M, Kucerova L, Matuskova M. ALDH1A3 upregulation and spontaneous metastasis formation is associated with acquired chemoresistance in colorectal cancer cells. *BMC Cancer* 2018; **18**: 848 [PMID: 30143021 DOI: 10.1186/s12885-018-4758-y]
 - 159 **Kozovska Z**, Patsalias A, Bajzik V, Durinkova E, Demkova L, Jargasova S, Smolkova B, Plava J, Kucerova L, Matuskova M. ALDH1A inhibition sensitizes colon cancer cells to chemotherapy. *BMC Cancer* 2018; **18**: 656 [PMID: 29902974 DOI: 10.1186/s12885-018-4572-6]
 - 160 **Pal D**, Kolluru V, Chandrasekaran B, Baby BV, Aman M, Suman S, Sirimulla S, Sanders MA, Alatassi H, Ankem MK, Damodaran C. Targeting aberrant expression of Notch-1 in ALDH+ cancer stem cells in breast cancer. *Mol Carcinog* 2017; **56**: 1127-1136 [PMID: 27753148 DOI: 10.1002/mc.22579]

P- Reviewer: Haider KH, He XH, Scuteri A, Zheng YW
S- Editor: Dou Y **L- Editor:** Filipodia **E- Editor:** Song H



Basic Study

Functional and molecular mechanism of intracellular pH regulation in human inducible pluripotent stem cells

Shih-Chi Chao, Gwo-Jang Wu, Shu-Fu Huang, Niann-Tzyy Dai, Hsu-Kai Huang, Mei-Fang Chou, Yi-Ting Tsai, Shiao-Pieng Lee, Shih-Hung Loh

Shih-Chi Chao, Shih-Hung Loh, Graduate Institute of Life Sciences, National Defense Medical Center, Taipei 11490, Taiwan

Gwo-Jang Wu, Department of Obstetrics and Gynecology, Tri-Service General Hospital, National Defense Medical Center, Taipei 11490, Taiwan

Shu-Fu Huang, Mei-Fang Chou, Shih-Hung Loh, Department of Pharmacy Practice, Tri-Service General Hospital, National Defense Medical Center, Taipei 11490, Taiwan

Niann-Tzyy Dai, Division of Plastic and Reconstructive Surgery, Department of Surgery, Tri-Service General Hospital, National Defense Medical Center, Taipei 11490, Taiwan

Hsu-Kai Huang, Division of Chest Surgery, Department of Surgery, Tri-Service General Hospital, National Defense Medical Center, Taipei 11490, Taiwan

Yi-Ting Tsai, Graduate Institute of Medical Sciences, National Defense Medical Center, Taipei 11490, Taiwan

Yi-Ting Tsai, Division of Cardiovascular Surgery, Department of Surgery, Tri-Service General Hospital, National Defense Medical Center, Taipei 11490, Taiwan

Shiao-Pieng Lee, Division of Oral and Maxillofacial Surgery, Department of Dentistry, School of Dentistry, Tri-Service General Hospital and National Defense Medical Center, Taipei 11490, Taiwan

Shih-Hung Loh, Department of Pharmacology, National Defense Medical Center, Taipei 11490, Taiwan

ORCID number: Shih-Chi Chao (0000-0002-0920-9340); Gwo-Jang Wu (0000-0001-5360-8018); Shu-Fu Huang (0000-0002-4593-1779); Niann-Tzyy Dai (0000-0003-2066-574X); Hsu-Kai Huang (0000-0002-4358-4822); Mei-Fang Chou (0000-0001-515-593X); Yi-Ting Tsai (0000-0001-9439-9734); Shiao-Pieng Lee (0000-0002-7345-2062); Shih-Hung Loh (0000-0001-9269-5580).

Author contributions: Chao SC and Loh SH performed the majority of experiments and analyzed the data; Chao SC, Wu GJ, Dai NT and Loh SH performed conception and design; Wu GJ, Dai NT and Loh SH participated equally in iPSC treatment and providing; Chao SC, Wu GJ, Huang SF, Dai NT, Huang SK, Tsai YT, Lee SP and Loh SH coordinated and interpreted the research; Chao SC and Loh SH wrote the paper; Chao SC, Wu GJ, Huang SF and Loh SH drafted the article or making critical revisions related to important intellectual content of the manuscript; Loh SH final approval of the version of the article to be published.

Supported by Ministry of Science and Technology Grants of Taiwan, No. MOST 106-2320-B-016-003-MY2 (to Loh SH) and No. MOST 106-2314-B-016-037-MY3 (to Tsai YT); National Defense Medical Center Grants of Taiwan, No. MAB-106-033 (to Loh SH), No. MAB-105-043 and No. MAB-106-034 (to Dai NZ); Teh-Tzer Study Group for Human Medical Research Foundation of Taiwan, No. A1061037 and No. A1061054 (to Loh SH).

Institutional review board statement: The manuscript is approved by Institutional Review Board of Tri-Service General Hospital.

Conflict-of-interest statement: All authors declare no potential conflict of interest.

Open-Access: This article is an open-access article which was selected by an in-house editor and fully peer-reviewed by external reviewers. It is distributed in accordance with the Creative Commons Attribution Non Commercial (CC BY-NC 4.0) license, which permits others to distribute, remix, adapt, build upon this work non-commercially, and license their derivative works on different terms, provided the original work is properly cited and the use is non-commercial. See: <http://creativecommons.org/licenses/by-nc/4.0/>

Manuscript source: Invited manuscript

Corresponding author to: Shih-Hung Loh, DPhil, Director, Full Professor, Department of Pharmacology, and Department of Pharmacy Practice, Tri-Service General Hospital, National

Defense Medical Center, No. 161, Sec. 6, Minquan E. Rd., Taipei 11490, Taiwan. shloh@ndmctsgh.edu.tw
Telephone: +886-2-87924861
Fax: +886-2-87924861

Received: October 17, 2018
Peer-review started: October 17, 2018
First decision: October 26, 2018
Revised: November 14, 2018
Accepted: December 4, 2018
Article in press: December 5, 2018
Published online: December 26, 2018

Abstract

AIM

To establish a functional and molecular model of the intracellular pH (pH_i) regulatory mechanism in human induced pluripotent stem cells (hiPSCs).

METHODS

hiPSCs (HPS0077) were kindly provided by Dr. Dai from the Tri-Service General Hospital (IRB No. B-106-09). Changes in the pH_i were detected either by microspectrofluorimetry or by a multimode reader with a pH-sensitive fluorescent probe, BCECF, and the fluorescent ratio was calibrated by the high K⁺/nigericin method. NH₄Cl and Na-acetate prepulse techniques were used to induce rapid intracellular acidosis and alkalization, respectively. The buffering power (β) was calculated from the ΔpH_i induced by perfusing different concentrations of (NH₄)₂SO₄. Western blot techniques and immunocytochemistry staining were used to detect the protein expression of pH_i regulators and pluripotency markers.

RESULTS

In this study, our results indicated that (1) the steady-state pH_i value was found to be 7.5 ± 0.01 ($n = 20$) and 7.68 ± 0.01 ($n = 20$) in HEPES and 5% CO₂/HCO₃⁻-buffered systems, respectively, which were much greater than that in normal adult cells (7.2); (2) in a CO₂/HCO₃⁻-buffered system, the values of total intracellular buffering power (β) can be described by the following equation: $\beta_{\text{tot}} = 107.79 (\text{pH}_i)^2 - 1522.2 (\text{pH}_i) + 5396.9$ (correlation coefficient $R^2 = 0.85$), in the estimated pH_i range of 7.1-8.0; (3) the Na⁺/H⁺ exchanger (NHE) and the Na⁺/HCO₃⁻ cotransporter (NBC) were found to be functionally activated for acid extrusion for pH_i values less than 7.5 and 7.68, respectively; (4) V-ATPase and some other unknown Na⁺-independent acid extruder(s) could only be functionally detected for pH_i values less than 7.1; (5) the Cl⁻/OH⁻ exchanger (CHE) and the Cl⁻/HCO₃⁻ anion exchanger (AE) were found to be responsible for the weakening of intracellular proton loading; (6) besides the CHE and the AE, a Cl⁻-independent acid loading mechanism was functionally identified; and (7) in hiPSCs, a strong positive correlation was observed between the loss of pluripotency and the weakening

of the intracellular acid extrusion mechanism, which included a decrease in the steady-state pH_i value and diminished the functional activity and protein expression of the NHE and the NBC.

CONCLUSION

For the first time, we established a functional and molecular model of a pH_i regulatory mechanism and demonstrated its strong positive correlation with hiPSC pluripotency.

Key words: Microspectrofluorimetry; Human induced pluripotent stem cells; Na⁺/H⁺ exchanger; Na⁺/HCO₃⁻ cotransporter; Cl⁻/OH⁻ exchanger; Cl⁻/HCO₃⁻ exchanger; V-ATPase; Intracellular buffering power; Intracellular pH; BCECF

© **The Author(s) 2018.** Published by Baishideng Publishing Group Inc. All rights reserved.

Core tip: For the first time, we established a model of the intracellular pH (pH_i) regulation mechanism in human induced pluripotent stem cells (hiPSCs). The steady-state pH_i value of hiPSCs was 7.50-7.68, which greater than that of normal adult cells. The Na⁺-H⁺ exchanger, the Na⁺-HCO₃⁻ cotransporter and vacuolar-ATPase were the main acid extruders, while the Cl⁻-HCO₃⁻ anion exchanger and the Cl⁻-OH⁻ exchanger were the main acid loaders. Moreover, the pH_i and acid-extruding mechanism were decreased during the loss of pluripotency in hiPSCs. pH_i regulators represent an attractive target for differentiation efficiency or culture quality.

Chao SC, Wu GJ, Huang SF, Dai NT, Huang HK, Chou MF, Tsai YT, Lee SP, Loh SH. Functional and molecular mechanism of intracellular pH regulation in human inducible pluripotent stem cells. *World J Stem Cells* 2018; 10(12): 196-211
URL: <https://www.wjgnet.com/1948-0210/full/v10/i12/196.htm>
DOI: <https://dx.doi.org/10.4252/wjsc.v10.i12.196>

INTRODUCTION

The homeostasis of intracellular pH (pH_i) affects many cellular functions, including cell proliferation, apoptosis, differentiation and epigenetic characteristics^[1-7]. The pH_i in mammalian cells is maintained within an optimal narrow range through the combined operation of transmembrane transporters and the intracellular buffering capacity. Thus far, pH_i control in mammalian cells has been divided into the following categories: (1) intracellular buffering; (2) acid extrusion systems; (3) acid loading systems; and (4) monocarboxylate-H⁺ transport^[7-11]. Intracellular buffering power (β) minimizes immediate changes in pH_i, either in an acidic or alkaline direction. The total intracellular buffering power (β_{tot}) has two components as follows: the intrinsic buffering power

of the cell (pH_i) caused by physicochemical buffers, such as weak acid/base moieties of cytoplasmic proteins, and the buffering capacity caused by intracellular CO_2/HCO_3^- (β_{CO_2})^[10]. Furthermore, different ion transporters are involved in the active pH_i regulatory mechanism. Acid-equivalent extruders, the Na^+-H^+ exchanger (NHE), the $Na^+-HCO_3^-$ cotransporter (NBC) and vacuolar-ATPase (V-ATPase) are the main active acid extruders that are activated against intracellular acidification^[7-9,12,13]. In contrast, the acid-equivalent loaders, such as the $Cl^-HCO_3^-$ anion exchanger (AE) and the Cl^-OH^- exchanger (CHE), are activated to prevent intracellular alkalization^[12,14,15]. In addition to acid extruders and acid loaders, there is also an H^+ -monocarboxylate transporter (MCT), which is very important for all mammalian cells because the metabolism and transport of lactate is essential for metabolism and function under physiological or pathological conditions, such as in tumors or hypoxic conditions. The MCT has been demonstrated to play a role either as an acid extruder or an acid loader, depending on the concentration gradient of monocarboxylates, such as lactate acid and pyruvate, between the intracellular and extracellular environments^[16,17]. The MCT carrier is stereoselective for L-lactate over D-lactate and has a stoichiometry of 1 H^+ with 1 lactate⁻ anion^[18,19].

Recently, the dysregulation of pH_i has been found to be a commonly adaptive feature in different types of cancer cells^[20]. In normally differentiated adult cells, the pH_i and extracellular pH (pH_e) are generally approximately 7.2 and 7.4, respectively^[8,9,13,21]. However, a reversed pH gradient of $pH_i \geq 7.2$ and $pH_e \leq 7.1$ has been demonstrated in cancer cells. This reversed pH gradient is caused by the overexpression and increased set-point of the acid extrusion mechanism^[12,20-23]. This dysregulated pH_i feature further promotes tumor progression, invasion and metastasis^[21,24-26]. Indeed, metabolic changes have been reported to be a substantial hallmark of cancer cells^[27]. Both in the absence or presence of oxygen, cancer cells tend to shift their metabolism from aerobic phosphorylation to aerobic glycolysis, which is known as the Warburg effect. However, the glycolytic by-products lactate and H^+ increase during aerobic glycolysis. Therefore, intracellular acid extruders, such as NHE and MCT, are activated to maintain pH_i homeostasis. The overactivation and/or overexpression of the acid extrusion mechanism results in an increased pH_i that further promotes proliferation and prevents apoptosis in cancer cells^[24,26,28,29]. Furthermore, accompanying extracellular acidification causes restructuring of the extracellular matrix and further promotes malicious metastasis and invasion^[26,30,31].

Human induced pluripotent stem cells (hiPSCs), which are reprogrammed from somatic cells by expressing pluripotent transcription factors, are defined by their ability for self-renewal and differentiation into the three germ layers^[32]. Pluripotent stem cells (PSCs) shared many similar properties with cancer cells, such as increased glycolysis, proliferation and adaptation

to hypoxia^[33-35]. Therefore, it has been proposed that the pH_i regulatory mechanism in hiPSCs is not typical compared to that in most adult cells. Indeed, a few studies have indicated that changes in pH_i affect the fate of stem cell differentiation. Decreased pH_i , either by a deficiency or the inhibition of NHE1, has been found to disturb retinoic acid-induced neuronal differentiation in mouse embryonal carcinoma cells. A similar phenomenon has been claimed to contribute to osteogenesis in human umbilical cord-derived mesenchymal stem cells^[1,36]. Furthermore, overexpressed NHE1 has been shown to increase cardiomyocyte differentiation in mouse embryonic stem cells (mESCs)^[6]. A recent study has reported that a decreased pH_i by knocking out or inhibiting NHE obstructed drosophila follicle stem cell differentiation and delayed the loss of pluripotency during spontaneous differentiation induced by the removal of LIF/2i^[6]. Therefore, an elevated pH_i is considered necessary for PSCs to differentiate. Furthermore, another study has shown that acidic culture medium, caused by the accumulation of lactic acid from glycolysis, promotes pluripotency in both mESCs and hESCs through several mechanisms. However, studies that have optimized the culture environment showed that although acidic culture medium ($pH < 7.0$) promotes the retention of OCT-4 and pluripotency, it also causes significant growth arrest and an apoptotic effect in mESCs^[37]. Notably, although decreasing pH_i has been shown to retain pluripotency during differentiation, the resting pH_i level in the pluripotent state is maintained at pH_i about 7.4 and is greater than that in differentiated adult cells^[6]. Therefore, these recent results implicate that PSCs might share a cancer-like pH_i regulatory mechanism and consequently create a reversed pH gradient to promote pluripotent properties. However, there is a lack of reports on the correlation between the pH_i regulatory mechanism and pluripotency in hiPSCs.

Because of the importance of pH_i regulation in hiPSCs, the aims of this study are to further investigate the underlying mechanisms of pH_i regulation in hiPSCs. To determine transporter-mediated membrane fluxes of acid equivalents from measurements of pH_i , an accurate knowledge of intracellular buffering power is essential. Therefore, the first aim of this study is to estimate β_i and β_{CO_2} , and the second aim is to characterize the active pH_i regulators in hiPSCs to provide the molecular and functional targets of pH_i regulators for future applications in clinics. Finally, the correlation between the pH_i regulatory mechanism and hiPSC pluripotency was examined in this study.

MATERIALS AND METHODS

Cell culture

The hiPSCs (HPS0077) were a kind gift from Dr. N.Z. Dai (TSGH-IRB No: 100-05-251) from the Tri-Service General Hospital, Taipei, Taiwan. In this study, vitronectin was used to support the growth and adhesion of HPS0077 cells. To prepare the vitronectin-coated culture

plate, 100 μ L vitronectin (500 μ g/mL) was directly added and mixed into cold DPBS. The vitronectin-DPBS solution was then added into the culture plate at a final concentration of 0.5 μ g/cm² and incubated at room temperature for at least 2 h. This vitronectin-coated culture plate could be used immediately or stored at 4 °C for later use within 2 wk. To maintain pluripotency, HPS0077 cells were continuously cultured with mTeSR1 or mTeSR-E8 medium. When the cell colonies were grown to a sufficient size, Accutase was added to the cells at 37 °C for 3 min to suspend the cells. The cell suspension was centrifuged at 1000 rpm for 3 min, and the collected cell pellet was resuspended in fresh medium. The vitronectin solution was aspirated, and the cells were seeded in a suitable ratio with mTeSR1 or mTeSR-E8 medium containing 10 μ mol/L Y-27632. The Y-27632-containing culture medium was replaced with Y-27632-free medium after 24 h, and the medium was subsequently changed every day. To induce the loss of pluripotency, the mTeSR1 or mTeSR-E8 medium was replaced by mTeSR-E6 medium for 1 to 4 d, and the medium was changed once every two days.

Immunocytochemistry staining and immunoblotting

For immunocytochemistry staining, a pluripotent stem cell 4-marker immunocytochemistry kit (Invitrogen), including primary antibodies against OCT4, SSEA4, SOX2 and TRA-1-60, was used to evaluate the pluripotency. Briefly, the experimental procedure was performed according to the manufacturer's instructions. For immunoblotting, whole cell lysates were prepared using RIPA lysis buffer containing 1% protease, 1% phosphatase, and 0.1% Triton X. The supernatant was collected after centrifugation at 12000 rpm for 30 min at 4 °C. A total of 40 μ g of total protein per sample was subjected to 10% SDS-PAGE and transferred to a PVDF membrane and subsequently blocked for 1 h with 5% bovine serum albumin in Tris-buffered saline containing 0.1% Tween 20 (TBST). The membranes were then incubated overnight with primary antibodies of different pH_i regulators and an internal control at 4 °C. Then, the membranes were washed three times in TBST to remove the unbound primary antibodies and the secondary antibody was then added and incubated for 60 min at room temperature. The membranes were washed three times in TBST, and chemiluminescence was detected using a Clarity™ Western ECL substrate.

Measurement of intracellular pH

The measurement of the pH_i has been described in detail in our previous reports^[12]. Briefly, to measure the change in pH_i, HPS0077 hiPSCs were analyzed by microspectrofluorimetry with a pH-sensitive fluorescent dye, BCECF-AM. When cell colonies (on a 24 mm round coverslip) were grown to a sufficient size, cells were then incubated with BCECF-AM (diluted to 6.25 μ g/mL with standard HEPES solution) for 1 h at room temperature. Then, the coverslip containing the cells

was moved to an inverted fluorescence microscope and excited with light at wavelengths of 490 and 440 nm. The change in the BCECF emission ratio of the 530 nm wavelength emission at a 490 and 440 nm excitation (490/440) was detected and indicated the change in pH_i. A high potassium/nigericin calibration method was used to convert the emission ratio to the pH_i value.

When the pH_i was measured using a Synergy 2 Multi-Mode Reader, the cells were seeded on 24-well culture plates. The solution was replaced with a pipette instead of a perfusion system (including a peristaltic pump and suction). The experimental procedure is similar to microspectrofluorimetry, and the details are described in our previous study^[23].

Weak acid/base prepulse technique

NH₄Cl and Na-acetate prepulse techniques were used to induce intracellular acidification and alkalization, respectively, and the subsequent recovery from induced acidification and alkalization represent the activity of the acid extruder(s) and acid loader(s), respectively^[12]. Taking NH₄Cl prepulse as an example, it can be described by 4 phases, as shown in Figure 1A. Cells were first perfused with 20 mmol/L NH₄Cl for 5 min, which caused an initial rapid alkalization. This mechanism is simply caused by the small molecular weight and nonpolar [NH₃]_e easily crossing the cell membrane and acquiring hydrogen in the cytosol to produce NH₄⁺ (phase 1: rapid alkalization, NH₃ + H⁺ → NH₄⁺). Then, the pH_i slowly recovered and stabilized through the activation of acid loaders, such as AE and CHE (phase 2: slow recovery). The removal of NH₄Cl caused rapid intracellular acidification because [NH₃]_i rapidly effluxed and further produced hydrogen from [NH₄⁺]_i in the cytosol (phase 3: rapid acidification, NH₄⁺ → NH₃ + H⁺). The subsequent pH_i recovery following NH₄Cl-induced intracellular acidification is due to the activation of acid extruders, such as NHE and NBC, and this recovery slope represents the function of acid extruders (phase 4: pH_i recovery). To accurately quantify the H⁺ flux through pH_i regulators, all pH_i recovery rate data was converted to the J_H (pH_i recovery rate multiplied by buffering power)^[10].

Measurement of intracellular buffering power to derive the net influx or the net efflux

After the loading of BCECF-AM, cells were sequentially perfused with Na⁺/Cl⁻-free HEPES or 5% CO₂/HCO₃⁻-buffered solution (the details of the composition of the solutions are listed in the *Solution* section below) containing different concentrations of (NH₄)₂SO₄ (40, 20, 10, 5, 2.5 and 0 mmol/L). Perfusion with (NH₄)₂SO₄ induced an initial intracellular alkalization, and the subsequent removal of (NH₄)₂SO₄ or decrease in (NH₄)₂SO₄ concentration caused acidification. The buffering power is defined as the ability to resist the change in pH_i induced by the impact of hydrogen, *i.e.*, (NH₄)₂SO₄. Therefore, if the buffering power is stronger, the change in pH_i will be smaller. The buffering power can be

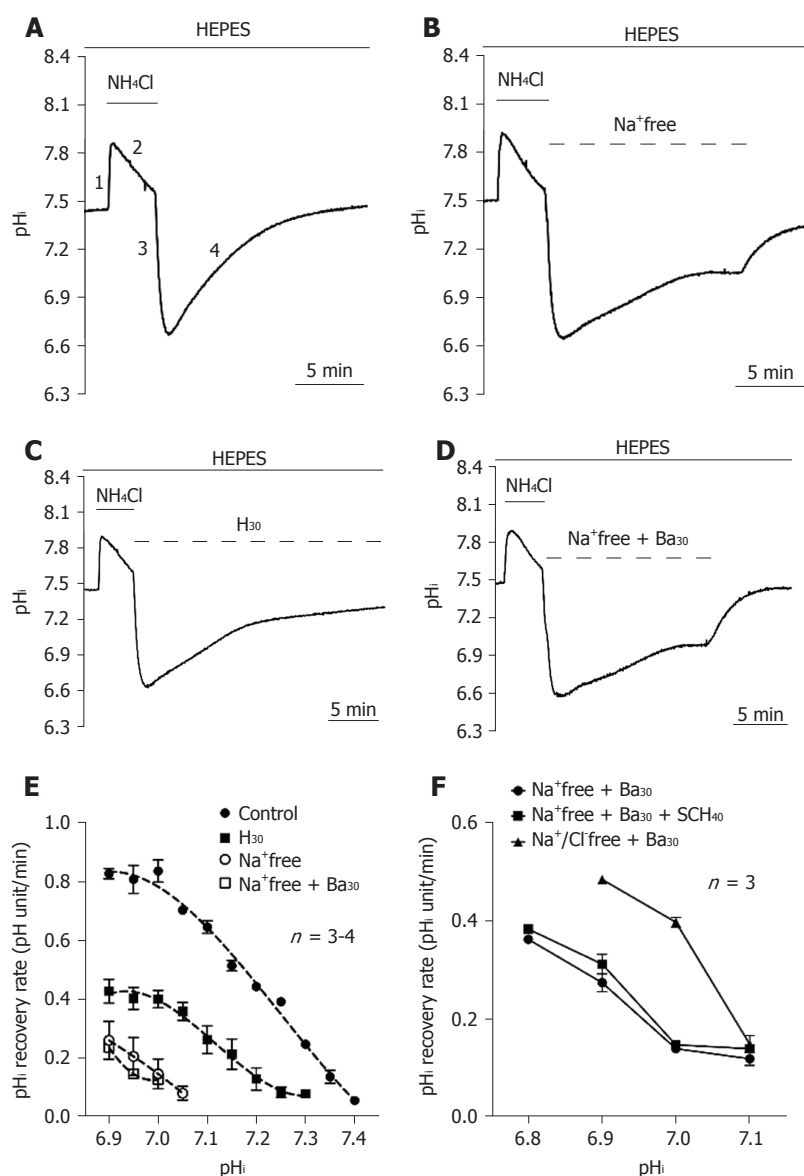


Figure 1 Functional characterization of acid extruders in the HEPES-buffered system. A-D: The top bar shows the buffer system used in perfusion experiments. The application of NH_4Cl and different conditions were respectively shown with the solid and dotted lines above the trace. The trace shown in A showed a typical pH recovery slope after NH_4Cl prepulse-induced intracellular acidosis in HEPES-buffered solution as a control. The traces shown in B-D showed the effect of the removal of extracellular Na^+ (Na^+ -free), addition of 30 $\mu\text{mol/L}$ HOE 694 (H_{30}) and Na^+ -free + 30 $\mu\text{mol/L}$ bafilomycin A1 (Ba_{30}) on the pH recovery slope. E: The curve of the pH recovery rates for Na^+ -free, H_{30} and Na^+ -free with Ba_{30} were collected from 3-6 similar experiments shown in A-D. F: After pre-treatment with NH_4Cl for 5 min, HPS0077 cells were treated with Na^+ -free + Ba_{30} , Na^+ -free + Ba_{30} + 40 $\mu\text{mol/L}$ SCH-28080 (SCH_{40}) and Na^+/Cl^- -free + Na^+ -free + Ba_{30} in HEPES-buffered solution, and the change in pH was detected by a multimode reader. Error bars represent the mean \pm SE.

defined by the following equation^[38]:

$$\beta(\text{mM}) = [\text{H}^+]_i / \Delta \text{pH}_i, \quad (\text{e.1})$$

Where $[\text{H}^+]_i$ is the change in the concentration of intracellular protons, and ΔpH_i is the resulting change in pH_i .

For experiments with the NH_4Cl prepulse technique, the application of $(\text{NH}_4)_2\text{SO}_4$ externally induces intracellular alkalinization. This is due to the rapid diffusion of NH_3 into the cell and its subsequent hydrogenation to form NH_4^+ . Upon the removal of extracellular $(\text{NH}_4)_2\text{SO}_4$, NH_4^+ exits the cell as uncharged NH_3 , leaving behind an equal concentration of H^+ and causing intracellular acidification. If $[\text{H}^+]_i$ is assumed to equal the intracellular concentration of NH_4^+ at the moment of their removal

from the external solution, then equation 1 can be expressed as follows:

$$\beta(\text{mM}) = [\text{NH}_4^+]_i / \Delta \text{pH}_i. \quad (\text{e.2})$$

According to the Henderson-Hasselbalch equation, the relationship between internal and external NH_4^+ concentration is as follows:

$$\text{pH}_o - \text{pH}_i = \log([\text{NH}_4^+]_i / [\text{NH}_4^+]_o). \quad (\text{e.3})$$

Equation 3 can then be rearranged as follows:

$$[\text{NH}_4^+]_i = [\text{NH}_4^+]_o \times 10^{(\text{pH}_o - \text{pH}_i)}. \quad (\text{e.4})$$

In the extracellular solution, $\text{pH}_o = \text{pK}_a + \log([\text{NH}_3]_o / [\text{NH}_4^+]_o)$ (Henderson-Hasselbalch equation). Therefore, this equation can be rearranged as follows:

$$[\text{NH}_4^+]_o = C / (10^{(\text{pH}_o - \text{pK})} + 1), \quad (\text{e.5})$$

where C is the total extracellular concentration of

NH_4^+ and pK is the dissociation constant of $(\text{NH}_4)_2\text{SO}_4$. Combining equations 4 and 5, we can derive $[\text{NH}_4^+]_i$ at a given pH_i as follows:

$$[\text{NH}_4^+]_i = [C/(10^{(\text{pH}_o - \text{pK})} + 1)] \times 10^{(\text{pH}_o - \text{pH}_i)}. \quad (\text{e.6})$$

In an open system, the theoretical β_{CO_2} can be calculated as follows:

$$\beta_{\text{CO}_2} = 2.3 \times [\text{HCO}_3^-]_i. \quad (\text{e.7})$$

Similar to the calculation procedures outlined above for NH_4^+ , $[\text{HCO}_3^-]_i$ can then be calculated as follows:

$$[\text{HCO}_3^-]_i = [C/(10^{(\text{pK} - \text{pH}_o)} + 1)] \times 10^{(\text{pH}_i - \text{pH}_o)}. \quad (\text{e.8})$$

Solutions and chemicals

Nigericin calibration solution was composed of 140 mmol/L KCl, 1 mmol/L MgCl_2 , 0.01 mmol/L nigericin and 10 mmol/L buffer (MES, HEPES or CAPSO), and the pH was adjusted to 5.5, 6.5, 7.0, 7.5, 8.5 or 9.5 with 6 mol/L NaOH. The buffers used in the calibration solution were in accordance with the pK_a of the buffers and the pH of the solution (MES was used for pH = 5.5 and 6.5; HEPES was used for pH = 7.0, 7.5 and 8.5; and CAPSO was used for pH = 9.5).

Standard HEPES-buffered solution was composed of 140 mmol/L NaCl, 4.5 mmol/L KCl, 1 mmol/L MgCl_2 , 2.5 mmol/L CaCl_2 , 11 mmol/L glucose, and 20 mmol/L HEPES. Standard bicarbonate-buffered Tyrode's solution (equilibrated with 5% $\text{CO}_2/22$ mmol/L HCO_3^-) was the same as above, except that the NaCl concentration was reduced to 117 mmol/L, and 22 mmol/L NaHCO_3 was added instead of HEPES (pH 7.40 at 37 °C).

Ion-substituted solutions: For Na^+ -free HEPES-buffered Tyrode's solution, NaCl was replaced with 140 mmol/L N-methyl-D-glucamine (NMDG). For Cl^- -free $\text{CO}_2/\text{HCO}_3^-$ -buffered Tyrode's solution contained 117 mmol/L sodium gluconate, 4.5 mmol/L potassium gluconate, 12 mmol/L calcium gluconate, 22 mmol/L NaHCO_3 , 1 mmol/L MgSO_4 , and 11 mmol/L glucose. The Na^+/Cl^- -free solution (for the buffering power experiment) was composed of 140 mmol/L NMDG, 4.5 mmol/L K-gluconate, 1 mmol/L Mg-gluconate, 2.5 mmol/L Ca-gluconate, 11 mmol/L glucose and 20 mmol/L HEPES (for 5% $\text{CO}_2/\text{HCO}_3^-$ -free system) or bubbled with 5% CO_2 (for 5% $\text{CO}_2/\text{HCO}_3^-$ system). The pH was adjusted to 7.4 with 6 mol/L NaOH, HCl or H_2SO_4 at 37 °C for all solutions. NH_4Cl , Na-acetate and $(\text{NH}_4)_2\text{SO}_4$ were directly added as solids to the buffered solutions before use. HOE 694 (HOE, a NHE1 specific inhibitor), S0859 (an NBC-specific inhibitor), bafilomycin A1 (Ba, a V-type ATPase-specific inhibitor) and SCH-28080 (SCH, a KHE-specific inhibitor) were added as stocks to solutions shortly before use. All drugs mentioned above were obtained from Sigma-Aldrich.

Statistical analysis

The data were expressed as the mean \pm SE of n preparations. The statistical significance was analyzed using one-way or two-way ANOVA followed by Tukey's

or Dunnett's multiple comparisons with GraphPad Prism 6 software, respectively. A P -value less than 0.05 were regarded as statistically significant.

RESULTS

In situ calibration of BCECF and the detection of hiPSC pluripotency markers

To monitor the change in pH_i , an *in situ* calibration was conducted in hiPSCs. A high potassium/nigericin calibration method was used to convert the emission ratio to the pH_i value. Briefly, BCECF-loaded cells were perfused with six different nigericin calibration solutions with different pH levels (5.5-9.5) (the details of the composition of the six nigericin calibration solutions are listed above in the solutions section) that caused the pH_i to equal the pH_o , as shown in Figure 2A. The calibration equation was obtained from ten similar experiments and a nonlinear BCECF fluorescence- pH_i curve of function, as shown below and in Figure 2B. The following equation was used to convert the fluorescence ratio into pH_i :

$$\text{pH}_i = \text{pK}_a + \log[(R_{\text{max}} - R)/(R - R_{\text{min}})] + \log(F_{440\text{min}}/F_{440\text{max}})$$

Where R is the ratio of the 530 nm fluorescence emission at 490 nm and 440 nm excitation (490/400), and F is the fluorescence value at 490 nm and 440 nm excitation. The maximum and minimum ratios (R_{max} and R_{min}) of 530/490 and 530/440 (Em/Ex) were obtained from perfusion with pH 9.5 and 5.5 calibration solutions, respectively.

Because the HPS0077 cell line was used as a representative example of hiPSCs in this study, we first examined whether pluripotency markers, such as OCT4, SOX2, SSEA-4 and TRA-1-60, are present in HPS0077 cells. As shown in Figure 2C, the four pluripotency markers were clearly identified by immunofluorescence staining and labeling. Our results support the hypothesis that the HPS0077 cell line possesses the characteristics of hiPSCs and is suitable as the subject for this study.

Functional characterization of acid extruders in HEPES buffered system

To investigate whether there is an acid extrusion mechanism in the cultured hiPSCs, the cells were first perfused in HEPES-buffered solution ($\text{CO}_2/\text{HCO}_3^-$ -free). As shown in Figure 1A, a pH_i recovery slope following NH_4Cl prepulse-induced intracellular acidification was a typical trace for the control ($n = 3$). Either removal of the extracellular Na^+ ($n = 3$) or application of 30 $\mu\text{mol/L}$ HOE 694 (H_{30} , $n = 4$) significantly inhibited the pH_i recovery rate, as shown in Figures 1B and 1C, respectively, which demonstrates the presence of Na^+ -dependent acid extruder(s) and NHE1 in HPS0077 cells.

However, besides Na^+ -dependent acid extruders, there is another acid extrusion mechanism responsible for the remaining acid extrusion in HEPES solution. Therefore, to further investigate whether the remain-

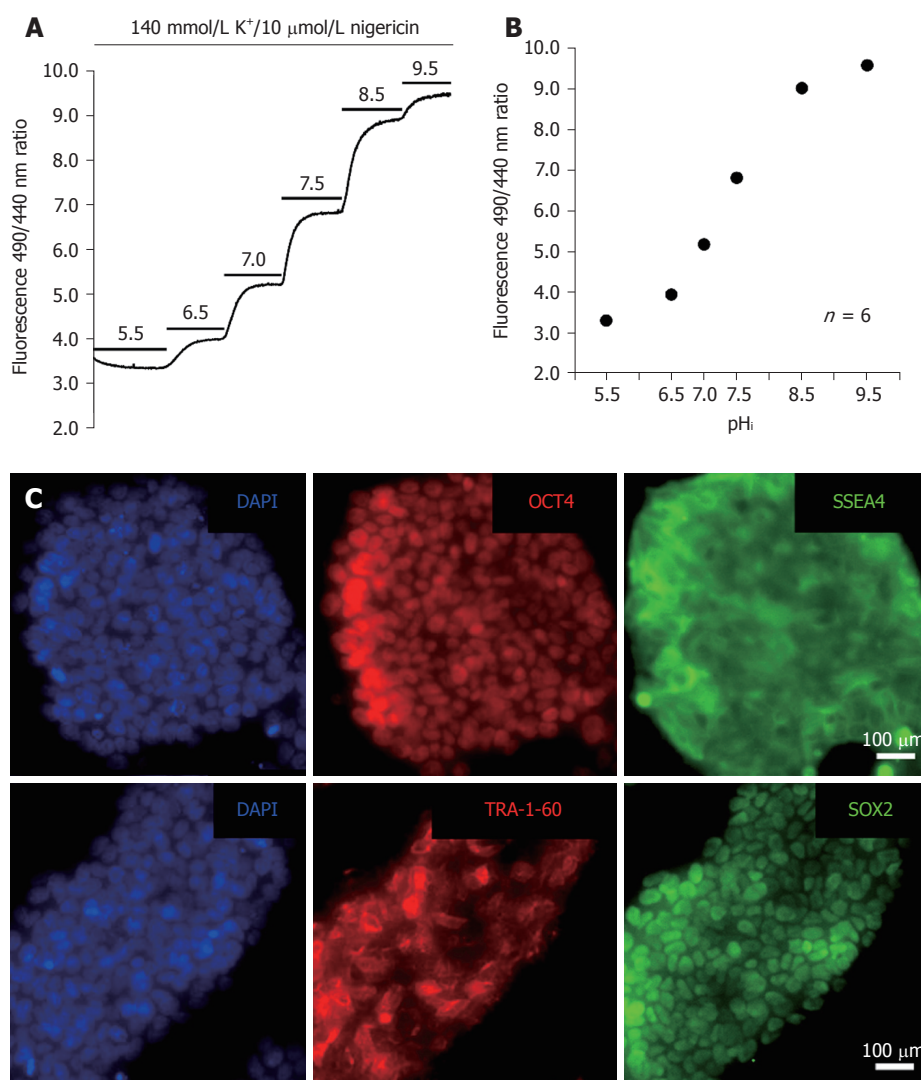


Figure 2 Calibration of the BCECF fluorescence ratio and pluripotency characterization. A: The trace showed the protocol of BCECF fluorescence ratio (510 nm emission at 490 nm and 440 nm excitations) calibration in HPS0077 cells. The top bars represent the application of different conditions; B: The plots of pH_i vs the BCECF fluorescence ratio were collected from 6 similar experiments shown in A; C: Immunofluorescence analysis showed the expression of pluripotency markers, OCT4, SSEA4, TRA-1-60 and SOX2, in HPS0077 cells.

ning Na^+ -independent pH_i recovery (*i.e.*, could not be inhibited by Na^+ -free solution) is caused by the vacuolar-type ATPase (V-ATPase), HPS0077 cells were perfused with an Na^+ -free solution pulse with 30 μ mol/L bafilomycin A1 (Ba_{30} ; V-ATPase-specific inhibitor, $n = 3$), as shown in Figure 1D. However, either no significant inhibition or slight inhibition of pH_i recovery was observed between the Na^+ -free solution group and the Na^+ -free solution + Ba_{30} group (Figures 1B and 1D, respectively). These results suggest that V-ATPase does not play a role in acid extrusion to the cytosol in hiPSCs. Experimental data similar to those shown in Figures 1A-D were summarized and plotted as a function of the pH_i recovery rate vs pH_i in Figure 1E. As shown in Figure 1E, in HEPES solution (*i.e.*, when HCO_3^- -dependent acid extruder(s) were not activated), the acid extrusion mechanism was mainly attributed to NHE1 (the difference between the trace of the Na^+ -free group and the trace of the H_{30} group), apart from other Na^+ -

dependent acid extruder(s) (the difference between the trace of H_{30} and the trace of Na^+ -free). Moreover, the other Na^+ -independent acid extruder(s) were activated when the pH_i was less than 7.1 ± 0.01 (see the trace of Na^+ -free + Ba_{30}).

To further examine whether the Na^+ -independent acid extruders shown in Figure 1E are KHE or Cl^- -dependent acid extruder(s), HPS0077 cells were either performed by adding 40 μ mol/L SCH-28080 (SCH_{40} , a KHE-specific inhibitor) or removing $[Cl^-]_o$. The change in pH_i in this series of experiments was detected using a Synergy 2 Multi-Mode Reader with BCECF-AM dye. The data for this series of experiments were summarized and plotted as a function of the pH_i recovery rate vs pH_i in Figure 1F. As shown in Figure 1F, the pH_i recovery rate between the trace before and after adding SCH_{40} ($n = 3$, solid circles and squares, respectively) was not significantly different. Moreover, the removal of $[Cl^-]$ ($n = 3$, solid triangles) surprisingly caused a dramatic

increase in the pH_i recovery rate instead of inhibition. This phenomenon is most likely caused by the inhibition of the activity of the Cl^- -dependent acid loader. In summary, these results provide clear pharmacological evidence that the NHE is mainly responsible for acid extrusion and functionally coexists with other Na^+ -dependent and -independent acid extrusion mechanisms in HPS0077 cells. Moreover, the Na^+ -independent acid extrusion mechanism is neither a KHE nor a Cl^- -dependent acid extruder(s).

Functional characterization of acid extruders in a 5% $\text{CO}_2/\text{HCO}_3^-$ -buffered system

To quantify the $[\text{H}_i]^+$ flux through pH_i regulators in 5% $\text{CO}_2/\text{HCO}_3^-$ -buffered conditions, we first quantified intracellular buffering (β). The experimental details are shown in the materials and methods section, and we found that β increased as pH_i increased at $\text{pH}_i = 7.0$ to 8.0 ($n = 35$, data not shown). The equation can be expressed as $\beta = 107.79 (\text{pH}_i)^2 - 1522.2 (\text{pH}_i) + 5396.9$ (correlation coefficient $R^2 = 0.85$). The obtained β can be used to calculate the $[\text{H}_i]^+$ flux through pH_i regulators by the following equation: $J_{\text{H}} = \beta \times \text{pH}_i$ recovery rate (pH_i value/minutes). To further investigate whether the NBC is functionally involved in the 5% $\text{CO}_2/\text{HCO}_3^-$ condition, we used a protocol similar to the previously mentioned experiments except for the replacement of HEPES-buffered solution with 5% $\text{CO}_2/\text{HCO}_3^-$ -buffered solution. The pH_i recovery slope following NH_4Cl prepulse-induced intracellular acidification in 5% $\text{CO}_2/\text{HCO}_3^-$ -buffered solution was a typical trace for the control ($n = 7$), as shown in Figure 3A. As shown in Figures 3B-E, the pH_i recovery rate was significantly inhibited under four different conditions as follows: removal of $[\text{Na}^+]$ ($n = 3$, addition of H_3O^+ ($n = 4$), addition of 90 $\mu\text{mol/L}$ S0859 (S_{90} ; an inhibitor of NBC, $n = 3$), and addition of H_3O^+ and S_{90} ($\text{H}_{30} + \text{S}_{90}$, $n = 3$). Experimental data similar to those shown in Figures 3A-E were summarized and plotted as a function of J_{H} vs pH_i in Figure 3F. As shown in Figure 3F, a similar pH_i recovery rate between Na^+ -free and $\text{H}_{30} + \text{S}_{90}$ conditions indicated that the NHE1 and the NBC were both involved in the Na^+ -dependent acid extrusion mechanism in the 5% $\text{CO}_2/\text{HCO}_3^-$ condition in HPS0077 cells.

Notably, the acid extrusion mechanism in the 5% $\text{CO}_2/\text{HCO}_3^-$ condition was regulated mainly by the NBC in the pH_i range of 7.50-7.68 because the pH_i recovery rate could be completely inhibited by S_{90} (Figure 3D). Moreover, the addition of S_{90} did not affect pH_i recovery when the pH_i was less than 6.9 ± 0.01 ($n = 3$, see the trace of S_{90}), which indicated that the NBC was not responsible for acid extrusion in the relatively acidic cytoplasm (Figure 3D). In summary, NHE1, NBC and Na^+ -independent acid extruder(s) were mainly functionally activated in the pH_i ranges of < 7.5 , 6.9-7.68 and < 7.1 , respectively.

Functional characterization of acid loaders

The homeostasis of pH_i is coregulated by both acid

extruders and acid loaders. The CHE and the AE are two known acid loaders in mammalian cells. Unlike the NHE and the NBC, the acid loading mechanism depends on $[\text{Cl}^-]_o$ and further exchange of $[\text{OH}^-]_i$ or $[\text{HCO}_3^-]_i$ out of the cytoplasm to neutralize intracellular alkalization. To estimate the function of acid loaders, an Na-acetate prepulse was used to induce intracellular alkalization in this study. The subsequent pH_i recovery slope was expressed as the acid loading activity of acid loaders. Figures 4A and 4C show the typical pH_i recovery slope following the Na-acetate prepulse either in HEPES or HCO_3^- -buffered solution, respectively ($n = 3$). Removal of $[\text{Cl}^-]_o$ in the 5% $\text{CO}_2/\text{HCO}_3^-$ -buffered solution completely inhibited the pH_i recovery ($n = 3$), as shown in Figure 4D, which indicated that the acid loading mechanism is completely Cl^- -independent in HPS0077 cells. However, interestingly, a rapid acid loading phenomenon was observed before the total inhibition at $\text{pH}_i = 7.9 \pm 0.01$ ($n = 3$) in HEPES solution, as shown in Figure 4B. These results indicated that CO_2 or HCO_3^- may inhibit this unknown Cl^- -dependent acid loader(s), but the characterization requires further studies. Due to the lack of specific inhibitors of the CHE and the AE, according to previous studies on the acid loading mechanism in mammalian cells conducted by Leem *et al.*^[39], we speculate that the Cl^- -independent acid loading mechanism is mainly attributed to the CHE and the AE^[39]. Notably, as shown in Figure 4E, the pH_i recovery rate is nearly identical between the 5% $\text{CO}_2/\text{HCO}_3^-$ system (solid circles) and the HEPES system (solid squares), which indicates that the CHE plays a more important role than the AE in the acid loading mechanism in HPS0077 cells.

Decrease in pH_i during the loss of pluripotency: molecular and functional evidence

Our previously mentioned results showed that the acid extruders NHE and NBC mainly functionally coexist in hiPSCs.

We further investigated the dynamic changes in pH_i during the loss of pluripotency in hiPSCs. In the pluripotent state, the resting pH_i observed from the pH_i completely recovered after NH_4Cl prepulse-induced intracellular acidification was found to be 7.5 ± 0.01 ($n = 20$) and 7.68 ± 0.01 ($n = 20$) in HEPES and 5% $\text{CO}_2/\text{HCO}_3^-$ conditions, respectively, as shown in Figures 5A and 5B. Moreover, in 5% $\text{CO}_2/\text{HCO}_3^-$ -buffered solution, as expected, the resting pH_i shifted to 7.46 ± 0.02 ($n = 5$) and 7.66 ± 0.02 ($n = 5$) after adding S0859 (S_{90}) and HOE694 (H_{30}), respectively (Figure 5B, the data were collected from the data shown in Figures 3C and 3D). Notably, there was no significant difference between the resting pH_i in HEPES and in the 5% $\text{CO}_2/\text{HCO}_3^-$ plus S_{90} conditions, which indicates that the set-point of NHE activation is $\text{pH}_i = 7.5$. In the 5% $\text{CO}_2/\text{HCO}_3^-$ condition, the resting pH_i showed no significant difference between the untreated and H_{30} -treated conditions, which indicates that the pH_i is regulated by the NBC instead of the NHE in the pH_i range of 7.50-7.68.

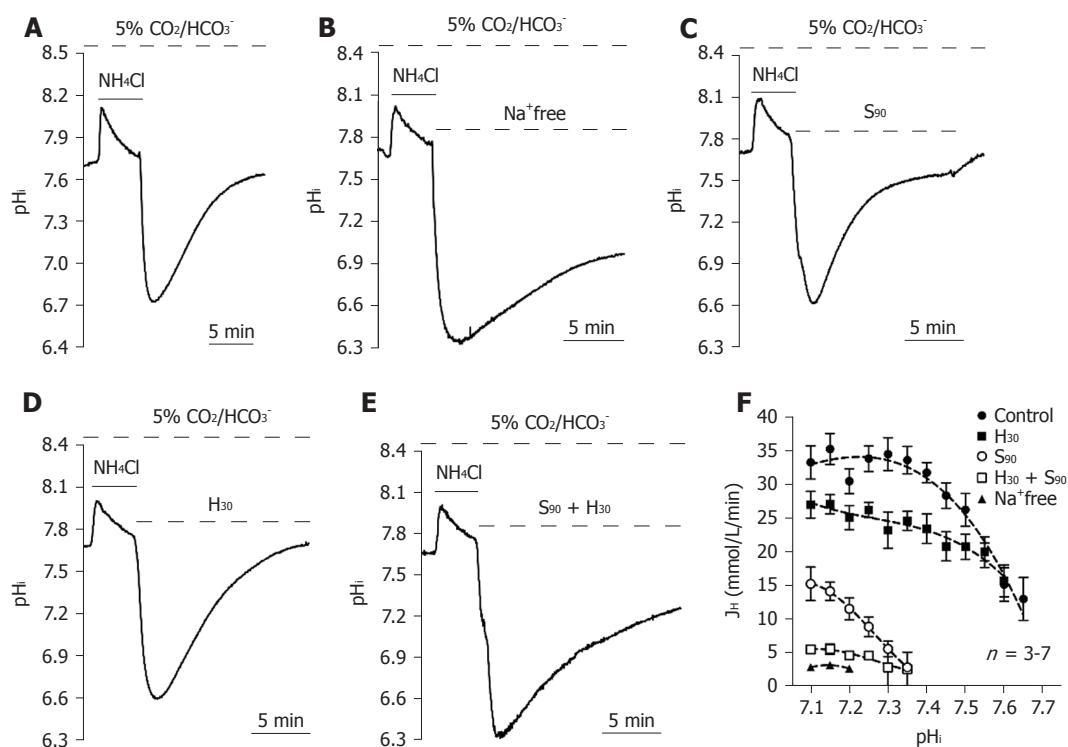


Figure 3 Functional characterization of acid extruders in the 5% CO₂/HCO₃⁻-buffered system. A-E: The trace shown in A showed a typical pH_i recovery slope after NH₄Cl prepulse-induced intracellular acidosis in HEPES-buffered solution as a control. The traces shown in B-E showed the effect of the removal of extracellular Na⁺ (Na⁺-free), addition of 90 μmol/L S0859 (S₉₀), addition of 30 μmol/L HOE 694 (H₃₀) and addition of S₉₀ + H₃₀ on the pH_i recovery slope; F: The curve of the pH_i recovery rates after the addition of Na⁺-free, S₉₀, H₃₀ and S₉₀ + H₃₀ were collected from 2-10 similar experiments shown in A-E. Error bars represent the mean ± SE.

To further induce the loss of pluripotency, HPS0077 cells were first transferred from mTeSR1 media (designed for maintaining long-term pluripotency) to mTeSR-E8 medium (containing fibroblast growth factor 2, FGF2, and transforming growth factor β1, TGFβ1) and then subsequently replaced with mTeSR-E6 medium (without FGF2 and TGFβ1) for 1 to 4 days (E6-1d to 4d) to induce the loss of pluripotency. Notably, the expression of the pluripotency marker OCT4 was significantly decreased after culture in mTeSR-E6 medium, as shown in Figure 5C. We also found that the expression of NHE1, NHE3, V-ATPase, NBCe1 and NBCe2 decreased during the loss of pluripotency, while the expression of NBCn1 did not decrease, as shown in Figure 5C.

To further investigate the role of the NHE and the NBC on the loss of pluripotency, we detected the pH_i recovery rate following NH₄Cl prepulse-induced intracellular acidification. The pH_i recovery traces in different culture mediums, *i.e.*, E8, E6-1d, E6-2d, E6-3d and E6-4d in HEPES and 5% CO₂/HCO₃⁻-buffered solution are shown in Figures 6A and 6D, respectively. The graphs in Figure 6B show the pH_i recovery rate in E6-1d to E6-4d normalized from the E8 condition (% of E8) in HEPES, estimated at pH_i = 6.9 and 7.2, respectively, and averaged for 3 experiments similar to that shown in Figure 6A. The NHE is mainly responsible for acid extrusion in the HEPES condition. When the pH_i recovery rate was measured at pH_i = 6.9, E6-1d showed no significant change, while E6-2d, E6-3d and E6-4d significantly decreased by 76.3%, 60.6% and 51.7%,

respectively (*n* = 3). When the pH_i recovery rate was measured at pH_i = 7.2, the pH_i recovery rates of E6-1d, E6-2d, E6-3d and E6-4d significantly decreased by 82.7%, 67.4%, 47.6% and 16.3%, respectively (*n* = 3). The max/min charts in Figure 6C show the resting pH_i in E8, E6-1d, E6-2d, E6-3d and E6-4d, respectively, averaged from similar experiments as shown in Figure 6A (*n* = 5-20). The resting pH_i decreased from 7.5 to 7.49, 7.4, 7.28 and 7.21 in E6-1d, E6-2d, E6-3d and E6-4d, respectively (*n* = 5 to 20).

The graphs shown in Figure 6E show the pH_i recovery rate in E6-1d to E6-4d normalized to E8 (control) in 5% CO₂/HCO₃⁻-buffered solution, which was estimated at pH_i = 6.9, 7.2 and 7.5, respectively, and averaged for 3 experiments similar to that shown in Figure 6D. As shown in Figure 6E, in the 5% CO₂/HCO₃⁻ condition (*i.e.*, where the NHE and the NBC were both involved in the acid extrusion mechanism), the pH_i recovery rate measured at pH_i = 6.9 and 7.2 showed no significant difference between E8 and E6-1d, but it was significantly decreased by 85.2% when measured at pH_i = 7.5. The pH_i recovery rate for E6-2d, E6-3d and E6-4d was significantly decreased by 88.7, 74.9 and 61%, respectively, when measured at pH_i = 6.9, decreased by 82%, 77.2% and 51.5%, respectively, when measured at pH_i = 7.2, and decreased by 53.4%, 44.8% and 22.3%, respectively, when measured at pH_i = 7.5 (*n* = 3). The max/min charts shown in Figure 6F show the resting pH_i in E8, E6-1d, E6-2d, E6-3d and E6-4d, averaged from similar experiments as those shown

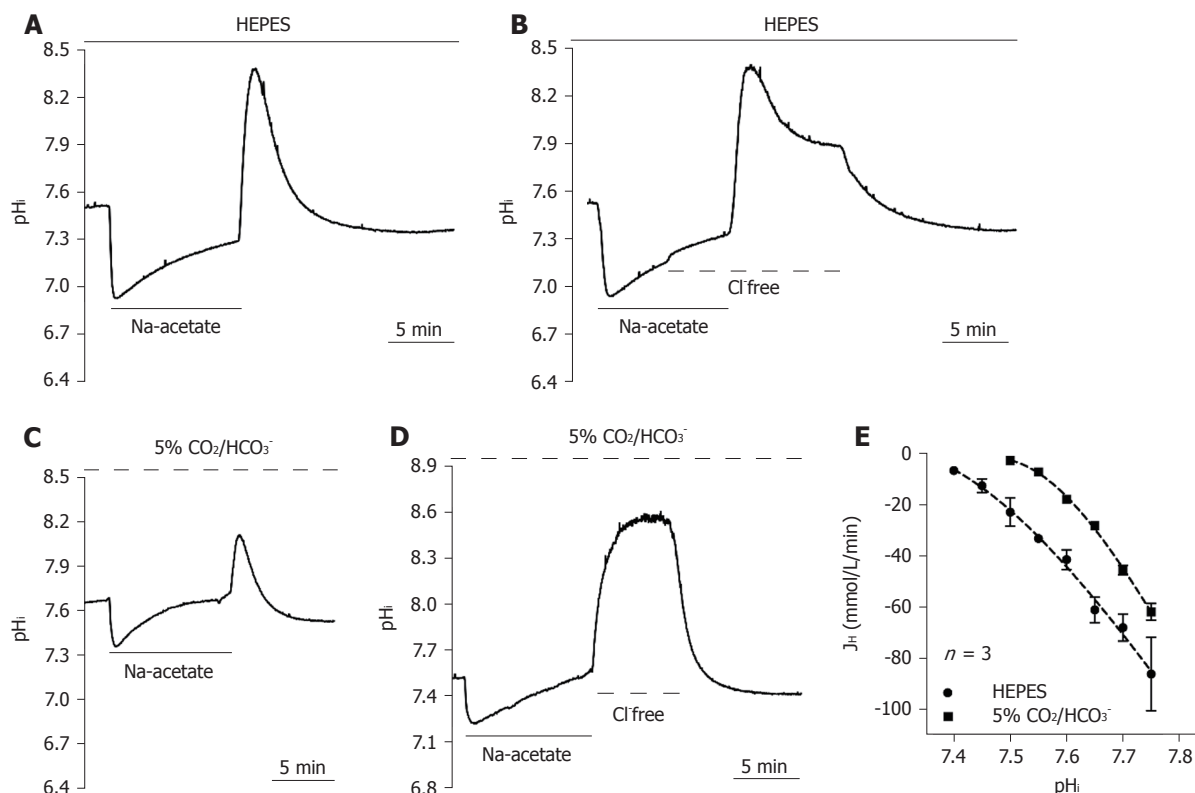


Figure 4 Functional characterization of the acid loader. A-D: The traces shown in A and C showed typical pH_i recovery slopes after Na-acetate prepulse-induced intracellular alkalinization in HEPES and 5% CO₂/HCO₃⁻ buffered solution as a control. The traces shown in B and D showed the effect of the removal of extracellular Cl⁻ (Cl⁻ free) on the pH_i recovery slope in HEPES and 5% CO₂/HCO₃⁻ buffered solution; E: The curve of the pH_i recovery rates in HEPES and 5% CO₂/HCO₃⁻ buffered solution were collected from 3-4 similar experiments shown in A and C. Error bars represent the mean ± SE.

in Figure 6D ($n = 5-20$). We found that the resting pH_i decreased from 7.68 to 7.64, 7.61, 7.56 and 7.48 in E6-1d, E6-2d, E6-3d and E6-4d, respectively ($n = 5$, Figure 6F). In summary, our results provide clear evidence that the loss of hiPSC pluripotency decreased the activity and expression of acid extruders (NHE and NBC), further resulting in a decrease in the pH_i recovery rate and resting pH_i.

DISCUSSION

The functional and molecular evidence of active transmembrane acid extruders and acid loaders in hiPSCs

In this study, we have clearly demonstrated that transmembrane active pH_i regulators, such as NHE1, NBC, AE and CHE, functionally coexisted in hiPSCs (Figures 3 and 4). Moreover, we successfully quantified the net acid efflux of each functional acid transporter, as shown in Figures 3 and 7, by considering intracellular buffering. From Figure 3F, we can clearly observe that the active efflux was mainly dependent on the activity of the NBC in hiPSCs in the pH_i range less than 7.35 because the S₉₀ group (*i.e.*, inhibiting NBC activity) substantially decreased the activity compared to other groups (inhibiting NHE1 or other Na-independent acid extruders). Moreover, the role of NHE1 on acid extrusion decreased as the pH_i increased (Figures 1,

3 and 7). Notably, the activity of NHE1 was nominally undetectable when the pH_i was greater than 7.50, as shown in Figures 1, 3 and 7.

Relevant molecular candidates for the NBC include at least five members of the slc4 family, including 2 electrogenic Na⁺-HCO₃⁻ cotransporters (NBCe1/SLC4A4 and NBCe2/SLC4A5), 1 electroneutral Na⁺-HCO₃⁻ cotransporter (NBCn1/SLC4A7) and 2 Na⁺-dependent Cl⁻-HCO₃⁻ exchangers (NCBE/SLC4A10 and NDCBE/SLC4A8)^[7,40,41]. In this study, we found that three isoforms of the NBC, NBCn1, NBCe1 and NBCe2, coexist in hiPSCs, which is similar to our previously reported results in cultured human renal artery smooth muscle cells^[7]. However, the Aalkjaer group has demonstrated that the NBC is NBCn1, *i.e.*, it is electroneutral, in rat and mouse smooth muscle cells^[42], which is similar to the results reported in guinea pig myocytes by the Vaughan-Jones group^[10]. In other words, the coexistence of 3 types of NBCs in hiPSCs is different from the results in mouse and rat models (*c.f.* Aalkjaer's group) and guinea pig models (*c.f.* Vaughan-Jones's group, which is likely due to differences in species/organs).

Moreover, in contrast to the results reported in our previous studies in cardiovascular cells, we found that Na⁺-independent acid extruder(s) and Cl⁻-independent acid loader(s) were substantially present for acid extrusion (pH_i < 7.1) and acid loading (pH_i > 7.9) in hiPSCs (Figures 1, 4 and 7). We further demonstrated

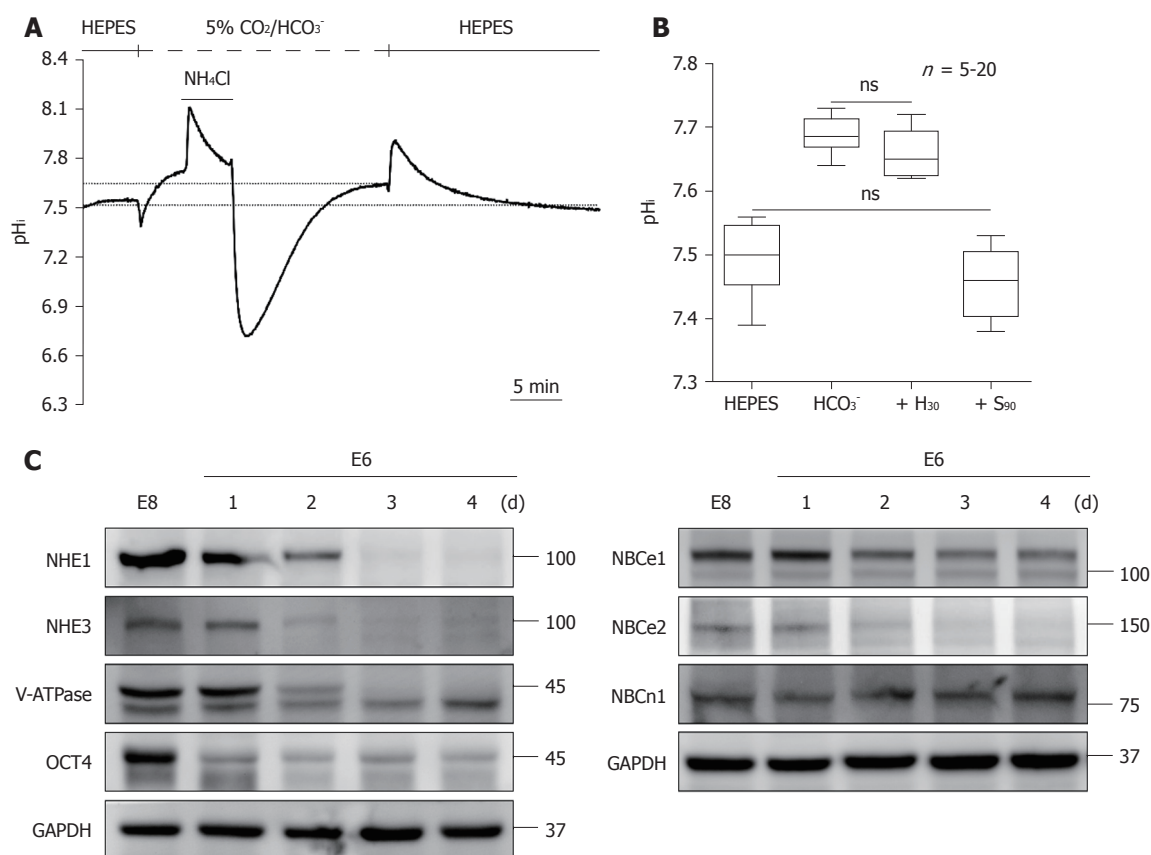


Figure 5 Steady-state pH_i in HEPES and 5% CO₂/HCO₃⁻-buffered solution and the change in the expression of pH_i regulators during the loss of pluripotency in human induced pluripotent stem cells. **A:** The resting pH_i was a steady-state taken from the completely recovered pH_i after intracellular acidification or alkalization. The dotted line indicates the value of the resting pH_i; **B:** The max/min chart of the resting pH_i in hiPSCs was collected from **A** ($n = 20$) and Figures 4C and D ($n = 5$). The means of the resting pH_i in HEPES and 5% CO₂/HCO₃⁻-buffered solution were found to be 7.50 ± 0.01 and 7.68 ± 0.01 , respectively. After treatment with H₃₀ and S₉₀ in 5% CO₂/HCO₃⁻-buffered solution, the resting pH_i shifted to 7.66 ± 0.02 and 7.46 ± 0.02 , respectively; **C:** Immunoblot analysis of the expression of NHE1, NHE3, V-ATPase, NBCe1, NBCe2, NBCn1 and OCT4 in hiPSCs in different culture media for different days (E8 and E6-1d to E6-4d). The histograms in **B** display the mean and the min to max values. hiPSCs: Human induced pluripotent stem cells; NHE: The Na⁺/H⁺ exchanger; NBC: The Na⁺/HCO₃⁻ cotransporter; V-ATPase: Vacuolar-ATPase.

that the unknown Na⁺-independent acid extruder(s) is not the V-ATPase, KHE^[43] or Cl⁻-dependent acid extruder (localized on lysosome and gastric cell membranes)^[44,45] (Figures 1D and 1F). Therefore, we hypothesize that this unknown Na⁺-independent mechanism is most likely an ATP-dependent transporter instead of a concentration gradient-driven transporter. For example, ATP deficiency, induced by the addition of oligomycin, combined with the addition of bafilomycin A1 during the perfusion experiments would allow us to observe whether it inhibits Na⁺/V-ATPase-independent acid extrusion in hiPSCs^[46]. However, functional and molecular characterization requires further studies in the future.

In addition to being an acid extruder, NBCe1 has been reported to be responsible for the acid loading mechanism during the process of changing from the HEPES-buffered solution to the 5% CO₂/HCO₃⁻-buffered solution in mouse astrocytes^[47]. However, in our findings, the addition of 50 μM S0859 still failed to inhibit the Cl⁻-independent acid extrusion mechanism in the HEPES-buffered condition (data not shown). This result suggested that the Cl⁻-independent acid

extruder(s) was not NBCe1 in hiPSCs. Due to this unknown Cl⁻-independent acid extrusion mechanism being completely inhibited in the CO₂/HCO₃⁻-buffered system and the lack of related studies, future works should further characterize the possible existence of a CO₂-related pH_i acid loading mechanism.

The implication of the existence of extra acid extrusion/loading mechanisms in hiPSCs

The existence of an unknown acid extrusion mechanism, *i.e.*, Na⁺-independent acid extruder(s) (see Figure 3F) and acid loading mechanisms, *i.e.*, Cl⁻-independent acid loader(s), in hiPSCs might imply that the ability to resist the acid/base impact is very important for the pluripotency of hiPSCs^[37,48,49]. It has been reported that hiPSCs share many cellular properties with cancer cells, such as increased cell proliferation and dependence on glycolysis for metabolism^[24,26,50,51]. Many studies showed that a lower pH_i decreased proliferation and energy production in either normal or cancer cells^[15,26]. Indeed, in this study, we found that the acid extrusion mechanism was fully activated at an acidic pH_i (< 7.2), including the NHE, the NBC

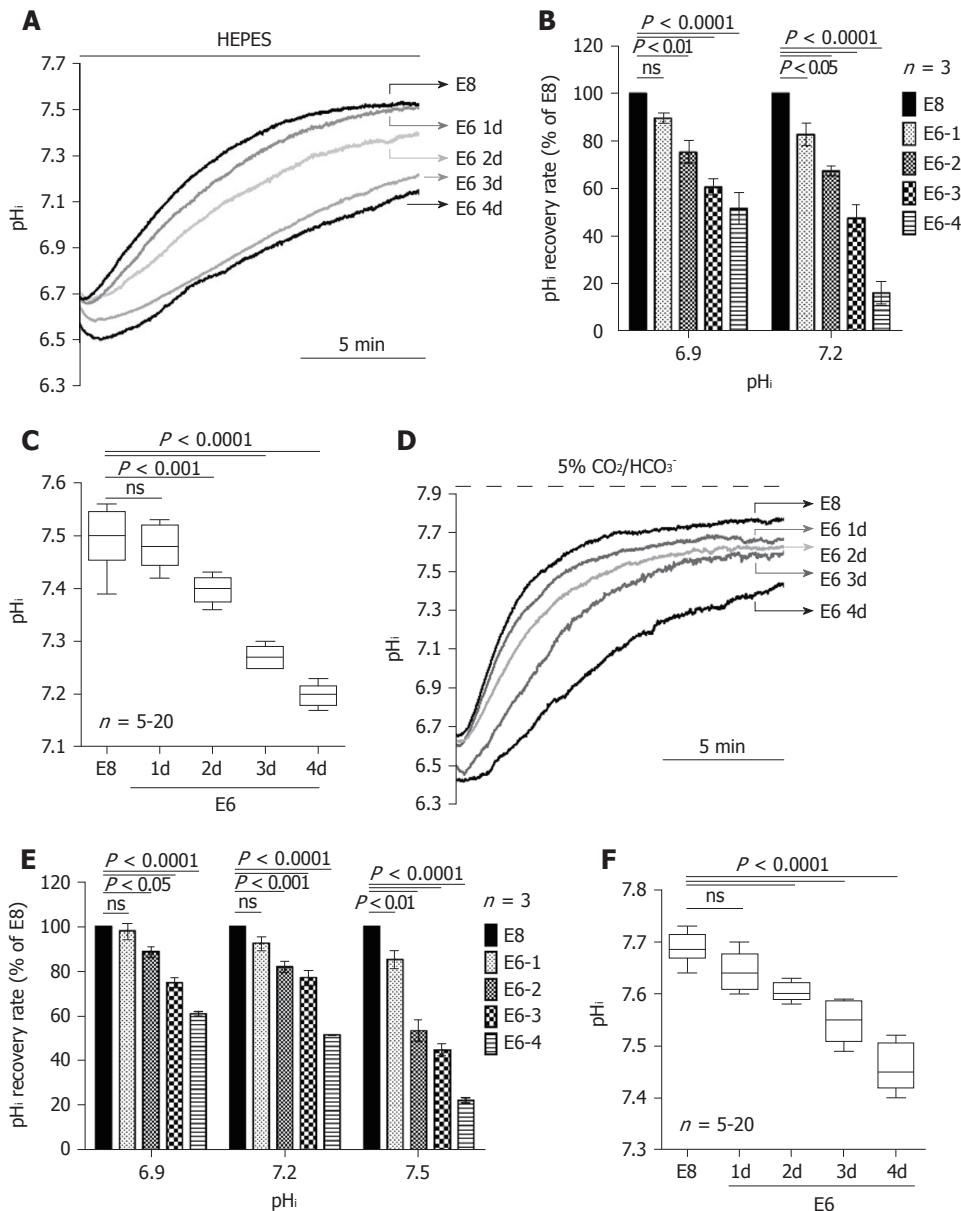


Figure 6 The change in the activity of the Na^+/H^+ exchanger and the Na^+/HCO_3^- cotransporter and the resting pH_i during the loss of pluripotency in human induced pluripotent stem cells. **A**: The traces showed the changes in pH_i recovery after NH_4Cl prepulse-induced intracellular acidification in E8 medium (containing fibroblast growth factor 2, FGF2, and transforming growth factor $\beta 1$, TGF $\beta 1$) and E6 medium (without FGF2 and TGF $\beta 1$) for 1 to 4 d (E6-1d to E6-4d) in HEPES-buffered solution; **B**: The charts showed the pH_i recovery rate in E6-1d to -4d normalized to the rate in E8 (% of E8) in HEPES-buffered solution, which was estimated at $pH_i = 6.9$ and 7.2 , respectively, and averaged for 3 experiments similar to that shown in **A** ($n = 5-20$); **C**: The max/min plots showed the resting pH_i in E8, E6-1d, E6-2d, E6-3d and E6-4d media that were averaged from similar experiments shown in **A** ($n = 5-20$); **D**: The traces showed the changes in pH_i recovery after NH_4Cl prepulse-induced intracellular acidification in E8 and E6-1d to E6-4d media in 5% CO_2/HCO_3^- -buffered solution; **E**: The graphs show the pH_i recovery rate in E6-1d to E6-4d normalized to the rate in E8 (control) in 5% CO_2/HCO_3^- -buffered solution, which was estimated at $pH_i = 6.9$, 7.2 and 7.5 , respectively, and averaged for 3 experiments similar to that shown in **D**; **F**: The max/min plots showed the resting pH_i in E8 E6-1d, E6-2d, E6-3d and E6-4d media, averaged from similar experiments shown in **D** ($n = 5-20$). Error bars represent the mean \pm SE. The histograms in **C** and **F** show the mean and min to max values. NS: No significant difference; hiPSCs: Human induced pluripotent stem cells.

and an unknown Na^+ -independent acid extruder(s), in hiPSCs. As expected, the resting pH_i in hiPSCs was found to be 7.5 and 7.68 in the HEPES and 5% CO_2/HCO_3^- conditions, respectively, and was relatively higher than that of normal differentiated adult cells (resting $pH_i = 6.9-7.2$), such as cardiovascular cells and tissues demonstrated in our previous studies^[7,13,52,53]. In cancer, the reversal of the intracellular/extracellular pH (pH_i/pH_e) gradient (alkaline pH_i and acidic pH_e) is

a common feature and further promotes carcinogenesis. The reason for the gradient reversal is that cancer cells overexpress and upregulate the set-point of acid extruders^[24-26]. Therefore, it is likely that hPSCs may upregulate the acid extrusion mechanism to adapt to cancer-like cellular properties. Some studies showed that, in addition to hiPSC growth being inhibited by an acidic culture environment, the alkalization of culture medium significantly decreases the cell growth rate and

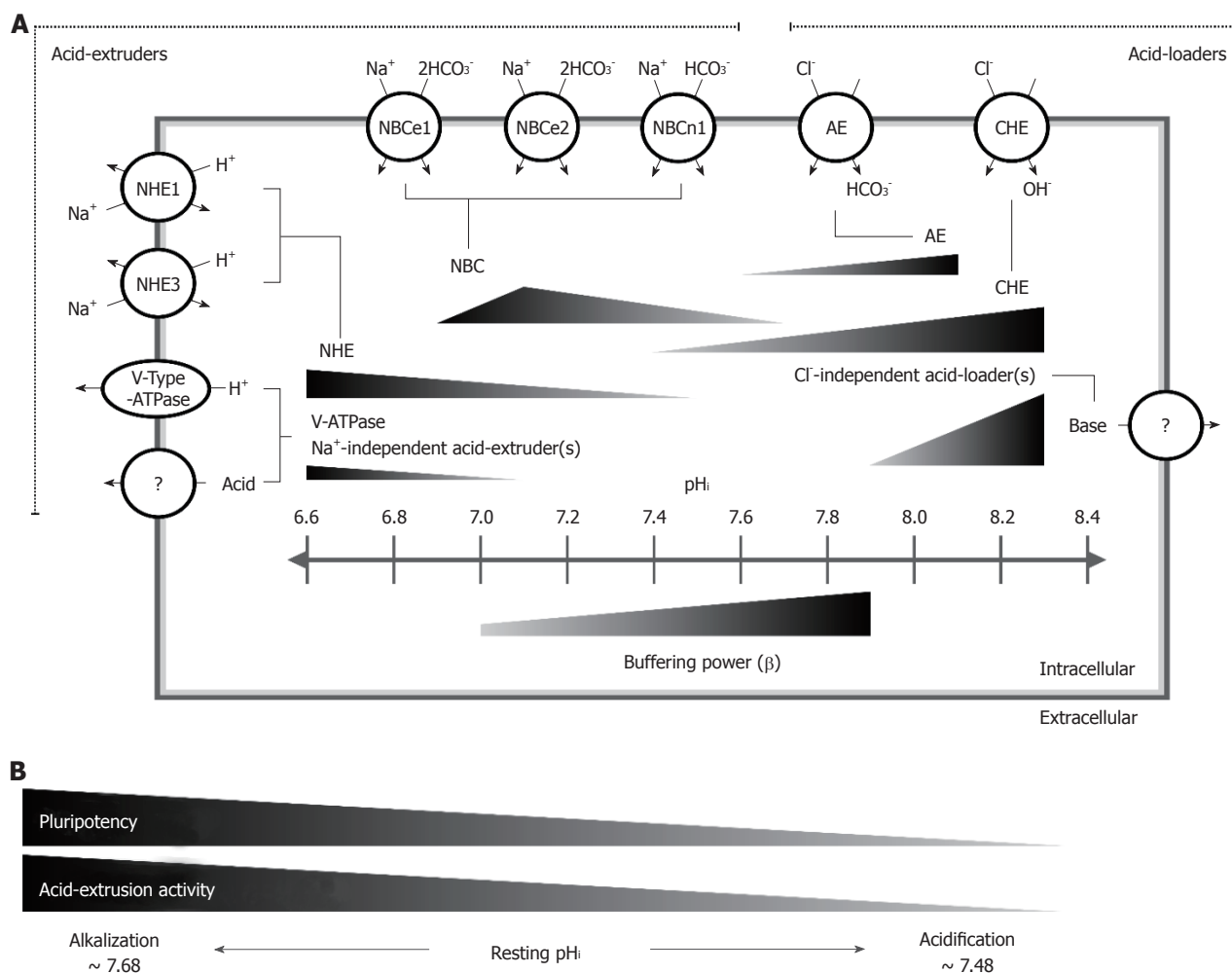


Figure 7 Kinetic model of the pHi regulatory mechanism in human induced pluripotent stem cells. A: A kinetic model illustrating the pHi regulatory mechanism in HPS0077 cell, including acid extrusion, acid loading and passive buffering power. For the first time, we demonstrated that the active membrane pH regulators NHE1, NHE3, V-ATPase, NBCe1, NBCe2, NBCn1, AE and CHE functionally coexisted in hiPSCs, and in addition, unknown Na⁺-independent acid extruder(s) and Cl⁻-independent acid loader(s) were also observed. The length of the triangle indicates the pHi range of pHi regulator activation, and the height indicates the magnitude of the pHi regulatory activity. For example, the NHE, NBC, AE and CHE were activated at pHi ≤ 7.5, between 6.9 and 7.68, ≥ 7.4 and between 7.6 and 8.1, respectively. The non-NHE acid extruders [V-ATPase, unknown Na⁺-independent acid extruder(s)] and unknown Cl⁻-independent acid loader(s) were activated during extreme intracellular acidification, *i.e.*, pHi < 7.1, and alkalinization, *i.e.*, pHi > 7.9, respectively. Moreover, the intracellular passive buffering capacity (β) increased as the pHi shifted to the alkalinization direction; B: In the process of the loss of pluripotency, the activity of the acid extrusion mechanism gradually decreased, including the participation of at least the NHE, the NBC and V-ATPase, and resulted in the resting pHi shifting from 7.68 to 7.48. hiPSCs: Human induced pluripotent stem cells; NHE: The Na⁺/H⁺ exchanger; NBC: The Na⁺/HCO₃⁻ cotransporter; V-ATPase: Vacuolar-ATPase; AE: Anion exchanger; CHE: Cl⁻/OH⁻ exchanger.

expression of pluripotency markers at a minimum pHi = 7.8^[37,48,49]. The proliferative ability and pluripotency in hPSCs are critical for development^[54]. Therefore, the expression of additional unknown Na⁺-independent and Cl⁻-independent acid-regulating extruder(s) in hiPSCs implicates the function of resisting the potential impact of intracellular proton changes in hPSCs. However, further study on characterizing the mechanisms should be conducted in the future.

Decreases in acid extrusion activity during the loss of pluripotency in hiPSCs

A previous study showed that during the early spontaneous differentiation of mESCs, the resting pHi significantly increased at 48 and 72 h and returned to baseline at 96 h, and this increase was dependent on the loss of NHE1 function^[6]. However, in this study,

the decrease in resting pHi and the downregulation of the acid extrusion mechanism were demonstrated during the early loss of pluripotency in hiPSCs either in HEPES-buffered conditions or in 5% CO₂/HCO₃⁻-buffered conditions. These contradictory results may be due to the different pluripotent states between mESCs and hiPSCs, *i.e.*, naïve and primed pluripotency, respectively^[54,55]. As expected, the cells in the preprimed (naïve) and primed states significantly increased the pHi at 48 and 72 hours during early differentiation in mESCs. This result implies that increasing resting pHi occurred during the naïve to primed pluripotency states^[6]. Subsequently, the resting pHi returned to baseline at 72-96 h, which may indicate that the primed state is further differentiated. Furthermore, to adapt to the intracellular acidification caused by increased glycolysis, *i.e.*, the Warburg effect, the acid extrusion

mechanism is upregulated and further alkalizes the resting pHi in cancer cells^[24,26]. During the processes of PSC development, metabolism has been found to rely on different metabolic pathways, *i.e.*, oxidative phosphorylation (OXPHOS), glycolysis and OXPHOS in naive, primed and early differentiation states, respectively^[51,56,57]. This switch between OXPHOS and glycolysis supports the dynamic changes in the resting pHi observed during the loss of pluripotency in mESCs and the decrease in the resting pHi and acid extrusion in hiPSCs demonstrated in this study.

The possible underlying mechanism for the observed decrease in the acid extrusion mechanism during the process of the loss of pluripotency in hiPSCs may be due to the crosstalk between the PI3K/AKT and MEK/ERK signaling pathways, which plays a curial role in pluripotency^[58]. To maintain pluripotency in hPSCs, FGF2 has been added to the culture medium to activate PI3K/AKT signaling^[58,59]. The activation of PI3K/AKT signaling further promotes the relative gene expression of pluripotency markers and inhibits differentiation by suppressing MEK/ERK signaling^[58]. Therefore, the removal of FGF2 decreases the ratio of AKT activity to ERK and further causes cell differentiation^[58,60]. ERK is a well-known activator of NHE1^[61,62], but we did not find that removal of FGF2 (in E6 medium) resulted in an increase of the NHE1-dependent acid extrusion rate in this study. Although AKT has been shown to inhibit NHE1 activity in cardiovascular cells^[63], AKT is stimulated by insulin and growth factors and further activates NHE1 in cancer cells and fibroblasts^[64,65]. Therefore, this study implicates that the removal of FGF2 causes the loss of AKT activity and thus decreases the acid extrusion rate in hiPSCs.

In conclusion, for the first time, we established a functional pHi regulatory model in hiPSCs, as shown in Figure 7. In this model, we demonstrated that the steady-state pHi value is approximately 7.50-7.68 in hiPSCs. Additionally, we showed that at least four types of acid extruders [NHE, NBC, V-ATPase and Na⁺-independent acid extruder(s)] and three types of acid loaders [CHE, AE and Cl⁻-independent acid loader(s)] coexist and are responsible for the pHi regulatory mechanism, and each is activated in different pHi ranges in hiPSCs. Moreover, the activity of the acid extrusion mechanism decreased by changing both the expression and activity of acid extruders during the process of the loss of pluripotency in hiPSCs.

ARTICLE HIGHLIGHTS

Research background

Homeostasis of intracellular pHi (pHi) affects many cellular functions, such as cell proliferation and differentiation. However, the knowledge of pHi regulation mechanism in human pluripotent stem cells still unknown.

Research motivation

The changes of acid-base kinetic were observed during the loss of pluripotency in mouse embryonic stem cells. Moreover, the balance of intracellular and

extracellular pH significantly affected the reprogramming efficiency and culture quality of human induced pluripotent stem cells (hiPSCs).

Research objectives

We aimed to establish the pHi regulation mechanism model and investigate the relationship of pHi regulation and pluripotency in hiPSCs.

Research methods

In the pluripotent state and during the loss of pluripotency in hiPSCs, we observed the activity of pHi regulation mechanism by acutely induced intracellular acidification and alkalization in the physiological buffered solution.

Research results

In hiPSCs, the Na⁺-H⁺ exchanger (NHE), the Na⁺-HCO₃⁻ cotransporter (NBC) and vacuolar-ATPase (V-ATPase) were the main active acid extruders that were activated against intracellular acidification. In contrast, the acid-equivalent loaders, such as the Cl⁻-HCO₃⁻ anion exchanger (AE) and the Cl⁻-OH⁻ exchanger (CHE), were activated to prevent intracellular alkalization. In addition to the classic pHi regulators NHE, NBC, V-ATPase, AE and CHE, we also demonstrated the functional existence of unknown acid-extruder(s) and -loader(s) in hiPSCs. Moreover, the pHi and acid-extruding mechanism were decreased during the loss of pluripotency in hiPSCs.

Research conclusions

For the first time, we established a model of the pHi regulation mechanism in hiPSCs. The higher resting pHi and acid-extruding mechanism might be the specific feature to adaptive the cancer-like cellular function and pluripotency in hiPSCs.

Research perspectives

In summary, we characterized the pHi regulation mechanism and its functional/expressional roles in maintenance of pluripotency of hiPSCs. We proposed that targeting either pHi regulators or pH environments of culture medium could be an effective way to modify the pluripotency state of hiPSCs, which may contribute the differentiation efficiency or culture quality.

REFERENCES

- Gao W, Zhang H, Chang G, Xie Z, Wang H, Ma L, Han Z, Li Q, Pang T. Decreased intracellular pH induced by cariporide differentially contributes to human umbilical cord-derived mesenchymal stem cells differentiation. *Cell Physiol Biochem* 2014; **33**: 185-194 [PMID: 24481225 DOI: 10.1159/000356661]
- Li X, Karki P, Lei L, Wang H, Fliegel L. Na⁺/H⁺ exchanger isoform 1 facilitates cardiomyocyte embryonic stem cell differentiation. *Am J Physiol Heart Circ Physiol* 2009; **296**: H159-H170 [PMID: 19011045 DOI: 10.1152/ajpheart.00375.2008]
- McBrian MA, Behbahan IS, Ferrari R, Su T, Huang TW, Li K, Hong CS, Christofk HR, Vogelauer M, Seligson DB, Kurdistan SK. Histone acetylation regulates intracellular pH. *Mol Cell* 2013; **49**: 310-321 [PMID: 23201122 DOI: 10.1016/j.molcel.2012.10.025]
- Park HJ, Lyons JC, Ohtsubo T, Song CW. Acidic environment causes apoptosis by increasing caspase activity. *Br J Cancer* 1999; **80**: 1892-1897 [PMID: 10471036 DOI: 10.1038/sj.bjc.6690617]
- Pouyssegur J, Franchi A, L'Allemain G, Paris S. Cytoplasmic pH, a key determinant of growth factor-induced DNA synthesis in quiescent fibroblasts. *FEBS Lett* 1985; **190**: 115-119 [PMID: 4043390 DOI: 10.1016/0014-5793(85)80439-7]
- Ulmschneider B, Grillo-Hill BK, Benítez M, Azimova DR, Barber DL, Nystul TG. Increased intracellular pH is necessary for adult epithelial and embryonic stem cell differentiation. *J Cell Biol* 2016; **215**: 345-355 [PMID: 27821494 DOI: 10.1083/jcb.201606042]
- Loh SH, Lee CY, Tsai YT, Shih SJ, Chen LW, Cheng TH, Chang CY, Tsai CS. Intracellular Acid-extruding regulators and the effect of lipopolysaccharide in cultured human renal artery smooth muscle cells. *PLoS One* 2014; **9**: e90273 [PMID: 24587308 DOI: 10.1371/journal.pone.0090273]

- 8 **Loh SH**, Chen WH, Chiang CH, Tsai CS, Lee GC, Jin JS, Cheng TH, Chen JJ. Intracellular pH regulatory mechanism in human atrial myocardium: functional evidence for Na⁽⁺⁾/H⁽⁺⁾ exchanger and Na⁽⁺⁾/HCO₃⁽⁻⁾ symporter. *J Biomed Sci* 2002; **9**: 198-205 [PMID: 12065894 DOI: 10.1159/000059420]
- 9 **Loh SH**, Jin JS, Tsai CS, Chao CM, Chiung CS, Chen WH, Lin CI, Chuang CC, Wei J. Functional evidence for intracellular acid extruders in human ventricular myocardium. *Jpn J Physiol* 2002; **52**: 277-284 [PMID: 12230804 DOI: 10.2170/jjphysiol.52.277]
- 10 **Lagadic-Gossmann D**, Buckler KJ, Vaughan-Jones RD. Role of bicarbonate in pH recovery from intracellular acidosis in the guinea-pig ventricular myocyte. *J Physiol* 1992; **458**: 361-384 [PMID: 1302269 DOI: 10.1113/jphysiol.1992.sp019422]
- 11 **Amos BJ**, Pocock G, Richards CD. On the role of bicarbonate as a hydrogen ion buffer in rat CNS neurones. *Exp Physiol* 1996; **81**: 623-632 [PMID: 8853270 DOI: 10.1113/expphysiol.1996.sp003963]
- 12 **Chen GS**, Lee SP, Huang SF, Chao SC, Chang CY, Wu GJ, Li CH, Loh SH. Functional and molecular characterization of transmembrane intracellular pH regulators in human dental pulp stem cells. *Arch Oral Biol* 2018; **90**: 19-26 [PMID: 29524788 DOI: 10.1016/j.archoralbio.2018.02.018]
- 13 **Lee CY**, Tsai YT, Chang CY, Chang YY, Cheng TH, Tsai CS, Loh SH. Functional characterization of intracellular pH regulators responsible for acid extrusion in human radial artery smooth muscle cells. *Chin J Physiol* 2014; **57**: 238-248 [PMID: 25241983 DOI: 10.4077/CJP.2014.BAD269]
- 14 **Vaughan-Jones RD**, Spitzer KW, Swietach P. Intracellular pH regulation in heart. *J Mol Cell Cardiol* 2009; **46**: 318-331 [PMID: 19041875 DOI: 10.1016/j.yjmcc.2008.10.024]
- 15 **Casey JR**, Grinstein S, Orlowski J. Sensors and regulators of intracellular pH. *Nat Rev Mol Cell Biol* 2010; **11**: 50-61 [PMID: 19997129 DOI: 10.1038/nrm2820]
- 16 **de Hemptinne A**, Marrannes R, Vanheel B. Influence of organic acids on intracellular pH. *Am J Physiol* 1983; **245**: C178-C183 [PMID: 6614155 DOI: 10.1152/ajpcell.1983.245.3.C178]
- 17 **Trosper TL**, Philipson KD. Functional characteristics of the cardiac sarcolemmal monocarboxylate transporter. *J Membr Biol* 1989; **112**: 15-23 [PMID: 2593136 DOI: 10.1007/BF01871160]
- 18 **Deuticke B**, Beyer E, Forst B. Discrimination of three parallel pathways of lactate transport in the human erythrocyte membrane by inhibitors and kinetic properties. *Biochim Biophys Acta* 1982; **684**: 96-110 [PMID: 7055558 DOI: 10.1016/0005-2736(82)90053-0]
- 19 **Wang X**, Poole RC, Halestrap AP, Levi AJ. Characterization of the inhibition by stilbene disulphonates and phloretin of lactate and pyruvate transport into rat and guinea-pig cardiac myocytes suggests the presence of two kinetically distinct carriers in heart cells. *Biochem J* 1993; **290**(Pt 1): 249-258 [PMID: 8439293 DOI: 10.1042/bj2900249]
- 20 **Reshetnyak YK**. Imaging Tumor Acidity: pH-Low Insertion Peptide Probe for Optoacoustic Tomography. *Clin Cancer Res* 2015; **21**: 4502-4504 [PMID: 26224874 DOI: 10.1158/1078-0432.CCR-15-1502]
- 21 **Damaghi M**, Wojtkowiak JW, Gillies RJ. pH sensing and regulation in cancer. *Front Physiol* 2013; **4**: 370 [PMID: 24381558 DOI: 10.3389/fphys.2013.00370]
- 22 **Swietach P**, Vaughan-Jones RD, Harris AL, Hulikova A. The chemistry, physiology and pathology of pH in cancer. *Philos Trans R Soc Lond B Biol Sci* 2014; **369**: 20130099 [PMID: 24493747 DOI: 10.1098/rstb.2013.0099]
- 23 **Lee SP**, Chao SC, Huang SF, Chen YL, Tsai YT, Loh SH. Expressional and Functional Characterization of Intracellular pH Regulators and Effects of Ethanol in Human Oral Epidermoid Carcinoma Cells. *Cell Physiol Biochem* 2018; **47**: 2056-2068 [PMID: 29975935 DOI: 10.1159/000491473]
- 24 **Webb BA**, Chimenti M, Jacobson MP, Barber DL. Dysregulated pH: a perfect storm for cancer progression. *Nat Rev Cancer* 2011; **11**: 671-677 [PMID: 21833026 DOI: 10.1038/nrc3110]
- 25 **Hanahan D**, Weinberg RA. Hallmarks of cancer: the next generation. *Cell* 2011; **144**: 646-674 [PMID: 21376230 DOI: 10.1016/j.cell.2011.02.013]
- 26 **Parks SK**, Chiche J, Pouyssegur J. Disrupting proton dynamics and energy metabolism for cancer therapy. *Nat Rev Cancer* 2013; **13**: 611-623 [PMID: 23969692 DOI: 10.1038/nrc3579]
- 27 **Moses C**, Garcia-Bloj B, Harvey AR, Blancafort P. Hallmarks of cancer: The CRISPR generation. *Eur J Cancer* 2018; **93**: 10-18 [PMID: 29433054 DOI: 10.1016/j.ejca.2018.01.002]
- 28 **Marchiq I**, Pouyssegur J. Hypoxia, cancer metabolism and the therapeutic benefit of targeting lactate/H⁽⁺⁾ symporters. *J Mol Med (Berl)* 2016; **94**: 155-171 [PMID: 26099350 DOI: 10.1007/s00109-015-1307-x]
- 29 **Lee ZW**, Teo XY, Song ZJ, Nin DS, Novera W, Choo BA, Dymock BW, Moore PK, Huang RY, Deng LW. Intracellular Hyper-Acidification Potentiated by Hydrogen Sulfide Mediates Invasive and Therapy Resistant Cancer Cell Death. *Front Pharmacol* 2017; **8**: 763 [PMID: 29163155 DOI: 10.3389/fphar.2017.00763]
- 30 **Amith SR**, Fliegel L. Regulation of the Na⁺/H⁺ Exchanger (NHE1) in Breast Cancer Metastasis. *Cancer Res* 2013; **73**: 1259-1264 [PMID: 23393197 DOI: 10.1158/0008-5472.CAN-12-4031]
- 31 **Lucien F**, Brochu-Gaudreau K, Arsenault D, Harper K, Dubois CM. Hypoxia-induced invadopodia formation involves activation of NHE-1 by the p90 ribosomal S6 kinase (p90RSK). *PLoS One* 2011; **6**: e28851 [PMID: 22216126 DOI: 10.1371/journal.pone.0028851]
- 32 **Takahashi K**, Tanabe K, Ohnuki M, Narita M, Ichisaka T, Tomoda K, Yamanaka S. Induction of pluripotent stem cells from adult human fibroblasts by defined factors. *Cell* 2007; **131**: 861-872 [PMID: 18035408 DOI: 10.1016/j.cell.2007.11.019]
- 33 **Gu W**, Gaeta X, Sahakyan A, Chan AB, Hong CS, Kim R, Braas D, Plath K, Lowry WE, Christofk HR. Glycolytic Metabolism Plays a Functional Role in Regulating Human Pluripotent Stem Cell State. *Cell Stem Cell* 2016; **19**: 476-490 [PMID: 27618217 DOI: 10.1016/j.stem.2016.08.008]
- 34 **Yoshida Y**, Takahashi K, Okita K, Ichisaka T, Yamanaka S. Hypoxia enhances the generation of induced pluripotent stem cells. *Cell Stem Cell* 2009; **5**: 237-241 [PMID: 19716359 DOI: 10.1016/j.stem.2009.08.001]
- 35 **Zhang J**, Nuebel E, Daley GQ, Koehler CM, Teitell MA. Metabolic regulation in pluripotent stem cells during reprogramming and self-renewal. *Cell Stem Cell* 2012; **11**: 589-595 [PMID: 23122286 DOI: 10.1016/j.stem.2012.10.005]
- 36 **Wang H**, Singh D, Fliegel L. The Na⁺/H⁺ antiporter potentiates growth and retinoic acid-induced differentiation of P19 embryonal carcinoma cells. *J Biol Chem* 1997; **272**: 26545-26549 [PMID: 9334233 DOI: 10.1074/jbc.272.42.26545]
- 37 **Chaudhry MA**, Bowen BD, Piret JM. Culture pH and osmolality influence proliferation and embryoid body yields of murine embryonic stem cells. *Biochem Eng J* 2009; **45**: 126-135 [DOI: 10.1016/j.bej.2009.03.005]
- 38 **Zaniboni M**, Swietach P, Rossini A, Yamamoto T, Spitzer KW, Vaughan-Jones RD. Intracellular proton mobility and buffering power in cardiac ventricular myocytes from rat, rabbit, and guinea pig. *Am J Physiol Heart Circ Physiol* 2003; **285**: H1236-H1246 [PMID: 12750065 DOI: 10.1152/ajpheart.00277.2003]
- 39 **Leem CH**, Lagadic-Gossmann D, Vaughan-Jones RD. Characterization of intracellular pH regulation in the guinea-pig ventricular myocyte. *J Physiol* 1999; **517** (Pt 1): 159-180 [PMID: 10226157 DOI: 10.1111/j.1469-7793.1999.0159z.x]
- 40 **Boedtker E**, Aalkjaer C. Acid-base transporters modulate cell migration, growth and proliferation: Implications for structure development and remodeling of resistance arteries? *Trends Cardiovasc Med* 2013; **23**: 59-65 [PMID: 23266155 DOI: 10.1016/j.tcm.2012.09.001]
- 41 **Romero MF**, Chen AP, Parker MD, Boron WF. The SLC4 family of bicarbonate (HCO₃⁻) transporters. *Mol Aspects Med* 2013; **34**: 159-182 [PMID: 23506864 DOI: 10.1016/j.mam.2012.10.008]
- 42 **Boedtker E**, Aalkjaer C. Intracellular pH in the resistance vasculature: regulation and functional implications. *J Vasc Res* 2012; **49**: 479-496 [PMID: 22907294 DOI: 10.1159/000341235]
- 43 **da Costa-Pessoa JM**, Damasceno RS, Machado UF, Beloto-

- Silva O, Oliveira-Souza M. High glucose concentration stimulates NHE-1 activity in distal nephron cells: the role of the Mek/Erk1/2/p90RSK and p38MAPK signaling pathways. *Cell Physiol Biochem* 2014; **33**: 333-343 [PMID: 24557342 DOI: 10.1159/000356673]
- 44 **Li X**, Wang T, Zhao Z, Weinman SA. The CIC-3 chloride channel promotes acidification of lysosomes in CHO-K1 and Huh-7 cells. *Am J Physiol Cell Physiol* 2002; **282**: C1483-C1491 [PMID: 11997263 DOI: 10.1152/ajpcell.00504.2001]
- 45 **Takahashi Y**, Fujii T, Fujita K, Shimizu T, Higuchi T, Tabuchi Y, Sakamoto H, Naito I, Manabe K, Uchida S, Sasaki S, Ikari A, Tsukada K, Sakai H. Functional coupling of chloride-proton exchanger CIC-5 to gastric H⁺K⁺-ATPase. *Biol Open* 2014; **3**: 12-21 [PMID: 24429108 DOI: 10.1242/bio.20136205]
- 46 **Dascalu A**, Nevo Z, Korenstein R. The control of intracellular pH in cultured avian chondrocytes. *J Physiol* 1993; **461**: 583-599 [PMID: 8394427 DOI: 10.1113/jphysiol.1993.sp019530]
- 47 **Theparambil SM**, Naoshin Z, Thyssen A, Deitmer JW. Reversed electrogenic sodium bicarbonate cotransporter 1 is the major acid loader during recovery from cytosolic alkalosis in mouse cortical astrocytes. *J Physiol* 2015; **593**: 3533-3547 [PMID: 25990710 DOI: 10.1113/JP270086]
- 48 **Kim N**, Minami N, Yamada M, Imai H. Immobilized pH in culture reveals an optimal condition for somatic cell reprogramming and differentiation of pluripotent stem cells. *Reprod Med Biol* 2016; **16**: 58-66 [PMID: 29259452 DOI: 10.1002/rmb2.12011]
- 49 **Gupta P**, Hourigan K, Jadhav S, Bellare J, Verma P. Effect of lactate and ph on mouse pluripotent stem cells: Importance of media analysis. *Biochem Eng J* 2017; **118**: 25-33 [DOI: 10.1016/j.bej.2016.11.005]
- 50 **Liu A**, Yu X, Liu S. Pluripotency transcription factors and cancer stem cells: small genes make a big difference. *Chin J Cancer* 2013; **32**: 483-487 [PMID: 23419197 DOI: 10.5732/cjc.012.10282]
- 51 **Varum S**, Rodrigues AS, Moura MB, Momcilovic O, Easley CA 4th, Ramalho-Santos J, Van Houten B, Schatten G. Energy metabolism in human pluripotent stem cells and their differentiated counterparts. *PLoS One* 2011; **6**: e20914 [PMID: 21698063 DOI: 10.1371/journal.pone.0020914]
- 52 **Tsai CS**, Loh SH, Jin JS, Hong GJ, Lin HT, Chiung CS, Chang CY. Effects of alcohol on intracellular pH regulators and electro-mechanical parameters in human myocardium. *Alcohol Clin Exp Res* 2005; **29**: 1787-1795 [PMID: 16269908 DOI: 10.1097/01.alc.0000183512.31705.74]
- 53 **Tsai YT**, Lee CY, Hsu CC, Chang CY, Hsueh MK, Huang EY, Tsai CS, Loh SH. Effects of urotensin II on intracellular pH regulation in cultured human internal mammary artery smooth muscle cells. *Peptides* 2014; **56**: 173-182 [PMID: 24768794 DOI: 10.1016/j.peptides.2014.04.011]
- 54 **Weinberger L**, Ayyash M, Novershtern N, Hanna JH. Dynamic stem cell states: naive to primed pluripotency in rodents and humans. *Nat Rev Mol Cell Biol* 2016; **17**: 155-169 [PMID: 26860365 DOI: 10.1038/nrm.2015.28]
- 55 **Altshuler A**, Verbuk M, Bhattacharya S, Abramovich I, Haklai R, Hanna JH, Kloog Y, Gottlieb E, Shalom-Feuerstein R. RAS Regulates the Transition from Naive to Primed Pluripotent Stem Cells. *Stem Cell Reports* 2018; **10**: 1088-1101 [PMID: 29456180 DOI: 10.1016/j.stemcr.2018.01.004]
- 56 **Folmes CD**, Dzeja PP, Nelson TJ, Terzic A. Metabolic plasticity in stem cell homeostasis and differentiation. *Cell Stem Cell* 2012; **11**: 596-606 [PMID: 23122287 DOI: 10.1016/j.stem.2012.10.002]
- 57 **Ryall JG**, Cliff T, Dalton S, Sartorelli V. Metabolic Reprogramming of Stem Cell Epigenetics. *Cell Stem Cell* 2015; **17**: 651-662 [PMID: 26637942 DOI: 10.1016/j.stem.2015.11.012]
- 58 **Singh AM**, Reynolds D, Cliff T, Ohtsuka S, Mattheyses AL, Sun Y, Menendez L, Kulik M, Dalton S. Signaling network crosstalk in human pluripotent cells: a Smad2/3-regulated switch that controls the balance between self-renewal and differentiation. *Cell Stem Cell* 2012; **10**: 312-326 [PMID: 22385658 DOI: 10.1016/j.stem.2012.01.014]
- 59 **Chen G**, Gulbranson DR, Hou Z, Bolin JM, Ruotti V, Probasco MD, Smuga-Otto K, Howden SE, Diol NR, Propson NE, Wagner R, Lee GO, Antosiewicz-Bourget J, Teng JM, Thomson JA. Chemically defined conditions for human iPSC derivation and culture. *Nat Methods* 2011; **8**: 424-429 [PMID: 21478862 DOI: 10.1038/nmeth.1593]
- 60 **Cho YM**, Kwon S, Pak YK, Seol HW, Choi YM, Park DJ, Park KS, Lee HK. Dynamic changes in mitochondrial biogenesis and antioxidant enzymes during the spontaneous differentiation of human embryonic stem cells. *Biochem Biophys Res Commun* 2006; **348**: 1472-1478 [PMID: 16920071 DOI: 10.1016/j.bbrc.2006.08.020]
- 61 **Malo ME**, Li L, Fliegel L. Mitogen-activated protein kinase-dependent activation of the Na⁺/H⁺ exchanger is mediated through phosphorylation of amino acids Ser770 and Ser771. *J Biol Chem* 2007; **282**: 6292-6299 [PMID: 17209041 DOI: 10.1074/jbc.M611073200]
- 62 **Javadov S**, Baetz D, Rajapurohitam V, Zeidan A, Kirshenbaum LA, Karmazyn M. Antihypertrophic effect of Na⁺/H⁺ exchanger isoform 1 inhibition is mediated by reduced mitogen-activated protein kinase activation secondary to improved mitochondrial integrity and decreased generation of mitochondrial-derived reactive oxygen species. *J Pharmacol Exp Ther* 2006; **317**: 1036-1043 [PMID: 16513848 DOI: 10.1124/jpet.105.100107]
- 63 **Snabaitis AK**, Cuello F, Avkiran M. Protein kinase B/Akt phosphorylates and inhibits the cardiac Na⁺/H⁺ exchanger NHE1. *Circ Res* 2008; **103**: 881-890 [PMID: 18757828 DOI: 10.1161/CIRCRESAHA.108.175877]
- 64 **Meima ME**, Webb BA, Witkowska HE, Barber DL. The sodium-hydrogen exchanger NHE1 is an Akt substrate necessary for actin filament reorganization by growth factors. *J Biol Chem* 2009; **284**: 26666-26675 [PMID: 19622752 DOI: 10.1074/jbc.M109.019448]
- 65 **Clement DL**, Mally S, Stock C, Lethan M, Satir P, Schwab A, Pedersen SF, Christensen ST. PDGFR α signaling in the primary cilium regulates NHE1-dependent fibroblast migration via coordinated differential activity of MEK1/2-ERK1/2-p90RSK and AKT signaling pathways. *J Cell Sci* 2013; **126**: 953-965 [PMID: 23264740 DOI: 10.1242/jcs.116426]

P- Reviewer: Saeki K, Tanabe S S- Editor: Ma YJ

L- Editor: A E- Editor: Song H



Basic Study

Platelet-rich plasma enhances adipose-derived stem cell-mediated angiogenesis in a mouse ischemic hindlimb model

Chia-Fang Chen, Han-Tsung Liao

Chia-Fang Chen, Han-Tsung Liao, Department of Plastic and Reconstructive Surgery, Chang Gung Memorial Hospital, Taoyuan 333, Taiwan

Han-Tsung Liao, Craniofacial Research Center, Chang Gung Memorial Hospital, College of Medicine, Chang Gung University, Taoyuan 333, Taiwan

ORCID number: Chia-Fang Chen (0000-0003-2911-7547); Han-Tsung Liao (0000-0001-9259-9839).

Author contributions: Liao HT contributed to study design, editing, reviewing, and final approval of article; Chen CF performed experiments, analyzed the data, and wrote the article.

Supported by grant from the National Sci-Tech Program, Ministry of Science and Technology, No. NRMPG3E0471 and No. NRMPG3D0231; and a Chang Gung Memorial Hospital grant, No. CMRPGHB0011.

Institutional review board statement: This study was approved by the Institutional Review Board of Chang Gung Memorial Hospital.

Institutional animal care and use committee statement: The animal use protocol has been reviewed and approved by the Institutional Animal Care and Use Committee of Chang Gung Memorial Hospital.

Conflict-of-interest statement: The authors have declared no conflicts of interest.

Data sharing statement: Requests for access to data should be addressed to the corresponding author.

ARRIVE guidelines statement: The authors have read the ARRIVE guidelines, and the manuscript was prepared and revised according to the ARRIVE guidelines.

Open-Access: This is an open-access article that was selected by an in-house editor and fully peer-reviewed by external reviewers. It is distributed in accordance with the Creative Commons Attribution Non Commercial (CC BY-NC 4.0) license, which permits others to distribute, remix, adapt, build upon this work non-commercially, and license their derivative works on different

terms, provided the original work is properly cited and the use is non-commercial. See: <http://creativecommons.org/licenses/by-nc/4.0/>

Manuscript source: Unsolicited manuscript

Corresponding author to: Han-Tsung Liao, MD, PhD, Associate Professor, Chief Doctor, Department of Plastic and Reconstructive Surgery, Chang Gung Memorial Hospital, No. 5 Fusing Street, Taoyuan 333, Taiwan. lia01211@gmail.com
Telephone: +886-3-3281200
Fax: +886-3-3972681

Received: August 9, 2018

Peer-review started: August 9, 2018

First decision: August 31, 2018

Revised: October 18, 2018

Accepted: November 7, 2018

Article in press: November 7, 2018

Published online: December 26, 2018

Abstract

AIM

To evaluate the angiogenic effect of platelet-rich plasma (PRP)-preconditioned adipose-derived stem cells (ADSCs) both in vitro and in a mouse ischemic hindlimb model.

METHODS

ADSCs were divided based on culture medium: 2.5% PRP, 5% PRP, 7.5% PRP, and 10% PRP. Cell proliferation rate was analyzed using the MTS assay. The gene expression of CD31, vascular endothelial growth factor, hypoxia-inducible factors, and endothelial cell nitric oxide synthase was analyzed using reverse transcription polymerase chain reaction. Cell markers and structural changes were assessed through immunofluorescence staining and the tube formation assay. Subsequently, we studied the *in vivo* angiogenic capabilities of ADSCs

by a mouse ischemic hindlimb model.

RESULTS

The proliferation rate of ADSCs was higher in the 2.5%, 5%, and 7.5% PRP groups. The expression of hypoxia-inducible factor, CD31, vascular endothelial growth factor, and endothelial cell nitric oxide synthase in the 5% and 7.5% PRP groups increased. The 5%, 7.5%, and 10% PRP groups showed higher abilities to promote both CD31 and vascular endothelial growth factor production and tubular structure formation in ADSCs. According to laser Doppler perfusion scan, the perfusion ratios of ischemic limb to normal limb were significantly higher in 5% PRP, 7.5% PRP, and human umbilical vein endothelial cells groups compared with the negative control and fetal bovine serum (FBS) groups (0.88 ± 0.08 , 0.85 ± 0.07 and 0.81 ± 0.06 for 5%, 7.5% PRP and human umbilical vein endothelial cells compared with 0.42 ± 0.17 and 0.54 ± 0.14 for the negative control and FBS, $P < 0.01$).

CONCLUSION

PRP-preconditioned ADSCs presented endothelial cell characteristics *in vitro* and significantly improved neovascularization in ischemic hindlimbs. The optimal angiogenic effect occurred in 5% PRP- and 7.5% PRP-preconditioned ADSCs.

Key words: Platelet-rich plasma; Adipose-derived stem cells; Mesenchymal stem cell; Angiogenesis; Endothelial differentiation; Mouse ischemic hindlimb model

© The Author(s) 2018. Published by Baishideng Publishing Group Inc. All rights reserved.

Core tip: We reported the *in vitro* angiogenic effect of platelet-rich plasma (PRP) treated adipose-derived stem cells (ADSCs) and the neovascularization ability of these cells in animal models. This is significant because we demonstrated that ADSCs presented endothelial cell characteristics after PRP treatment. We were the first to observe that treatment with PRP-preconditioned ADSCs significantly enhanced circulation in mouse ischemic hindlimbs models. Our result further showed that 5% and 7.5% PRP exerted the optimal effect on promoting angiogenesis of ADSCs and improving perfusion. We developed a stem cell-based, safe, and efficient way to promote peripheral circulation in animal model.

Chen CF, Liao HT. Platelet-rich plasma enhances adipose-derived stem cell-mediated angiogenesis in a mouse ischemic hindlimb model. *World J Stem Cells* 2018; 10(12): 212-227
URL: <https://www.wjgnet.com/1948-0210/full/v10/i12/212.htm>
DOI: <https://dx.doi.org/10.4252/wjsc.v10.i12.212>

INTRODUCTION

Peripheral artery disease (PAD) is caused by peripheral

artery obstruction, which may lead to ischemic changes in the extremities. Due to insufficient blood flow in the musculature, patients may present with symptoms such as pain, claudication, or even tissue necrosis. Smoking, diabetes mellitus, hypercholesterolemia, hypertension, and renal insufficiency have all been reported to have high correlations with PAD. The pathological features of PAD include lumen obstruction caused by atherosclerotic plaques and destruction of vessel walls. Research has shown that elderly individuals and patients with diabetes mellitus are prone to these vasculature problems^[1]. The current trend of the increasing populations of elder people and patients with diabetes mellitus is accompanied with the increased prevalence of PAD.

Current therapies for PAD are primarily aimed at relieving the discomfort and slowing the progress of the disease. In advanced PAD, revascularization surgery is indicated for large to medium-sized peripheral arteries with obstructions. However, ideal treatment for small arteries with obstructions has not been established. Therefore, treatments for obstructive lesions in small vessels are urgently required. Therapeutic angiogenesis provides a novel strategy for managing PAD; this strategy induces new vessel development in ischemic tissue, which can improve local perfusion.

Angiogenesis comprises many steps. Establishing stable and functional vascular networks is complicated. During ischemia, the damaged tissue releases growth factors to attract endothelial progenitor cells (EPCs). These cells proliferate, migrate, and form tubular structures, and finally achieve angiogenesis^[2]. Microscopically, many growth factors are involved in angiogenesis. The angiogenic switch is initiated by hypoxia. Hypoxia-inducible factors (HIFs) are transcription factors that respond to hypoxia, and they play crucial roles in maintaining hemostasis during low oxygen conditions. During hypoxia, HIFs bind to targets, including the vascular endothelial growth factor (VEGF) gene, subsequently increasing the expression of downstream factors including transforming growth factor alpha and platelet-derived growth factor. Angiogenesis promotes endothelial cell proliferation and migration^[3]. Endothelial cell nitric oxide synthase (eNOS), which is secreted by endothelial cells, exerts synergistic effects on neovascularization by increasing vessel wall permeability and promoting endothelial cell migration. CD31 also plays a crucial role in angiogenesis. It is a cell-cell adhesion molecule located on the endothelial cell membrane. Without CD31 stimulation, endothelial cells cannot form tubular structures. Through the synergistic effects of the mentioned factors, endothelial cells form new vessels at the ischemic site and subsequently establish a stable and functional perfusion system. Therefore, in research, these factors are commonly used as angiogenic markers for evaluating endothelial cell differentiation.

A previous study proved that mesenchymal stem cells (MSCs) can be used to form EPCs and promote

angiogenesis, and MSCs are thus useful for vascular tissue engineering^[4]. However, limited stem cell numbers circulate in the blood, which poses a major problem to the clinical application of these cells^[5]. Although human adult stem cells can be obtained from many accessible sources, such as the bone marrow, teeth, and skeletal muscle, isolating human adult stem cells from the aforementioned tissue is difficult due to limited cell numbers and high donor site morbidities^[6]. Recently, researchers have focused their attention on fat tissue-derived MSCs, adipose-derived stem cells (ADSCs). ADSCs were discovered in 2002 by researchers at University of California at Los Angeles; they have become a popular therapeutic strategy in current stem cell research. Abundant ADSCs can be retrieved from autologous fat tissue, and no controversy and ethical concerns are associated with these cells. In contrast to bone marrow-, teeth-, or skeletal muscle-derived stem cells, ADSCs are much easier to obtain. ADSCs can be collected through liposuction, which is a commonly performed cosmetic procedure^[7,8]. Furthermore, after appropriate induction, ADSCs exhibit endothelial cell properties. All these characteristics render ADSCs more suitable for clinical use than other types of stem cells.

Fetal bovine serum (FBS) is widely used in research settings for the *in vitro* culture of ADSCs. However, culturing cells for therapeutic purposes in patients is associated with zoonotic disease transmission and xenotransplantation concerns. Alternative culture medium for ADSCs should be human-derived and should meet the criteria proposed by the International Society of Cellular Therapy (ISCT) and International Fat Applied Technology Society (IFATS)^[9,10]. Because human serum is a natural reservoir of growth factors, and it has already been proved to be effective endothelial lineage differentiation media, several researchers have applied human serum products to culture ADSCs and induce angiogenesis *in vitro*. Recently, autologous conditioned serum, namely platelet-rich plasma (PRP), has shown great potential. PRP is an autologous reservoir of growth factors and cytokines. In summary, PRP has great potential to replace animal serum as culture medium.

To date, limited data are available on the effects of PRP on ADSCs. Our study evaluated the angiogenic potential of PRP-preconditioned ADSCs. In addition, ADSCs' biological characteristics and their capability to induce angiogenesis both *in vitro* and *in vivo* were evaluated.

MATERIALS AND METHODS

All experimental procedures were performed as per hospital regulations and medical ethics standards.

Preparation of PRP

Concentrated human PRP (UltraGRO™) was purchased from AventaCell BioMedical Co., Ltd. ([http://www.](http://www.atcbiomed.com)

[atcbiomed.com](http://www.atcbiomed.com), United States). Blood donors were tested by the supplying company as per the United States regulations for the preparation of blood components. These donors were negative for mycoplasma, human immunodeficiency virus, hepatitis B virus, hepatitis C virus, human T-lymphotropic virus type 1 [determined by polymerase chain reaction (PCR) and serologic testing], anti-*Trypanosoma cruzi* antibody, and syphilis (determined by serologic testing).

Preparation of human ADSCs from human fat

Human raw lipoaspirates were derived from our patients undergoing selective suction-assisted lipectomy and were isolated following the procedure described by Zuk *et al.*^[11] with modifications. After harvesting, the lipoaspirates were washed extensively to remove blood cells, and the lipoaspirates, which were obtained under local anesthetics, were digested with 0.075% collagenase in a 37 °C water bath for 30 min. Subsequently, the cell pellet was collected through centrifugation and was incubated overnight in Dulbecco's modified eagle medium (DMEM) supplemented with 10% FBS at 37 °C in 5% CO₂.

Flow cytometry analysis

Flow cytometry analysis was performed to characterize the phenotypes of ADSCs. Cells were cultured in medium containing different concentrations of PRP (2.5%, 5%, 7.5%, and 10% PRP) or 10% FBS (control group). At least 1×10^6 cells per well were incubated with fluorescence-labeled monoclonal antibodies against human CD34 (BD Biosciences, San Jose, CA, United States), CD45 (BD Biosciences), CD73 (R&D Systems), CD90 (BD Biosciences), and CD105 (R&D Systems). After washing, the labeled cells were analyzed through flow cytometry using BD FACSCalibur™ and the BD CellQuest™ Pro.

Cell proliferation assay

To determine the optimal concentration of PRP for ADSC proliferation, ADSCs were cultured in medium containing different concentrations of PRP (2.5%, 5%, 7.5%, and 10% PRP) or 10% FBS (control group). At least 5×10^3 ADSCs were seeded per well and were incubated at 37 °C in 5% CO₂. Subsequently, the proliferation of ADSCs in each group was determined using the CellTiter 96 AQueous One Solution Reagent (Promega Co., Madison, WI, United States), which contains a novel tetrazolium salt (MTS). The tetrazolium salt MTS is reduced by living cells into a colored formazan product. The quantity of the formazan product is directly proportional to the number of viable cells. In our experiment, the colorimetric measurement of the formazan dye was performed at a wavelength of 490 nm on an enzyme-linked immuno sorbent assay plate reader (Molecular Devices, Sunnyvale, CA, United States). Cell numbers were determined using a calibration curve plotting the

number of ADSCs vs the absorbance values on days 0, 3, 5, and 7.

Reverse transcription-PCR

Mature and functional endothelial markers were evaluated through reverse transcription-PCR (RT-PCR). ADSCs were incubated in culture medium containing different concentrations of PRP (2.5%, 5%, 7.5%, and 10% PRP); 10% FBS was used as the control group. After culturing for 14 d, RNA was isolated using a GeneJET RNA Purification Kit (Thermo Fisher Scientific, Waltham, MA, United States) in accordance with the manufacturer's protocols. The expression of angiogenic-related genes, namely CD31 and CD34, was analyzed. The constitutively expressed gene encoding β -actin was used as an internal control in RT-PCR to normalize the amounts of mRNA in each sample.

Immunofluorescence staining

ADSCs were cultured in medium containing different concentrations of PRP (2.5%, 5%, 7.5%, and 10% PRP) or 10% FBS (control group). Approximately 1×10^4 cells were incubated at 37 °C in 5% CO₂. On days 7 and 14, to identify the endothelial differentiation of ADSCs, immunofluorescence staining was performed using the following antibodies: rabbit polyclonal antibody (1:200) against human CD31 (1:50) and rabbit polyclonal antibody against VEGF. Antibodies with fluorescent labels were used. The immunostaining intensity was observed through confocal microscopy and was then quantified using Image J. The corrected total cellular fluorescence ratio was calculated using the following formula: corrected total cellular fluorescence = integrated density (area of selected cell \times mean fluorescence of background readings).

Tube formation assay

Matrigel was thawed and suspended in 96-well plates and solidified at 37 °C for 30 min. ADSCs were cultured in medium containing different concentrations of PRP (2.5%, 5%, 7.5%, and 10% PRP) or 10% FBS (control group) for 14 d. Cells were then seeded at a density of approximately 1×10^5 cells per well and were labeled using Live-Dead Cell Staining Kits. The tubular structure was examined under a confocal microscope. Endothelial differentiation was assessed by determining the average length, total tube length, branch numbers, and total branch points through Image J.

Animal care protocol and nude mouse ischemic hindlimb model

Animal care and experiments were approved by the Local Ethics Committee for Animal Research Studies at Chang Gung Memorial Hospital. All nude mice were kept in laboratory conditions (controlled temperature 23 °C and humidity 50%) with free access to water and food for 4 wk prior to experimentation. ADSCs were pre-conditioned by culturing in medium containing 5% PRP,

7.5% PRP, and 10% FBS. Additionally, human umbilical vein endothelial cells (HUVECs) were used as a positive control. Mice administered with local injections of phosphate buffer solution (PBS) only (no ADSCs) were used as negative controls. General anesthesia was done by mixture of Zoletil and Xylazine 0.1 cc intraperitoneal injection before all experiments. The proximal portion of the right femoral artery of 8-wk-old nude mice was ligated using an electrosurgical pencil. About 3×10^6 preconditioned ADSCs and HUVECs were directly injected over the medial thigh muscle and lateral thigh muscle groups. Blood flow in both the ischemic hindlimb and normal hindlimb was measured using a laser Doppler blood flow meter on days 0, 1, 4, 7, 11, 14, and 18.

Immunohistochemistry study

Nude mice were sacrificed on day 18. All mice were euthanized by carbon dioxide overdose for tissue collection. The muscle of the ischemic hindlimb was fixed in paraformaldehyde and sectioned into slices. To identify endothelial cells, immunohistochemical analysis was performed using rabbit polyclonal antibody against mouse CD31 antibody. The sections were then treated with diaminobenzidine and were stained using hematoxylin and eosin stain. Capillary density was determined by measuring the capillary numbers/mm² under a microscope.

Statistical analysis

All the data are reported as mean \pm standard deviation. Statistical analyses among the multiple group data are carried out using a one-way analysis of variance test to determine the significant differences. Turkey's *post-hoc* test is used to determine the difference between any two groups with $P < 0.05$ considered statistically significant.

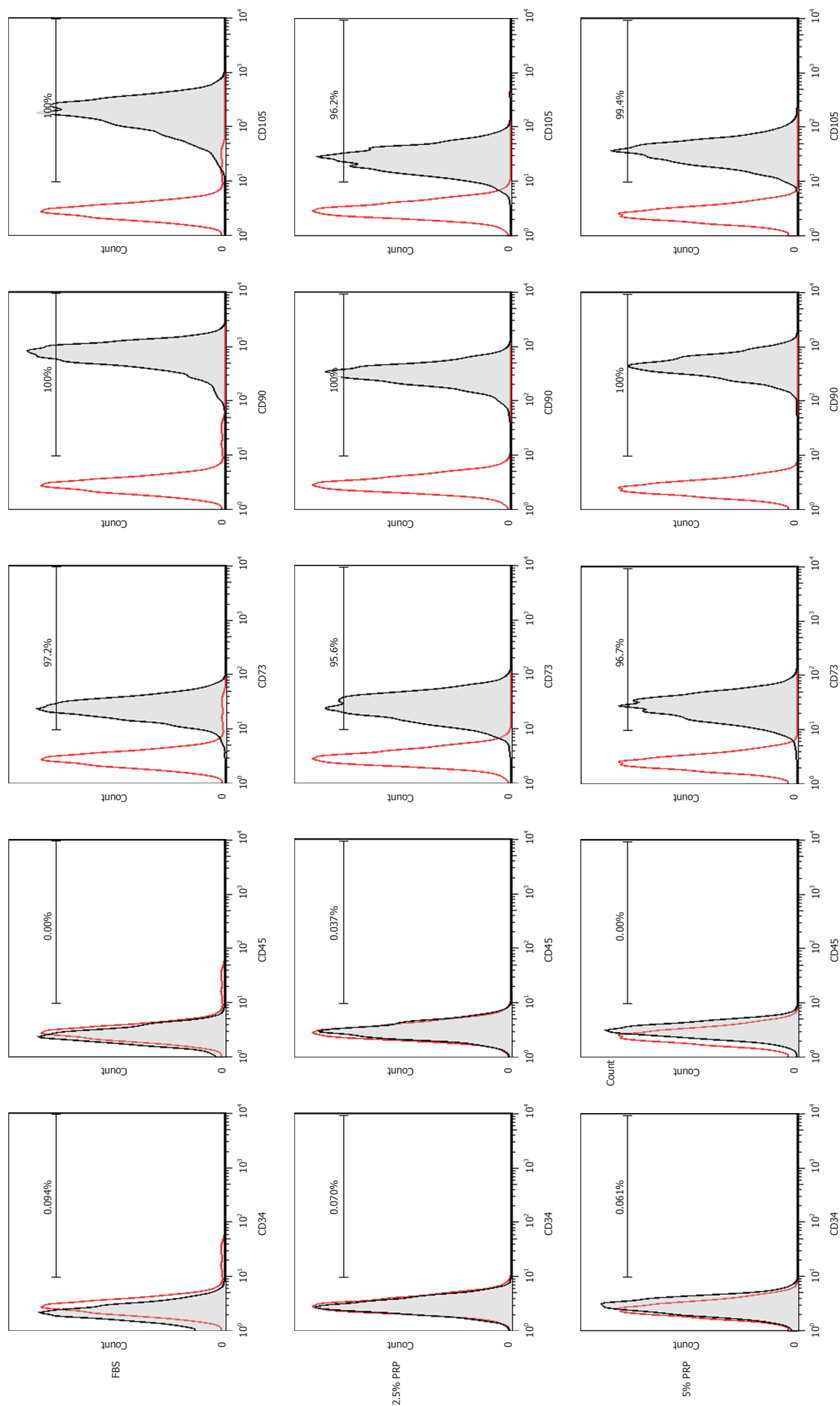
RESULTS

Characterization of ADSCs

Flow cytometry was performed to characterize the phenotypes of ADSCs after their culture in medium containing PRP (Figure 1). Most of PRP- preconditioned ADSCs (98%-99%) were positive for endoglin receptor (CD105), the surface enzyme ecto-59-nucleotidase (CD73), and extracellular matrix protein (CD90). However, they were negative for markers of hematopoietic lineage (CD34) and the leukocyte common antigen (CD45). The cells presented cell markers specific to MSCs and these phenotypes meet the criteria proposed by the ISCT and IFATS for ADSCs.

Cell proliferation assay

The cell proliferation rate is presented as the growth ratio (%), which was calculated using the following formula: ADSC numbers on day 3, 5, or 7/ADSC numbers on day 0. The cell proliferation rate was increased from



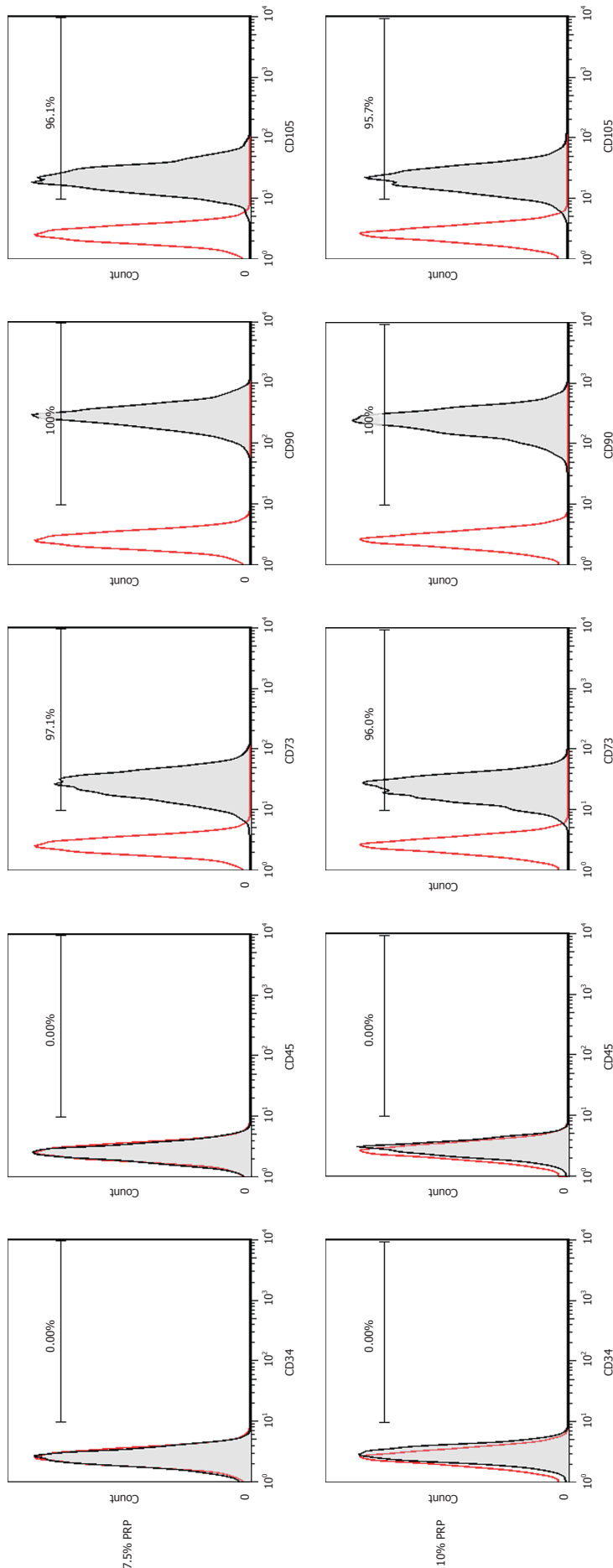


Figure 1 Flow cytometry of platelet-rich plasma preconditioned adipose-derived stem cells. Most of the platelet-rich plasma preconditioned cells (98%-99%) were positive for CD105, CD73 and CD90, but negative for hematopoietic lineage markers including CD34 and CD45. The cells presented cell markers specific to mesenchymal stem cells. PRP: Platelet-rich plasma; FBS: Fetal bovine serum.

day 3 in PRP groups compared with the FBS group. At the endpoint (day 7), the proliferation rate of ADSCs was significantly higher in the 2.5%, 5%, and 7.5% PRP groups (25.348 ± 2.572 , 31.778 ± 2.523 , 33.400 ± 5.428 for 2.5% PRP, 5% PRP, 7.5% PRP, respectively) than in the 10% FBS (control group) and 10% PRP groups (15.483 ± 3.071 and 14.168 ± 2.650 for 10% FBS and 10% PRP; $P < 0.01$). The results suggested that 2.5%, 5%, and 7.5% PRP showed a higher ability to increase ADSC proliferation compared with FBS (Figure 2).

RT-PCR

Angiogenic-related gene expression was analyzed by RT-PCR. Relative quantification of RT-PCR was done by calculating the difference of the dCt value between the target groups and the FBS group. Compared with the FBS group, the expression of HIF mRNA was significantly increased in the 5% and 7.5% PRP groups ($P < 0.01$; Figure 3A). The mRNA expression of endothelial cell markers, including CD31 and VEGF, was markedly higher in the 5%, 7.5%, and 10% PRP groups than in the 2.5% PRP and FBS groups ($P < 0.01$; Figure 3B and C). The eNOS mRNA expression level was also increased in the 5%, 7.5%, and 10% PRP groups ($P < 0.01$; Figure 3D). RT-PCR analysis revealed that the expression levels of *HIF*, *CD31*, *VEGF*, and *eNOS* genes were significantly higher in the 5% PRP and 7.5% PRP groups ($P < 0.01$). In RT-PCR, the expression of angiogenic-related genes was higher in the 5% and 7.5% PRP groups.

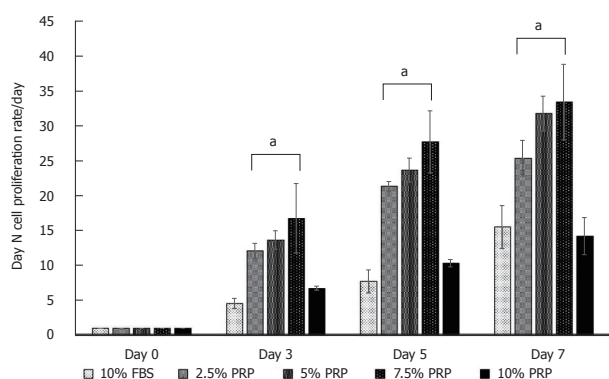


Figure 2 Cell proliferation assay. At the endpoint (day 7), the proliferation rate of ADSCs was significantly higher in the 2.5%, 5%, and 7.5% PRP groups (25.348 ± 2.572 , 31.778 ± 2.523 , 33.400 ± 5.428 for 2.5% PRP, 5% PRP, 7.5% PRP, respectively) than in the 10% FBS (control group) and 10% PRP groups (15.483 ± 3.071 and 14.168 ± 2.650 for 10% FBS and 10% PRP; $P < 0.01$). The results suggested that 2.5%, 5%, and 7.5% PRP showed a higher ability to increase ADSC proliferation compared with FBS. Data are expressed as mean \pm standard deviation. ^a $P < 0.01$ vs 10% FBS group. ADSC: Adipose-derived stem cell; PRP: Platelet-rich plasma; FBS: Fetal bovine serum.

Immunofluorescence staining for angiogenic protein expression

The protein production level was analyzed through immunofluorescence staining. After culturing for 14 d, CD31 expression was significantly higher in all PRP groups compared with the FBS group ($P < 0.01$; Figure 4A and C). According to the immunofluorescence staining results, the early elevated production of VEGF was noted from day 7 in the 5% and 7.5% PRP groups. On day 14, 5%, 7.5%, and 10% PRP groups showed considerable increases in VEGF production (Figure 4B and D). VEGF and CD31, which are produced by endothelial cells, are key proteins in angiogenesis. VEGF and CD31 production increased after ADSCs were cultured in medium containing PRP. The 5%, 7.5%, and 10% PRP groups showed a higher ability to promote both CD31 and VEGF production by ADSCs.

Morphological changes in ADSCs

EPCs form tubes, connecting to each other, and are then arranged in clusters. Thus, morphological change is also a crucial parameter for evaluating the level of endothelial differentiation. Microscopy revealed the tubular structure of ADSCs in all PRP groups (Figure 5A). We quantified tube formation by determining the average length, tube numbers, and branch points (Figure 5B). Overall performance was evaluated based on the total tube length, which was calculated using the following formula: average length \times tube numbers. Although the tubular structure was observed through microscopy, morphological changes in ADSCs cultured in 2.5% PRP were nonsignificant compared with those in the control group ($P > 0.05$). The result showed that ADSCs in the 5%, 7.5%, and 10% PRP groups showed more tube formation, more cell-cell interconnections (evaluated by branch points), and longer tubes ($P < 0.01$).

PRP-preconditioned ADSCs improved revascularization in the ischemic mouse hindlimb

In our *in vitro* studies, 5% PRP and 7.5% PRP had higher abilities to promote the endothelial differentiation of ADSCs. We further designed an *in vivo* study to evaluate the angiogenic potential of these two groups. Blood vessel ligation was performed on the right hindlimb of nude mice. ADSCs from the PBS, FBS, 5% PRP, and 7.5% PRP groups and from HUVECs were applied to the wound immediately after surgery. Blood perfusion was measured immediately after surgery and on postoperative day 18 by using the laser Doppler blood flow meter. In representative images, red and blue indicated areas with normal blood perfusion and ischemia, respectively (Figure 6A). Image J was used to quantify laser Doppler images, and the result was expressed as the perfusion ratio (%), which was calculated using the following formula: blood flow in operated hindlimb/blood flow in non-operated hindlimb. Data revealed improved blood flow in the ischemic hindlimb after PRP treatment (Figure 6B). The revascularization rate remained low in the PBS and 10% FBS groups, with the ratios of 0.42 ± 0.16 and 0.54 ± 0.14 , respectively, on day 18. The PRP and HUVEC groups showed significantly higher ratios on day 18 (0.88 ± 0.08 , 0.85 ± 0.07 , 0.81 ± 0.06 for 5% PRP, 7.5% PRP, and HUVECs, respectively) than the PBS group (0.42 ± 0.17 ; $P < 0.01$). No significant difference was observed in the perfusion ratios of the PRP and HUVEC groups ($P > 0.05$). Although serial laser Doppler images showed some natural recovery of hindlimb blood flow in control groups, administering PRP-preconditioned ADSCs to the ischemic site significantly increased tissue perfusion.

Histological staining of muscle sections

CD31 is a key glycoprotein expressed at endothelial cell intercellular junctions, and it is often used as an angiogenesis marker in research. In the present study, CD31 was used to demonstrate the presence of endothelial cells in histological tissue sections. Capillary density was assessed through quantification of CD31-positive capillaries, and the density was determined by measuring capillary numbers/mm². Consistent with the findings obtained from laser Doppler image analysis, the capillary densities of the PRP groups were significantly higher than those of the control and FBS groups, as shown in Figure 7A and quantified in Figure 7B (26.95 ± 9.21 , 30.22 ± 4.80 , 13.03 ± 4.46 , and 14.22 ± 4.14 for 5% PRP, 7.5% PRP, 10% FBS, and the control group, respectively). The 5% PRP and HUVEC groups had similar angiogenesis effects, and the 7.5% PRP group had the optimal result among all groups. The capillary density significantly increased in the 7.5% PRP group, even when compared with the positive control HUVEC group (30.22 ± 4.80 and 20.03 ± 5.67 for 7.5% PRP and HUVEC, respectively; $P < 0.05$). Overall, these data demonstrated that 5% PRP and 7.5% PRP-preconditioned ADSCs significantly enhanced

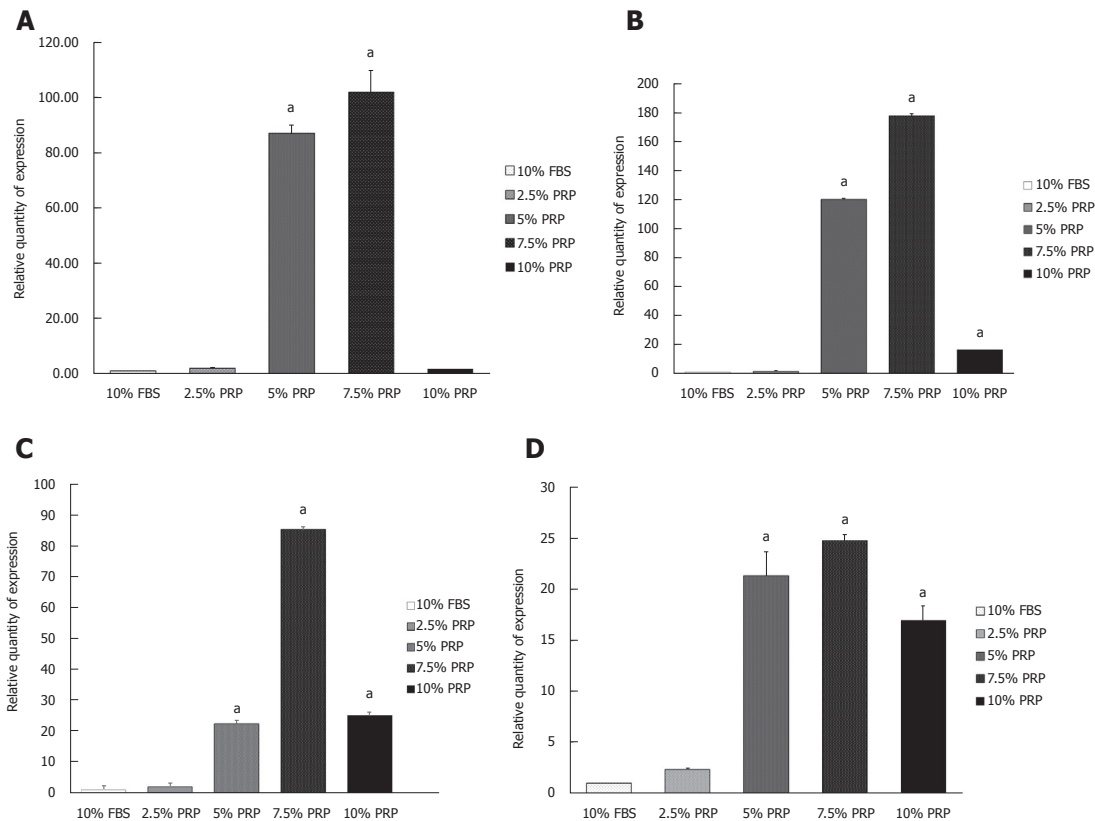


Figure 3 Analysis of gene expression of adipose-derived stem cell by reverse transcription polymerase chain reaction. A: The expression of hypoxia-inducible factor mRNA was significantly increased in the 5% and 7.5% PRP groups compared with the FBS group; B: The expression of CD31 mRNA was significantly higher in the 5%, 7.5%, and 10% PRP groups compared with the FBS group; C: The expression of vascular endothelial growth factor was markedly higher in the 5% and 7.5% PRP groups compared with the FBS group; D: The expression of endothelial cell nitric oxide synthase was significantly increased in the 5% and 7.5% PRP groups compared with the FBS group. Data are expressed as means \pm standard deviation. ^a $P < 0.01$ vs 10% FBS group. ADSC: Adipose-derived stem cell; PRP: Platelet-rich plasma; FBS: Fetal bovine serum.

physiologic neovascularization in ischemic tissue.

DISCUSSION

Our results showed that ADSCs cultured in medium containing PRP exhibited the properties of endothelial cells in terms of gene expression, angiogenic-related protein production, and morphological changes (*i.e.*, tubular structure formation). The ischemic hindlimb model showed significantly improved blood perfusion after local injection with PRP-preconditioned ADSCs. Histochemical analysis of CD31 in muscle sections also provided the same result. Notably, compared with FBS, PRP exhibited a higher ability to promote the endothelial differentiation of ADSCs. The 5% PRP and 7.5% PRP groups had the optimal result among all groups. These findings suggest that 5% PRP and 7.5% PRP are suitable substitutes for FBS when culturing ADSCs and can achieve angiogenesis and improve perfusion in ischemic tissue.

Flow cytometry

Cell surface markers such as CD105, CD73, and CD90 are associated with the stemness of MSCs. Any change in cell surface markers indicates that stem cells may

have committed to other lineages. In our study, PRP was added to medium to culture ADSCs. However, some concerns still exist that PRP might change the stem cell characteristics of MSCs. Li *et al.*^[12] found that after culturing in PRP, MSCs maintained their stem cell marker expression as well as multilineage differentiation capacity. Moreover, another study found that the percentage of surface markers remained the same in ADSCs after culturing in PRP^[13]. We showed similar findings in flow cytometry. Our ADSCs presented cell markers specific to stromal stem cells after PRP treatment.

Cell proliferation

PRP is a human blood derivative that is rich in growth factors. A previous paper reported that PRP could promote proliferation of ADSCs^[14]. The ability of PRP to accelerate cell proliferation of stem cells may come from α -granules, which have many growth factors in a physiological ratio, such as platelet-derived growth factor, transforming growth factor- β , VEGF, epidermal growth factor, insulin-like growth factor, *etc.*^[15]. These growth factors all play crucial roles for enhancing cell proliferation. However, only a few studies report the effects of different PRP concentrations on ADSC

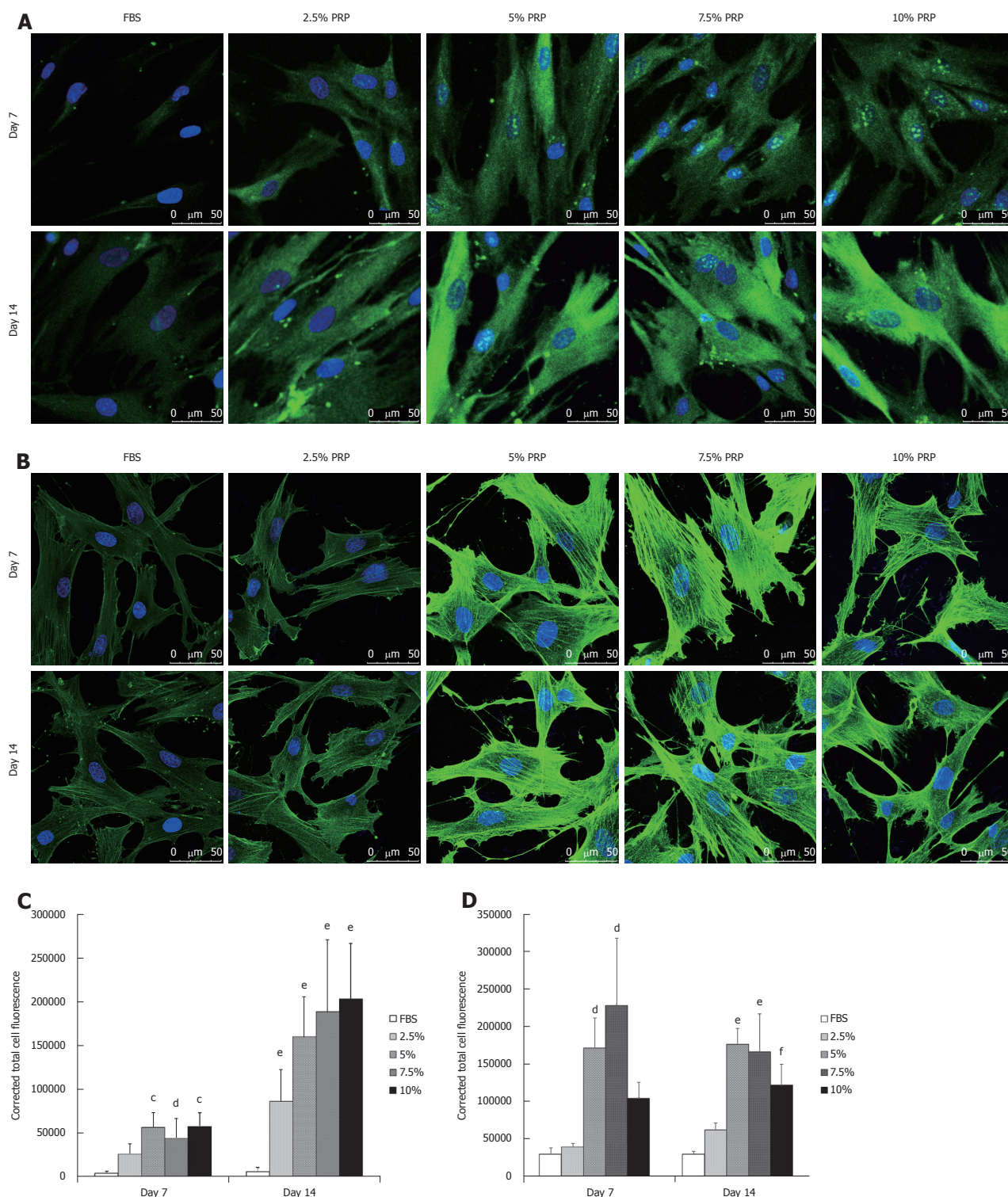


Figure 4 Immunofluorescence staining of CD31 and vascular endothelial growth factor. A: After culturing for 14 d, CD31 expression (in green) was higher in all PRP groups; B: After culturing for 14 d, VEGF expression (in green) was higher in all PRP groups; C: The immunostaining intensity was observed through confocal microscopy and was then quantified using Image J. The corrected total cellular fluorescence ratio was calculated using the following formula: corrected total cellular fluorescence = integrated density (area of selected cell × mean fluorescence of background readings). After culturing for 14 d, CD31 expression (in green) was significantly higher in all PRP groups than in the FBS group. D: The early elevated production of VEGF was noted from day 7 in the 5% and 7.5% PRP groups. On day 14, 5%, 7.5%, and 10% PRP groups showed considerable increases in VEGF production. Data are expressed as means ± standard deviation. ^c $P < 0.01$ vs 10% FBS group at day 7; ^d $P < 0.05$ vs 10% FBS group at day 7; ^e $P < 0.01$ vs 10% FBS group at day 14; ^f $P < 0.05$ vs 10% FBS group at day 14. PRP: Platelet-rich plasma; FBS: Fetal bovine serum; VEGF: Vascular endothelial growth factor.

proliferation. Early studies found that PRP had a dose dependent effect on proliferation of ADSCs^[16-18]. How-

ever, later studies had opposite opinions. One study demonstrated that a PRP concentration of 10% to 20%

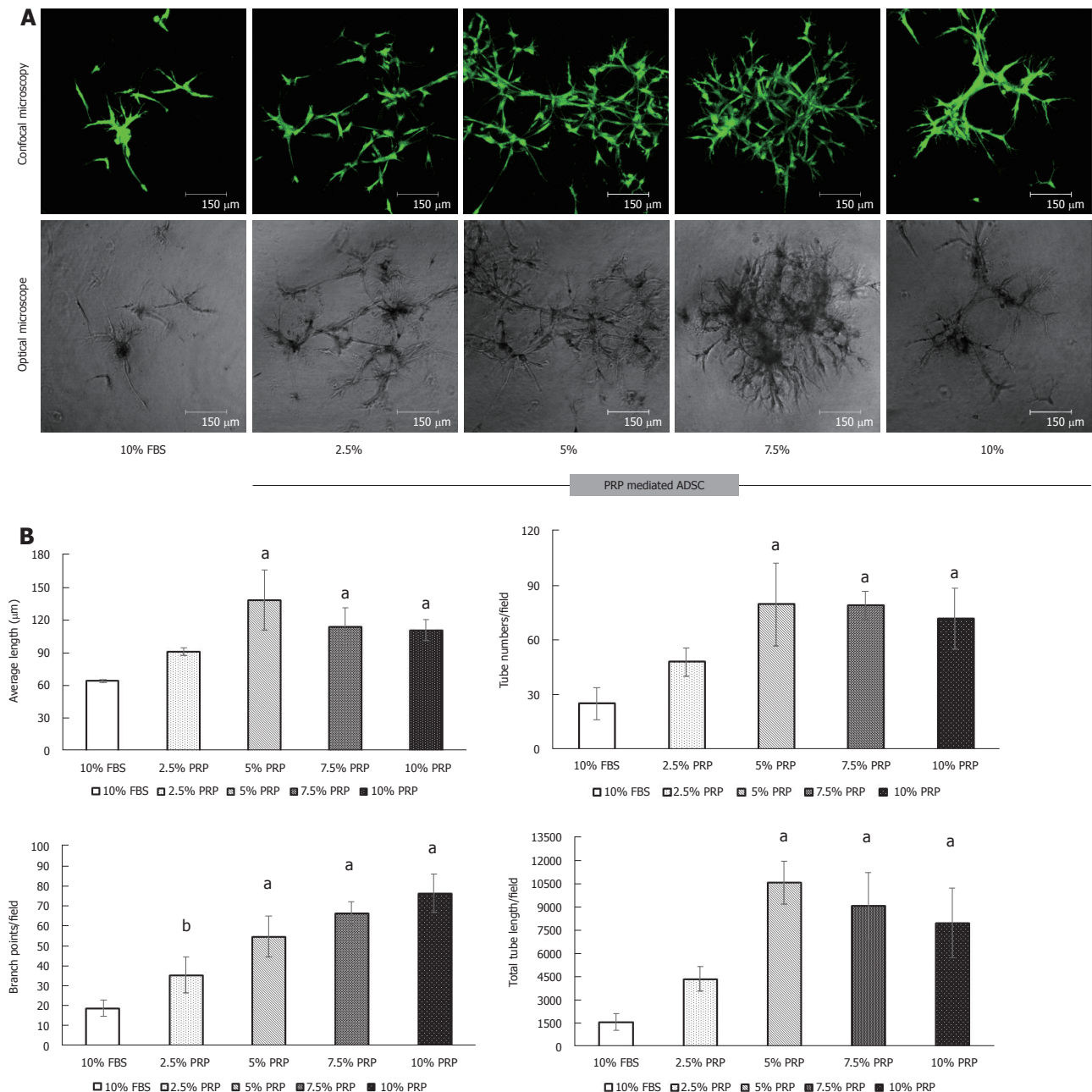


Figure 5 Tube formation assay. A: Tubular structure was noted in all PRP-treated ADSC groups; B: Tube formation was quantified by average length, tube numbers, and branch points. Overall performance was evaluated based on the total tube length, which was calculated using the following formula: average length \times tube numbers. The result showed that ADSCs in the 5%, 7.5%, and 10% PRP groups showed more tube formation, more cell-cell interconnections (evaluated by branch points), and longer tubes. Data are expressed as means \pm standard deviation. $^aP < 0.01$ vs 10% fetal bovine serum group. PRP: Platelet-rich plasma; FBS: Fetal bovine serum; ADSC: Adipose-derived stem cell.

had the highest impact on cell proliferation. Proliferation rates declined with higher PRP concentration^[19]. In another study, ADSCs were cultured in medium with PRP concentrations from 1% to 30%. The result showed that ADSCs were better grown in 5% and 10% PRP^[20]. Another paper had a similar result that 10% PRP in the culture medium markedly promoted cell proliferation while a higher concentration (30%) of PRP had less effect on cell proliferation^[21]. It is possible that an inhibitory effect is exerted if the concentration of growth factors or cytokines is too high. In our study, we noted that PRP significantly increased ADSC proliferation

compared with 10% FBS based medium. However, the PRP concentration was not directly proportional to the proliferation rate. It is notable that 2.5%, 5%, and 7.5% PRP had better results compared with others. Kakudo *et al.*^[22] also observed a similar finding. The best dose of PRP for cell proliferation of ADSC may vary from study to study due to different ADSC and PRP preparation methods. It is difficult to compare results between studies due to the lack of standardized protocols for ADSC and PRP collection.

Platelets contain abundant α -granules. These α -granules play important roles in regulating secretory and

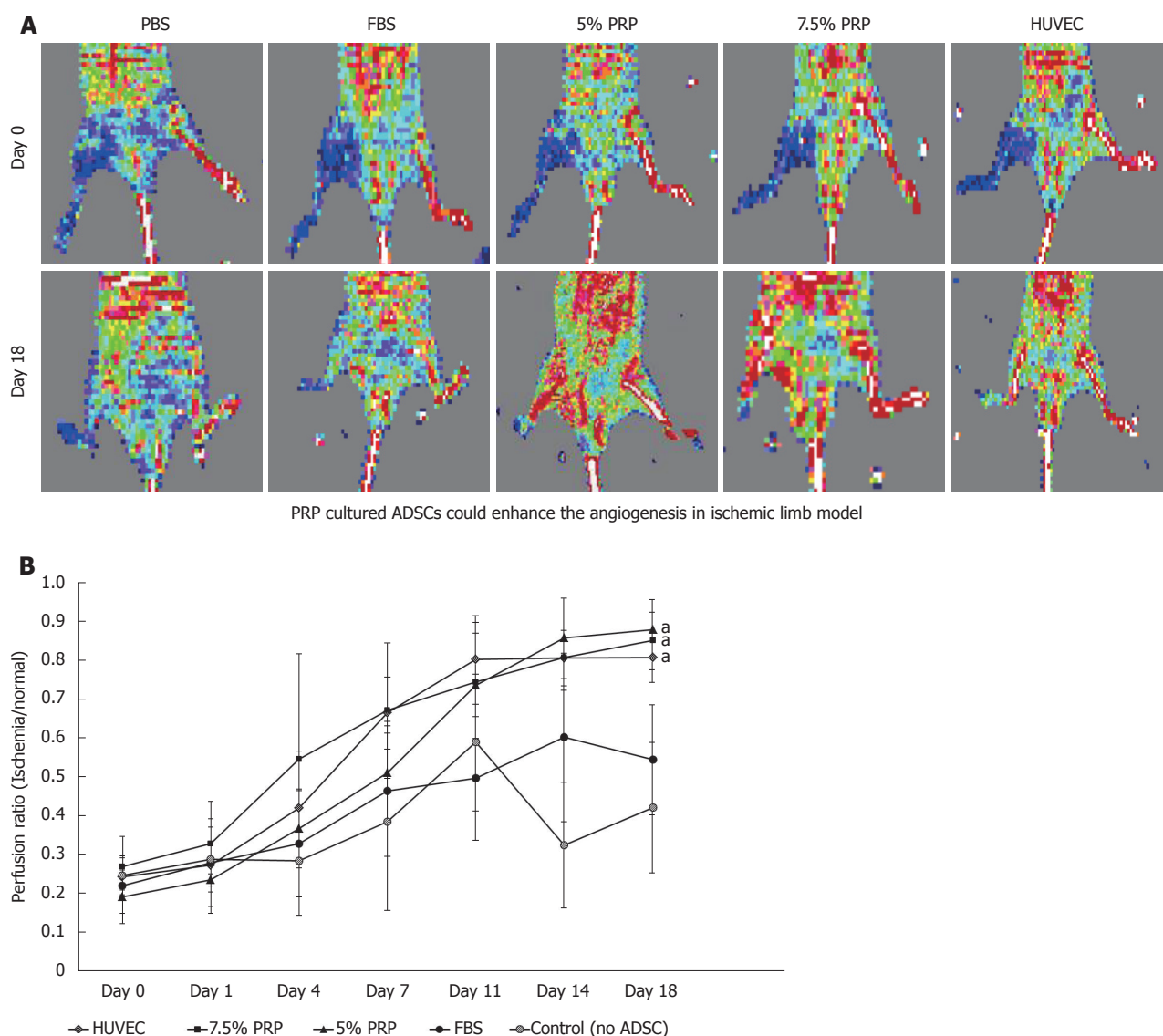


Figure 6 Ischemic hindlimb model. A: Red and blue indicate areas with normal blood perfusion and ischemia, respectively. Although serial laser Doppler images showed some natural recovery of hindlimb blood flow in control groups, administering PRP-preconditioned ADSCs to the ischemic site increased tissue perfusion; B: Quantification was done by perfusion ratio (%): blood flow in operated hindlimb/blood flow in non-operated hindlimb. The revascularization rate remained low in the phosphate buffer solution and 10% FBS groups, with the ratios of 0.42 ± 0.16 and 0.54 ± 0.14 , respectively, on day 18. The PRP and HUVEC groups showed significantly higher ratios on day 18 (0.88 ± 0.08 , 0.85 ± 0.07 , 0.81 ± 0.06 for 5% PRP, 7.5% PRP, and HUVECs, respectively) than the phosphate buffer solution group (0.42 ± 0.17). Data are expressed as means \pm standard deviation. $^*P < 0.01$ vs 10% FBS group. PRP: Platelet-rich plasma; FBS: Fetal bovine serum; ADSC: Adipose-derived stem cell; HUVEC: Human umbilical vein endothelial cell; PBS: Phosphate buffer solution.

angiogenesis pathways. However, α -granules not only release a variety of growth factors, but also contain regulatory proteins like the thrombospondin family. Thrombospondin-1 inhibits adhesion, proliferation, and tube formation of endothelial cells in culture, and it has been found to block neovascularization. Thrombospondin-2 also inhibits the migration and proliferation of endothelial cells. One study correlated large amounts of thrombospondin-1 detected in PRP with high concentrations of PRP could significantly decrease cell proliferation^[23]. Whether the thrombospondin family is the most critical regulatory factor compromising angiogenic ability of PRP during high concentration needs further investigation.

RT-PCR and immunofluorescence staining

In this study, markers including HIF, VEGF, CD31, and eNOS were used to evaluate ADSC-mediated angiogenesis. Gene expression was also confirmed through immunofluorescence staining. ADSCs cultured in PRP gained an endothelial phenotype, as demonstrated by the high expression of CD31 and VEGF. In a previous study, HIF was upregulated in ischemic tissues in response to low oxygen status^[24]. Another study showed that through HIF-1 production, downstream genes were activated to achieve angiogenesis, cell proliferation, and cell survival^[25]. ADSCs produced more HIF under low oxygen conditions^[26]. The present study is the first to report that not only oxygen deprivation but also PRP

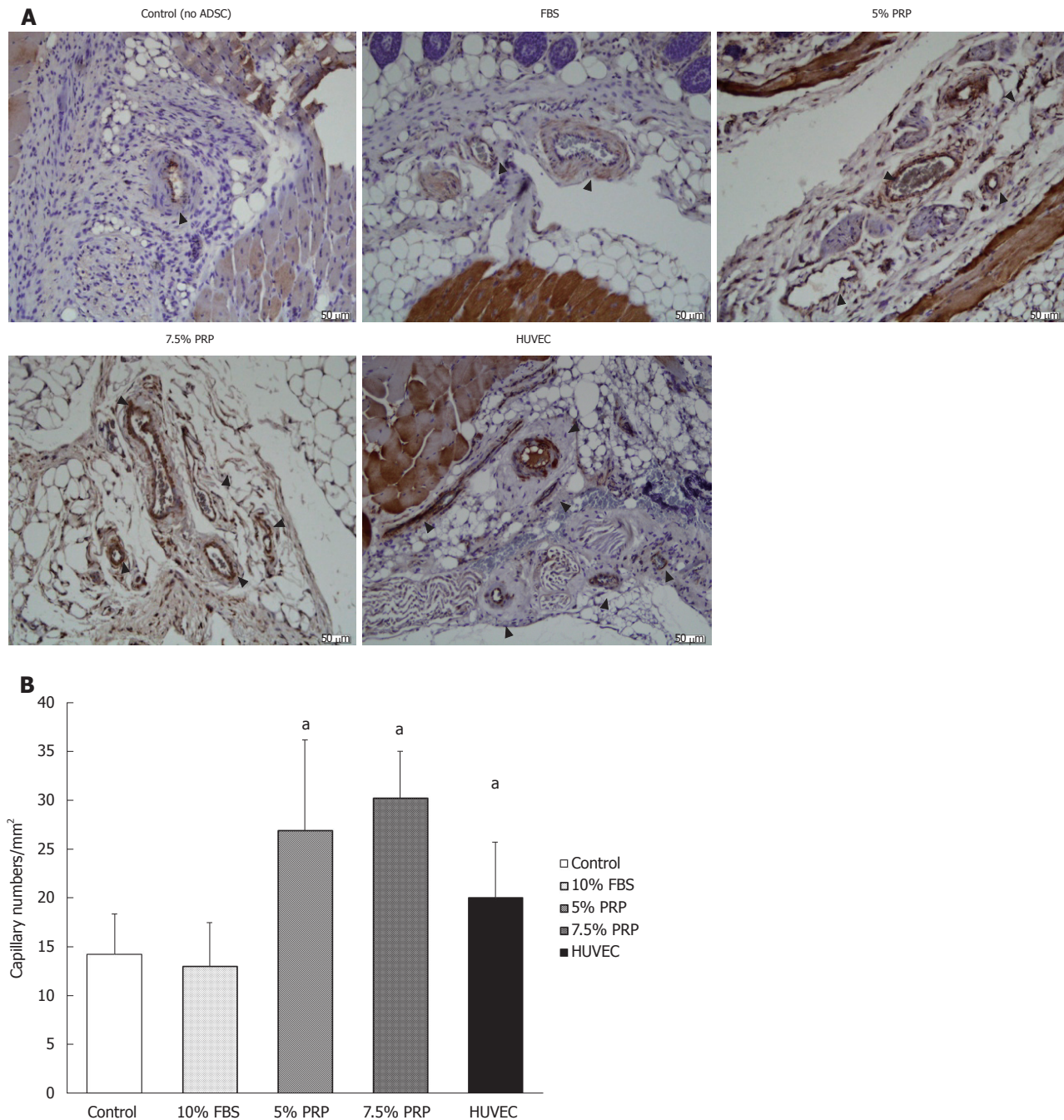


Figure 7 Histological staining of muscle sections. A: The capillary densities of the PRP groups were higher than those of the control and FBS groups; B: We used CD31 stained sections to identify capillary numbers under microscopy. Capillary density was determined by measuring capillary numbers/mm². The 5% PRP, 7.5% PRP, and human umbilical vein endothelial cell groups had better results than the FBS group. Data are expressed as means \pm standard deviation. ^a $P < 0.01$ vs 10% FBS group. PRP: Platelet-rich plasma; FBS: Fetal bovine serum; ADSC: Adipose-derived stem cell; HUVEC: Human umbilical vein endothelial cell.

treatment can assist ADSCs to produce more HIF, further activating angiogenesis.

HIF-1 α is a subunit of HIF-1, and it can activate several angiogenic genes and their receptors under hypoxic status. VEGF is upregulated by HIF-1 α , and it is the principal stimulatory factor in angiogenesis^[27,28]. VEGF binds to VEGF receptor and activates the mitogen-activated protein kinase/extracellular signal-regulated kinase pathway to achieve cell proliferation. VEGF also activates the phosphatidylinositol 3-kinase/protein

kinase B pathway to increase eNOS production^[29]. eNOS then increases vessel wall permeability and facilitates the chemotactic migration of EPCs toward VEGF. VEGF also attracts cells including EPCs, mural cells, and hematopoietic stem cells to the ischemic site. These stem cells produce capillary plexuses and eventually form mature vessels. All these processes together cause the development of new vessels for vascular supply in ischemic limbs^[30]. PRP is rich in VEGF and has been proven to enhance angiogenesis both *in vitro* and *in*

vivo. ADSCs were also able to increase the VEGF level in the nude mouse model established through local injection, enabling vessel growth in ischemic tissue^[31]. We hypothesized that local VEGF concentration could be further elevated through both work from PRP and ADSC. In our study, we proved that HIF and the downstream angiogenic-related genes VEGF and eNOS were upregulated in the PRP groups. High expression of the endothelial cell surface marker CD31 in the PRP groups was also strong evidence that PRP treatment induced the endothelial differentiation of ADSCs.

Tube formation assay

A variety of stem cells had been adopted to cell therapy. Regardless of their tissue origins, MSCs from different origins can express similar endothelial-relevant functions *in vitro*^[32]. ADSCs are a kind of MSC, with the capacity to become various cells including adipocytes, chondrocytes, and osteocytes. ADSCs also retained the ability to differentiate toward an endothelial lineage. The elder age, cardiovascular disease, obesity, or tobacco use of donors does not alter the isolation. Besides endothelial cell related molecular expression, functional characteristics were evaluated by the tube formation assay. After proper differentiation, ADSCs formed tubular structures upon plating on Matrigel, indicating that ADSCs were able to differentiate toward endothelial cells and participate in angiogenesis. Our finding was consistent to previous studies that demonstrated that ADSCs participate in angiogenesis.

Single growth factor VEGF or boosting VEGF expression by curcumin had been applied in a tubular formation assay to promote capillary structure formation of stem cells^[33,34]. However, stimulation of neovascularization involves complex steps and the result is influenced by multiple growth factors. Single growth factor VEGF use may have limitations to establish stable blood vessels. It is notable that PRP is a natural growth factor reservoir and had been proved to accelerate proliferation and stimulate capillary tube formation of endothelial cells^[35]. Compared with FBS, PRP better supported the formation of lumen-like structures and the alignment of multicentric junctions of endothelial cells^[36]. One study had found that formation of capillary like structures of HUVECs became maximal at 5% PRP^[37]. Another study demonstrated that capillary-like structures were more prevalent in certain concentrations of PRP (0.5%, 1% and 3% PRP) compared with either the control group (0% PRP) or higher concentrations (5% and 10% PRP) in a co-culture system of HUVECs and human dermal fibroblast cells^[38]. These two studies demonstrated PRP induced capillary-like structures of HUVECs in a bell-shaped dose-response curve. A previous study has proven that ADSCs differentiated into endothelial cells and produced capillary-like structures as HUVECs did *in vitro*^[7]. However, no studies worked on the dose-dependent effect of PRP on ADSCs for formation of capillary-like structures. In our study, we found PRP

significantly induced morphologic change of ADSCs. Further investigation indicated that tubular formation was proportional to PRP concentration between 2.5% to 7.5% PRP level, suggesting that proper ratio of angiogenic factors in PRP is important for formation of functional blood vessels by ADSCs.

From our results, the higher concentration of PRP lowered the proliferation rate of ADSCs and further reduced endothelial differentiation. Pro-angiogenic and anti-angiogenic molecules released by activation of plasma thrombin receptors during tissue injury gives an explanation to above phenomenon. As mentioned above, α -granules in the platelets contain regulatory proteins like the thrombospondin family. These proteins regulate angiogenesis by inhibiting MSC proliferation, tubular formation, and migration. Besides, the pro-angiogenic VEGF in α -granules and the anti-angiogenic endostatin in plasma were released upon platelet activation^[39]. Balance between local VEGF and endostatin concentration accounts for the net biological effect on injured tissue^[40]. High levels of anti-angiogenic molecules present in plasma should be considered when using high concentrations of PRP in tissue engineering.

Nude mouse ischemic hindlimb model

Increasing research attention has been paid to PAD due to the increased disease prevalence. Various treatment strategies have been developed to induce new vessel formation and restore tissue perfusion through the use of exogenous molecular and cellular agents. The ischemic hindlimb model of mice has been widely used for the *in vivo* investigation of cell therapy.

Although preclinical results of single-dose growth factor use in ischemic animal models were promising, the therapy did not have long-lasting clinical effects due to the short half-life of growth factors^[41]. Maintaining a stable level of growth factors is essential. Early studies have demonstrated that compared with the single-dose administration of VEGF, a drug delivery system that enabled the sustained release of growth factors significantly increased tissue blood flow, number of arterioles, and vascular density in the rabbit ischemic hindlimb model^[42,43]. Gelatin hydrogels, polylactic-co-glycolic acid, and alginate are commonly used to make such granules. However, degradation time varies among different granules, and complete degradation may not be achieved. The residual foreign body is associated with a higher risk of infection and safety concerns, limiting the clinical application of granules. Gaining a comprehensive understanding of EPCs has enabled various stem cells to be utilized for endothelial differentiation and ischemic tissue repair. The focus has moved toward stem cell-based therapeutic angiogenesis, and ADSCs are promising stem cell types in therapeutic angiogenesis.

Many studies have demonstrated the angiogenic potential of ADSCs not only *in vitro* but also *in vivo*. In mouse ischemic hindlimb models, increased circu-

lating endothelial cells were detected after local ADSC injection. The ischemic limbs recovered from muscle injury, and muscle sections exhibited increased vascular density^[44,45]. Studies have found that neovascularization in ischemic tissue is attributed not only to the endothelial differentiation of ADSCs but also to their paracrine effects. Conditioned media obtained from ADSCs contained multiple angiogenic cytokines, including HIF, VEGF, fibroblast growth factor, and hepatocyte growth factor^[46]. Through these growth factors, ADSCs augmented surrounding cell remodeling, reduced endothelial cell atrophy, and stimulated angiogenesis. However, the survival rates of ADSCs transplanted in the animal ischemic hindlimb model were variable. Multiple treatments have been developed to increase the survival and modify the angiogenic potential of ADSCs for cell therapy.

Under hypoxic conditions, the survival rate of ADSCs and the revascularization of animal ischemic hindlimbs are improved with the upregulation of HIF-1 α and VEGF as the underlying mechanism^[47,48]. Although researchers have reported that growth factors may have positive effects on the proliferation and endothelial differentiation of ADSCs, PRP treated ADSCs have never been applied in animal models. This study is the first to apply PRP, which is a natural reservoir of growth factors, to culture ADSCs and to evaluate cell angiogenic potential *in vivo*. Our hypothesis was that synergistic effects of multiple growth factors in PRP would increase the survival rate and endothelial differentiation of ADSCs. Application of these preconditioned ADSCs to ischemic tissue may achieve higher revascularization. PRP-preconditioned ADSCs had a higher ability to promote neovascularization *in vivo* compared with ADSCs preconditioned in common culture medium (*i.e.*, FBS).

In the present study, we determined the effect of PRP concentration on cell angiogenic potential. HUVECs, which are known to have a strong ability to promote angiogenesis in animal ischemic hindlimb models, providing nearly 80% blood perfusion recovery (compared with the normal hindlimb) in our mouse experiment. However, 5% and 7.5% PRP-preconditioned ADSCs provided even more favorable results in the animal model. In the ischemic hindlimb, 5% and 7.5% PRP-preconditioned ADSCs achieved perfusion rates as high as 85% and 88%, respectively. The result of muscle histological sections staining was consistent with those obtained from laser Doppler image analysis.

Conclusion

In conclusion, our study provided a new therapeutic strategy for PAD. Both ADSCs and PRP offer many advantages, including abundant resources, efficient preparation, and safety. Moreover, the clinical application of ADSCs and PRP is associated with lower risks of xeno-immune responses and zoonotic disease transmission. Previous studies reported that PRP had limited effects on the recovery of blood perfusion and

wound healing, which was mostly likely due to the rapid degradation of PRP *in vivo*. Therefore, instead of direct injection into tissue, ADSCs were preconditioned with PRP before cell implantation, which improved the angiogenic potential of cells and thus increased neovascularization in ischemic limbs. The balance between local angiogenic and proangiogenic factors accounts for the net biological effect on injured tissue. We further observed that 5% and 7.5% PRP provided the optimal effect on enhancing the angiogenic potential of ADSCs. Based on this finding, we believe that PRP treated ADSCs may be clinically applied for treating ischemic tissues and promoting wound healing in the future. Further research should focus on increasing the rate of ADSC differentiation into mature endothelial cells and finding key regulators for three-dimensional tubular structure formation in these cells. The optimal goal is to use ADSCs to form stable and functional vessels for patients with PAD.

ARTICLE HIGHLIGHTS

Research background

Peripheral artery disease (PAD) is caused by peripheral artery obstruction, which may lead to ischemic changes in the extremities. In advanced PAD, revascularization surgery is indicated for large to medium-sized peripheral arteries with obstructions. However, ideal treatment for small arteries with obstructions has not been established until now.

Research motivation

Therapeutic angiogenesis provides a novel strategy for managing PAD. Mesenchymal stem cells can be used to promote tissue angiogenesis. Among all mesenchymal stem cells, adipose-derived stem cells (ADSCs) are plentiful, easy to retrieve with less donor site morbidity, and free from ethical concerns, making it a good candidate for therapeutic angiogenesis. Fetal bovine serum (FBS) is widely used in research settings for culturing ADSCs. However, culturing cells for therapeutic purposes in patients is associated with zoonotic disease transmission and xeno-immunization concerns. Platelet-rich plasma (PRP) is an autologous reservoir of growth factors and cytokines, which have great potential to replace animal serum as culture medium.

Research objectives

To date, limited data are available on the effects of PRP on ADSCs. Our study evaluated the angiogenic potential of PRP-preconditioned ADSCs. In addition, ADSCs' biological characteristics and their capability to induce angiogenesis both *in vitro* and *in vivo* were evaluated.

Research methods

ADSCs were divided based on culture medium: 2.5% PRP, 5% PRP, 7.5% PRP, 10% PRP, or FBS as control. *In vitro*, we studied the cell proliferation rate, endothelial cell specific genes expression and cell morphology change. *In vivo*, we studied the angiogenic capability of ADSCs by mouse ischemic hindlimb mode.

Research results

The proliferation rate of ADSCs was higher in the 2.5%, 5%, and 7.5% PRP groups. The expression of hypoxia-inducible factor, CD31, vascular endothelial growth factor, and endothelial cell nitric oxide synthase increased in the 5% and 7.5% PRP groups. The 5%, 7.5%, and 10% PRP groups showed higher abilities to promote both CD31 and vascular endothelial growth factor production and tubular structure formation in ADSCs. According to laser Doppler perfusion scan, the perfusion ratios of ischemic limb to normal limb were significantly higher in the 5% PRP, 7.5% PRP and human umbilical vein endothelial cell

groups compared with the negative control and FBS groups.

Research conclusions

Our results showed that PRP-preconditioned ADSCs had a better ability to present endothelial cell characteristics *in vitro*. After PRP treatment, ADSCs significantly improved blood perfusion in ischemic hindlimbs. Furthermore, 5% PRP- and 7.5% PRP-preconditioned ADSCs exert the optimal angiogenic effect both *in vitro* and *in vivo*.

Research perspectives

We were the first study to observe the angiogenic effect of PRP-preconditioned ADSCs on ischemic hindlimb models. We were also the first to discuss the correlation between PRP concentration and angiogenesis of ADSCs. Based on our results, we believe that PRP and ADSCs could be clinically applied for treating ischemic tissues and promoting wound healing in the future. Further research should focus on increasing the rate of ADSC differentiation into mature endothelial cells and finding key regulators for three-dimensional tubular structure formation in these cells. The optimal goal is to use ADSCs to form stable and functional vessels for patients with PAD.

REFERENCES

- Zhou R, Zhu L, Fu S, Qian Y, Wang D, Wang C. Small Diameter Blood Vessels Bioengineered From Human Adipose-derived Stem Cells. *Sci Rep* 2016; **6**: 35422 [PMID: 27739487 DOI: 10.1038/srep35422]
- Adair TH, Montani JP. Angiogenesis. San Rafael: Morgan & Claypool Life Sciences, 2010 [PMID: 21452444]
- Ziello JE, Jovin IS, Huang Y. Hypoxia-Inducible Factor (HIF)-1 regulatory pathway and its potential for therapeutic intervention in malignancy and ischemia. *Yale J Biol Med* 2007; **80**: 51-60 [PMID: 18160990]
- Fujita Y, Kawamoto A. Stem cell-based peripheral vascular regeneration. *Adv Drug Deliv Rev* 2017; **120**: 25-40 [PMID: 28912015 DOI: 10.1016/j.addr.2017.09.001]
- Nakagami H, Maeda K, Morishita R, Iguchi S, Nishikawa T, Takami Y, Kikuchi Y, Saito Y, Tamai K, Ogihara T, Kaneda Y. Novel autologous cell therapy in ischemic limb disease through growth factor secretion by cultured adipose tissue-derived stromal cells. *Arterioscler Thromb Vasc Biol* 2005; **25**: 2542-2547 [PMID: 16224047 DOI: 10.1161/01.ATV.0000190701.92007.6d]
- Zhao L, Johnson T, Liu D. Therapeutic angiogenesis of adipose-derived stem cells for ischemic diseases. *Stem Cell Res Ther* 2017; **8**: 125 [PMID: 28583178 DOI: 10.1186/s13287-017-0578-2]
- Cao Y, Sun Z, Liao L, Meng Y, Han Q, Zhao RC. Human adipose tissue-derived stem cells differentiate into endothelial cells in vitro and improve postnatal neovascularization in vivo. *Biochem Biophys Res Commun* 2005; **332**: 370-379 [PMID: 15896706 DOI: 10.1016/j.bbrc.2005.04.135]
- Planat-Benard V, Silvestre JS, Cousin B, André M, Nibbelink M, Tamarat R, Clergue M, Manneville C, Saillan-Barreau C, Duriez M, Tedgui A, Levy B, Pénicaud L, Casteilla L. Plasticity of human adipose lineage cells toward endothelial cells: physiological and therapeutic perspectives. *Circulation* 2004; **109**: 656-663 [PMID: 14734516 DOI: 10.1161/01.CIR.0000114522.38265.61]
- Bourin P, Bunnell BA, Casteilla L, Dominici M, Katz AJ, March KL, Redl H, Rubin JP, Yoshimura K, Gimble JM. Stromal cells from the adipose tissue-derived stromal vascular fraction and culture expanded adipose tissue-derived stromal/stem cells: a joint statement of the International Federation for Adipose Therapeutics and Science (IFATS) and the International Society for Cellular Therapy (ISCT). *Cytotherapy* 2013; **15**: 641-648 [PMID: 23570660 DOI: 10.1016/j.jcyt.2013.02.006]
- Dominici M, Le Blanc K, Mueller I, Slaper-Cortenbach I, Marini F, Krause D, Deans R, Keating A, Prockop Dj, Horwitz E. Minimal criteria for defining multipotent mesenchymal stromal cells. The International Society for Cellular Therapy position statement. *Cytotherapy* 2006; **8**: 315-317 [PMID: 16923606 DOI: 10.1080/14653240600855905]
- Zuk PA, Zhu M, Ashjian P, De Ugarte DA, Huang JI, Mizuno H, Alfonso ZC, Fraser JK, Benhaim P, Hedrick MH. Human adipose tissue is a source of multipotent stem cells. *Mol Biol Cell* 2002; **13**: 4279-4295 [PMID: 12475952 DOI: 10.1091/mbc.e02-02-0105]
- Li H, Usas A, Poddar M, Chen CW, Thompson S, Ahani B, Cummins J, Lavasani M, Huard J. Platelet-rich plasma promotes the proliferation of human muscle derived progenitor cells and maintains their stemness. *PLoS One* 2013; **8**: e64923 [PMID: 23762264 DOI: 10.1371/journal.pone.0064923]
- Cervelli V, Scioli MG, Gentile P, Doldo E, Bonanno E, Spagnoli LG, Orlandi A. Platelet-rich plasma greatly potentiates insulin-induced adipogenic differentiation of human adipose-derived stem cells through a serine/threonine kinase Akt-dependent mechanism and promotes clinical fat graft maintenance. *Stem Cells Transl Med* 2012; **1**: 206-220 [PMID: 23197780 DOI: 10.5966/sctm.2011-0052]
- Shen J, Gao Q, Zhang Y, He Y. Autologous platelet-rich plasma promotes proliferation and chondrogenic differentiation of adipose-derived stem cells. *Mol Med Rep* 2015; **11**: 1298-1303 [PMID: 25373459 DOI: 10.3892/mmr.2014.2875]
- Fréchette JP, Martineau I, Gagnon G. Platelet-rich plasmas: growth factor content and roles in wound healing. *J Dent Res* 2005; **84**: 434-439 [PMID: 15840779 DOI: 10.1177/154405910508400507]
- Tavakolinejad S, Khosravi M, Mashkani B, Ebrahimzadeh Bideskan A, Sanjar Mossavi N, Parizadeh MR, Hamidi Alamdari D. The effect of human platelet-rich plasma on adipose-derived stem cell proliferation and osteogenic differentiation. *Iran Biomed J* 2014; **18**: 151-157 [PMID: 24842141]
- Van Pham P, Bui KH, Ngo DQ, Vu NB, Truong NH, Phan NL, Le DM, Duong TD, Nguyen TD, Le VT, Phan NK. Activated platelet-rich plasma improves adipose-derived stem cell transplantation efficiency in injured articular cartilage. *Stem Cell Res Ther* 2013; **4**: 91 [PMID: 23915433 DOI: 10.1186/srct277]
- Xiong BJ, Tan QW, Chen YJ, Zhang Y, Zhang D, Tang SL, Zhang S, Lv Q. The Effects of Platelet-Rich Plasma and Adipose-Derived Stem Cells on Neovascularization and Fat Graft Survival. *Aesthetic Plast Surg* 2018; **42**: 1-8 [PMID: 29302732 DOI: 10.1007/s00266-017-1062-1]
- Felthaus O, Prantl L, Skaff-Schwarze M, Klein S, Anker A, Ranieri M, Kuehlmann B. Effects of different concentrations of Platelet-rich Plasma and Platelet-Poor Plasma on vitality and differentiation of autologous Adipose tissue-derived stem cells. *Clin Hemorheol Microcirc* 2017; **66**: 47-55 [PMID: 28269759 DOI: 10.3233/CH-160203]
- Amable PR, Teixeira MV, Carias RB, Granjeiro JM, Borojovic R. Mesenchymal stromal cell proliferation, gene expression and protein production in human platelet-rich plasma-supplemented media. *PLoS One* 2014; **9**: e104662 [PMID: 25115920 DOI: 10.1371/journal.pone.0104662]
- Cho HS, Song IH, Park SY, Sung MC, Ahn MW, Song KE. Individual variation in growth factor concentrations in platelet-rich plasma and its influence on human mesenchymal stem cells. *Korean J Lab Med* 2011; **31**: 212-218 [PMID: 21779198 DOI: 10.3343/kjlm.2011.31.3.212]
- Kakudo N, Minakata T, Mitsui T, Kushida S, Notodihardjo FZ, Kusumoto K. Proliferation-promoting effect of platelet-rich plasma on human adipose-derived stem cells and human dermal fibroblasts. *Plast Reconstr Surg* 2008; **122**: 1352-1360 [PMID: 18971718 DOI: 10.1097/PRS.0b013e3181882046]
- Hsu CW, Yuan K, Tseng CC. The negative effect of platelet-rich plasma on the growth of human cells is associated with secreted thrombospondin-1. *Oral Surg Oral Med Oral Pathol Oral Radiol Endod* 2009; **107**: 185-192 [PMID: 18805712 DOI: 10.1016/j.tripleo.2008.07.016]
- Krock BL, Skuli N, Simon MC. Hypoxia-induced angiogenesis: good and evil. *Genes Cancer* 2011; **2**: 1117-1133 [PMID: 22866203 DOI: 10.1177/1947601911423654]
- Ke Q, Costa M. Hypoxia-inducible factor-1 (HIF-1). *Mol Pharmacol* 2006; **70**: 1469-1480 [PMID: 16887934 DOI: 10.1124/

- mol.106.027029]
- 26 **Andreeva ER**, Lobanova MV, Udartseva OO, Buravkova LB. Response of Adipose Tissue-Derived Stromal Cells in Tissue-Related O₂ Microenvironment to Short-Term Hypoxic Stress. *Cells Tissues Organs* 2015; **200**: 307-315 [PMID: 26407140 DOI: 10.1159/000438921]
 - 27 **Zimna A**, Kurpisz M. Hypoxia-Inducible Factor-1 in Physiological and Pathophysiological Angiogenesis: Applications and Therapies. *Biomed Res Int* 2015; **2015**: 549412 [PMID: 26146622 DOI: 10.1155/2015/549412]
 - 28 **Kakudo N**, Morimoto N, Ogawa T, Taketani S, Kusumoto K. Hypoxia Enhances Proliferation of Human Adipose-Derived Stem Cells via HIF-1 α Activation. *PLoS One* 2015; **10**: e0139890 [PMID: 26465938 DOI: 10.1371/journal.pone.0139890]
 - 29 **Hoeben A**, Landuyt B, Highley MS, Wildiers H, Van Oosterom AT, De Bruijn EA. Vascular endothelial growth factor and angiogenesis. *Pharmacol Rev* 2004; **56**: 549-580 [PMID: 15602010 DOI: 10.1124/pr.56.4.3]
 - 30 **Bir SC**, Esaki J, Marui A, Yamahara K, Tsubota H, Ikeda T, Sakata R. Angiogenic properties of sustained release platelet-rich plasma: characterization in-vitro and in the ischemic hind limb of the mouse. *J Vasc Surg* 2009; **50**: 870-879.e2 [PMID: 19679427 DOI: 10.1016/j.jvs.2009.06.016]
 - 31 **Ii M**, Horii M, Yokoyama A, Shoji T, Mifune Y, Kawamoto A, Asahi M, Asahara T. Synergistic effect of adipose-derived stem cell therapy and bone marrow progenitor recruitment in ischemic heart. *Lab Invest* 2011; **91**: 539-552 [PMID: 21135814 DOI: 10.1038/labinvest.2010.191]
 - 32 **Du WJ**, Chi Y, Yang ZX, Li ZJ, Cui JJ, Song BQ, Li X, Yang SG, Han ZB, Han ZC. Heterogeneity of proangiogenic features in mesenchymal stem cells derived from bone marrow, adipose tissue, umbilical cord, and placenta. *Stem Cell Res Ther* 2016; **7**: 163 [PMID: 27832825 DOI: 10.1186/s13287-016-0418-9]
 - 33 **Trojan K**, Oliveri RS, Glovinski PV, Kirchhoff M, Mathiasen AB, Elberg JJ, Andersen PS, Drzewiecki KT, Fischer-Nielsen A. Pooled human platelet lysate versus fetal bovine serum-investigating the proliferation rate, chromosome stability and angiogenic potential of human adipose tissue-derived stem cells intended for clinical use. *Cytotherapy* 2013; **15**: 1086-1097 [PMID: 23602579 DOI: 10.1016/j.jcyt.2013.01.217]
 - 34 **You J**, Sun J, Ma T, Yang Z, Wang X, Zhang Z, Li J, Wang L, Ii M, Yang J, Shen Z. Curcumin induces therapeutic angiogenesis in a diabetic mouse hindlimb ischemia model via modulating the function of endothelial progenitor cells. *Stem Cell Res Ther* 2017; **8**: 182 [PMID: 28774328 DOI: 10.1186/s13287-017-0636-9]
 - 35 **Bir SC**, Esaki J, Marui A, Sakaguchi H, Kevil CG, Ikeda T, Komeda M, Tabata Y, Sakata R. Therapeutic treatment with sustained-release platelet-rich plasma restores blood perfusion by augmenting ischemia-induced angiogenesis and arteriogenesis in diabetic mice. *J Vasc Res* 2011; **48**: 195-205 [PMID: 21099226 DOI: 10.1159/000318779]
 - 36 **Li X**, Hou J, Wu B, Chen T, Luo A. Effects of platelet-rich plasma and cell coculture on angiogenesis in human dental pulp stem cells and endothelial progenitor cells. *J Endod* 2014; **40**: 1810-1814 [PMID: 25175848 DOI: 10.1016/j.joen.2014.07.022]
 - 37 **Kakudo N**, Morimoto N, Kushida S, Ogawa T, Kusumoto K. Platelet-rich plasma releasate promotes angiogenesis in vitro and in vivo. *Med Mol Morphol* 2014; **47**: 83-89 [PMID: 23604952 DOI: 10.1007/s00795-013-0045-9]
 - 38 **Kakudo N**, Morimoto N, Ogawa T, Hihara M, Notodihardjo PV, Matsui M, Tabata Y, Kusumoto K. Angiogenic effect of platelet-rich plasma combined with gelatin hydrogel granules injected into murine subcutis. *J Tissue Eng Regen Med* 2017; **11**: 1941-1948 [PMID: 26489691 DOI: 10.1002/term.2091]
 - 39 **Etulain J**, Mena HA, Meiss RP, Frechtel G, Gutt S, Negrotto S, Schattner M. An optimised protocol for platelet-rich plasma preparation to improve its angiogenic and regenerative properties. *Sci Rep* 2018; **8**: 1513 [PMID: 29367608 DOI: 10.1038/s41598-018-19419-6]
 - 40 **Etulain J**, Mena HA, Negrotto S, Schattner M. Stimulation of PAR-1 or PAR-4 promotes similar pattern of VEGF and endostatin release and pro-angiogenic responses mediated by human platelets. *Platelets* 2015; **26**: 799-804 [PMID: 26082997 DOI: 10.3109/09537104.2015.1051953]
 - 41 **Eppler SM**, Combs DL, Henry TD, Lopez JJ, Ellis SG, Yi JH, Annex BH, McCluskey ER, Zioncheck TF. A target-mediated model to describe the pharmacokinetics and hemodynamic effects of recombinant human vascular endothelial growth factor in humans. *Clin Pharmacol Ther* 2002; **72**: 20-32 [PMID: 12152001 DOI: 10.1067/mcp.2002.126179]
 - 42 **Xie J**, Wang H, Wang Y, Ren F, Yi W, Zhao K, Li Z, Zhao Q, Liu Z, Wu H, Gu C, Yi D. Induction of angiogenesis by controlled delivery of vascular endothelial growth factor using nanoparticles. *Cardiovasc Ther* 2013; **31**: e12-e18 [PMID: 22954162 DOI: 10.1111/j.1755-5922.2012.00317.x]
 - 43 **Doi K**, Ikeda T, Marui A, Kushibiki T, Arai Y, Hirose K, Soga Y, Iwakura A, Ueyama K, Yamahara K, Itoh H, Nishimura K, Tabata Y, Komeda M. Enhanced angiogenesis by gelatin hydrogels incorporating basic fibroblast growth factor in rabbit model of hind limb ischemia. *Heart Vessels* 2007; **22**: 104-108 [PMID: 17390205 DOI: 10.1007/s00380-006-0934-0]
 - 44 **Moon MH**, Kim SY, Kim YJ, Kim SJ, Lee JB, Bae YC, Sung SM, Jung JS. Human adipose tissue-derived mesenchymal stem cells improve postnatal neovascularization in a mouse model of hindlimb ischemia. *Cell Physiol Biochem* 2006; **17**: 279-290 [PMID: 16791003 DOI: 10.1159/000094140]
 - 45 **Kondo K**, Shintani S, Shibata R, Murakami H, Murakami R, Imaizumi M, Kitagawa Y, Murohara T. Implantation of adipose-derived regenerative cells enhances ischemia-induced angiogenesis. *Arterioscler Thromb Vasc Biol* 2009; **29**: 61-66 [PMID: 18974384 DOI: 10.1161/ATVBAHA.108.166496]
 - 46 **Kamihata H**, Matsubara H, Nishiue T, Fujiyama S, Tsutsumi Y, Ozono R, Masaki H, Mori Y, Iba O, Tateishi E, Kosaki A, Shintani S, Murohara T, Imaizumi T, Iwasaka T. Implantation of bone marrow mononuclear cells into ischemic myocardium enhances collateral perfusion and regional function via side supply of angioblasts, angiogenic ligands, and cytokines. *Circulation* 2001; **104**: 1046-1052 [PMID: 11524400 DOI: 10.1161/hc3501.093817]
 - 47 **Yu WY**, Sun W, Yu DJ, Zhao TL, Wu LJ, Zhuang HR. Adipose-derived stem cells improve neovascularization in ischemic flaps in diabetic mellitus through HIF-1 α /VEGF pathway. *Eur Rev Med Pharmacol Sci* 2018; **22**: 10-16 [PMID: 29364466 DOI: 10.26355/eurrev_201801_14094]
 - 48 **Rehman J**, Traktuev D, Li J, Merfeld-Clauss S, Temm-Grove CJ, Bovenkerk JE, Pell CL, Johnstone BH, Considine RV, March KL. Secretion of angiogenic and antiapoptotic factors by human adipose stromal cells. *Circulation* 2004; **109**: 1292-1298 [PMID: 14993122 DOI: 10.1161/01.CIR.0000121425.42966.F1]

P- Reviewer: Yamaguchi DT, Zaminy A S- Editor: Ma RY

L- Editor: Filipodia E- Editor: Song H





Published by **Baishideng Publishing Group Inc**
7901 Stoneridge Drive, Suite 501, Pleasanton, CA 94588, USA
Telephone: +1-925-223-8242
Fax: +1-925-223-8243
E-mail: bpgoffice@wjgnet.com
Help Desk: <https://www.f6publishing.com/helpdesk>
<https://www.wjgnet.com>

